DEMONSTRATION OF POC BIOSENSOR TOWARD CLINICAL TRANSLATION FOR PATIENT BED-SIDE MONITORING

by

Ambalika Sanjeev Tanak

APPROVED BY SUPERVISORY COMMITTEE:

Shalini Prasad, Chair

Sriram Muthukumar

Soudeh Khoubrouy

Shashank Sirsi

Dedicated to my parents Sanjeev Tanak, Amita Tanak and my brother Ambarish Tanak for all the sacrifices you've made for letting me achieve my dream.

DEMONSTRATION OF POC BIOSENSOR TOWARD CLINICAL TRANSLATION FOR PATIENT BED-SIDE MONITORING

by

AMBALIKA SANJEEV TANAK, BE, MS

DISSERTATION

Presented to the Faculty of

The University of Texas at Dallas

in Partial Fulfillment

of the Requirements

for the Degree of

DOCTOR OF PHILOSOPHY IN

BIOMEDICAL ENGINEERING

THE UNIVERSITY OF TEXAS AT DALLAS

December 2021

ACKNOWLEDGMENTS

As an immense part of my academic journey comes close to an end, I would like to revisit all the beautiful moments that came along with it. There have been so many people who have directly or indirectly been a part of this incredible journey who I would personally like to acknowledge. I thank everyone I met during all the conferences who inspired me or discussed my research. It would be nearly impossible to mention everyone who has helped throughout this learning process, but I would like to thank every one of you from the bottom of my heart for giving your valuable feedback and spending time for me.

First and foremost, I am extremely grateful to my advisor Dr. Shalini Prasad who gave me this wonderful opportunity, supported me with utmost patience, provided guidance not only academically, but also towards my professional development and personal growth. Dr. Prasad has constantly encouraged me to push myself beyond my comfort zone and appreciated my efforts towards solving difficult situations. Thank you for sparing the time for me for all your scientific feedback, funding support, and encouragement towards my academic pursuit and making me an independent researcher. I am deeply grateful to my mentor, Dr. Sriram Muthukumar, who took time out every week to review my progress, provide constructive criticism and appreciate my creative efforts towards all my research projects. Thank you for all the effective long discussions which have helped me come up with newer perspectives and expand my understandings. I would like to extend my thanks to my committee members Dr. Soudeh Khoubroy and Dr. Shashank Sirsi for their valuable suggestions, comments and for agreeing to be a part of my committee. I would like to thank my collaborator Dr. Ibrahim Hashim, who provided patient samples for my research from UT Southwestern, valuable

clinical guidance on assay validation, and feedback and comments as co-author on my journal publications. Thank you for your encouragement, advice and introducing me to your lab members, especially during the American Association for Clinical Chemistry conference in Chicago! I would like to specially acknowledge Mrs. Indu Raman from UT Southwestern Medical Center for all the support, discussion, and guidance on LUMINEX assays throughout the work on sepsis. A special thanks to Texas Instruments and Dr. Srikanth Krishnan for the providing the opportunity to explore my understanding and apply my statistical expertise towards a different area of semi-conducting sensor research and funding. I would like to thank all my co-authors for their comments, feedback, suggestions, and contributions. I am thankful to all the Biomedical Microdevices and Nanotechnology Laboratory (BMNL) colleagues, past (Rujuta Munje, Vikramshankar Kamakoti, Jon Craven, David Kinnamon, and Hunter Stevenson) and present (Badrinath Jagannath, Ashlesha Bhide, Sayali Upasham, Devang Sankhala, Dr. Lin, and Madhavi Pali) members for their comments and feedback. I deeply acknowledge the contributions of all the undergraduate students who have helped me in data collection, literature search and creative graphical figures throughout my research. Thank you for accepting me as your mentor and guide and I hope you learnt a few things during your time in the lab. I am thankful to the bioengineering and cleanroom staff at UT Dallas for their support. I would like to express my sincere gratitude to Badri, who always supported me with his technical expertise, comments, and new ideas that provided valuable feedback throughout my doctoral journey. I am thankful for all the extensive technical discussions, debates, and working together after hours, having tireless conversations, especially before deadlines. I am grateful for all my close friends and roommates who have made my time in UTD most

delightful! I will treasure all the memories that we had throughout! A very special thanks to my closest circle who I call family away from home (Nikita Deshmukh, Gayatri Dabadghao and Manasi Deshpande) who have supported and encouraged me throughout this long and enduring journey- I will be forever indebted! They have been my emotional and mental support systems in my highest of highs and lowest of lows. Thank you for understanding me, making compromises, keeping a constant check on me, and adjusting to my schedule throughout this journey!

Finally, no words can ever express how grateful I am to my parents for making me who I am today. I thank my father, Sanjeev Tanak, who has always believed in me and guided me through all the times when I doubted myself. He has encouraged me to always be the best version of myself and never restricted my ambitions. I have learnt to work harder looking at his zeal and enthusiasm even today. I thank my mother, Amita Tanak, who has taught me to become a fearless independent, ambitious woman like herself with the most selfless nature. She has supported me in every possible way and sacrificed so much for me to be here today. Thank you, mom, and dad, for loving me the way I am, accepting my flaws and making me believe in myself to reach beyond my potential. I would like to thank my brother, Ambarish Tanak, who has been my stressbuster and guide during my tough times! I cannot express how much I miss all of them every day. I am thankful for my extended family (Rajan Tanak, Rushikesh and Payal) who have always been a major support to my parents and me, especially in my absence.

Lastly, a huge shoutout to all my friends in the U.S., India and Dubai who have been a part of my doctoral journey one way or another!

November 2021

DEMONSTRATION OF POC BIOSENSOR TOWARD CLINICAL TRANSLATION FOR PATIENT BED-SIDE MONITORING

Ambalika Sanjeev Tanak, PhD
The University of Texas at Dallas, 2021

Supervising Professor: Shalini Prasad

The research presented in this dissertation focuses on developing and characterizing a multiplexed affinity based electrochemical biosensing device toward clinical translation. The goal of this work is to establish a portable POC device for early disease detection across diverse healthcare applications using low sample volume, rapid response time and usability amongst minimally trained individual relying on ASSURED (Affordable, Sensitive, Specific, User friendly, rapid, and Robust, Equipment free and Deliverable to end users) criteria. Primarily, we designed a robust, non-faradaic electrochemical affinity biosensing platform for the rapid assessment of parathyroid hormone (PTH) as a single biosensing system. Unique high density semiconducting nanostructured arrays on a flexible sensing surface were used to create the analytical nanobiosensor. The surface modification technique was specifically designed to improve the interaction of the nanostructure–biological interface to capture the desired PTH level in HS and plasma. This was followed by evaluating the analytical performance of the developed biosensor with clinical rigor. The assay validation results were compared with laboratory standard as reference with results that demonstrated comparable performance with

higher accuracy. Next, the scope of the biosensor was expanded to solve a clinically challenging problem of detecting host immune markers for life-threatening sepsis infection. Herein, we demonstrate a first-of-a-kind multiplexed POC biosensing device that simultaneously detects a panel of eight key immune response cytokine biomarkers in sample volume equivalent to two drops of plasma and whole blood within 5 minutes without sample dilution. Moreover, this work focuses on validating the developed biosensing device with LUMINEX standard reference method for clinical translation using nearly 200 patient samples. The DeTecT (Direct Electrochemical Technique Targeting) Sepsis biosensing device is surface engineered with specific capture probes that utilizes EIS to measure the capacitive impedance change reflecting binding interactions between the capture probe and target biomarker enabling multiplexed detection. Specificity of the biosensor was validated using cross-reactive studies, which displayed insignificant interference from non-specific biomarkers. The biosensor also displays stable and repeatable performance. The novelty presented in this research combines the effectiveness of choosing specific host immune response biomarkers for detection of sepsis combined with unique surface modification strategy coupled with EIS technique to enable efficient clinical decision-making process. This unique sensor technology would allow medical practitioners to facilitate targeted interventions for septic patients as a rapid prognostic approach, preventing complications arriving from sepsis.

TABLE OF CONTENTS

CURRICULUM VITAE

LIST OF FIGURES

CHAPTER 1

INTRODUCTION

Biosensors and POC diagnostic devices are already revolutionizing healthcare in one form or another. From 2021 to 2026, the biosensors market is estimated to increase at a CAGR of 7.5%, from a value of USD 25.5 billion in 2021 to USD 36.7 billion in 2026 [1]. The advent of nanotechnology-based biosensors, with significant technological breakthroughs in recent years, growing the use of glucose biosensors for diabetes management, surging demands for home-based POC devices due to COVID-19 pandemic, and growing government initiatives toward diagnostics are amongst the pivotal motivating factors in the biosensing market. Biosensing research demands an interdisciplinary approach that integrates several branches of study such as chemistry, biology, and engineering. A biosensor is a device that translates biological response into a measurable quantifiable signal. These biological elements are converted into different forms of outputs based on the type of physicochemical transducer. An ideal sensor is expected to have typical characteristics such as wide detection range, good sensitivity and selectivity, linearity, reproducibility, repeatability, and fast response time. Accordingly, much focus is attributed towards the design and development of biosensors which have a wide range of application, especially in the last decade. A typical biosensor consists of the following components:

Analyte: A molecule of significance, that must be detected. In a biosensor designed to detect glucose, for instance, the analyte will be glucose.

Bioreceptor: A bioreceptor is a molecule that recognizes the analyte precisely. Bioreceptors include enzymes, cells, aptamers, deoxyribonucleic acid (DNA) and antibodies.

Biorecognition is the process of signal production (in the form of light, heat, pH, charge or shift in mass etc) when a bioreceptor interacts with an analyte.

Transducer: A transducer is device that transforms one form of energy into another. The responsibility of a transducer in a biosensing system is to convert the bio-recognition event into a quantifiable signal. For instance, converting biochemical interaction into an electric signal output.

Electronics: This is the portion of the biosensor that process and presents the transduced signal. It consists of specialized electronic circuitry that performs signal conditioning functions such as amplification and digital signal conversion. The display device of the biosensor then quantifies the processed signals.

Display: A user interpretation system, such as a computer, a portable mobile device or specialized screen. This component is often a combination of hardware and software that delivers user-friendly biosensing results. Depending on the application and the user requirement, the display can be numeric in terms of concentration, a range indicating low or high value or an image.

1.1 Need for biosensor sand POC devices

The need for faster results, user friendly test, and understanding infectious disease progression has been much appreciated with the advent of the current COVID-19 pandemic. While sensitive and specific assays such as blood culture, high-throughput immunoassays, polymerase chain reaction (PCR), and mass spectroscopy (MS) tests are available in central laboratories, they are often labor intensive, expensive, and reliant on sophisticated instruments and well-trained operators [2], [3]. Timely diagnosis with rapid treatment methodology has

been reported to improve the chances of preventing adverse complications, and thus, reduce mortality rate, particularly in infectious diseases[4]. For instance, in case of identifying the infected pathogen, traditional blood culture takes 1-3 days to increase bacterial concentration to the detectable limit for molecular diagnostic testing which could cause more harm in sensitive diseases like sepsis where rate of mortality is increased every hour the patient is undiagnosed. POC biosensors on the other hand offer an immediate on-site result, particularly in resource-constrained situations, allowing for timely and proper treatment, overcoming the existing shortcomings of laboratory-based tests[5], [6]. Patients may be able to self-test in the privacy of their own homes using POC tests. POC can also reduce costs associated with tests by making it convenient for healthcare providers as well as patients. Treatment can be implemented faster, thus providing opportunities to saving more lives. Having described the advantages of using POC biosensors within healthcare systems it is crucial to standardize the results including method of validation for consistency in results. This has given rise to the ASSURED criteria guided by the World Health Organization- which is Affordable, Sensitive, Specific, User friendly, rapid, and Robust, Equipment free and Deliverable to end users.

Multiple factors are involved in designing an optimal POC sensor. The major aspect that governs the success of a POC sensor is the rapid response time. Traditional diagnosis is performed by sending the patient sample to a laboratory for tests. This not only requires large sample volumes, but also takes several hours to provide results. POC sensors offer provocative possibilities of providing instant results without the laboratory hustle. Use of POC biosensor near patient bedside offers more opportunities for personalized medicine and healthcare. POC diagnostic devices must enable low sample consumption, easily accessible body fluid, rapid

turn-around times, sensitive detection limits that are in accordance with clinical findings, low cost, portable and easy to use. Key aspects that dictate the success of a POC device is the ability for rapid detection. The possibility to conduct diagnostic tests easily and frequently opens up opportunities in clinical practice. POC innovations are even more essential in developing and resource limited environments where timely diagnosis tailored to patient requirements can be utilized to curb the spread of infectious diseases. Detection strategies involving the use of biomarkers have revolutionized the healthcare field. Complex diseases can be easily diagnosed by measuring multiple biomarkers simultaneously, with multiple analytes using least sample volume along with the biosensor being portable.

1.2 Characteristics of POC biosensors

Certain features are required while implementing the biosensor design use of POC biosensors for highly effective outcomes which are listed as follow:

1.2.1 Selectivity

While establishing a bioreceptor for a specific biosensor, selectivity is an important factor to consider. In a sample containing mixed species and undesired impurities, a bioreceptor may detect a certain target analyte biomolecule.

1.2.2 Sensitivity

Sensitivity can be defined as the minimum amount of analyte that can be detected correctly in a few steps and in low concentrations to confirm the presence of analyte traces within a given sample.

1.2.3 Linearity

The accuracy of the measured result is assisted by linearity. The better the linearity, the more accurate detection of substrate concentration.

1.2.4 Response time

The time taken to display 95% of results is reported as the response time of the POC biosensor.

1.2.5 Reproducibility

Reproducibility is characterized as the precision (consistent results when the sample is measured multiple times) and accuracy (sensors capability to generate mean value closer to actual value when measured multiple times).

1.2.6 Stability

One of the key features of a biosensing device is stability of the biosensor. The degree of susceptibility to environmental perturbations within the biosensing device is referred to as stability. The affinity of the bioreceptor (binding capability to the bioreceptor) and the bioreceptor's degradation with time are the two elements that affects stability of the biosensor.

1.3 Innovation

The novelty presented in this research combines the effectiveness of specific capture probe antibodies with EIS technique for detection of target analytes to enable clinically efficient decision-making process. To provide a complete patient profile on the diseased state, we have targeted key biomarkers that help diagnose sepsis accurately and detecting PTH for determining the success during parathyroidectomy (further discussed in chapter 2 and 3). The

innovation lies in designing an electrochemical POC sensing platform that can measure single molecule or a multiplexed system that is compatible for seven biomarkers to be detected

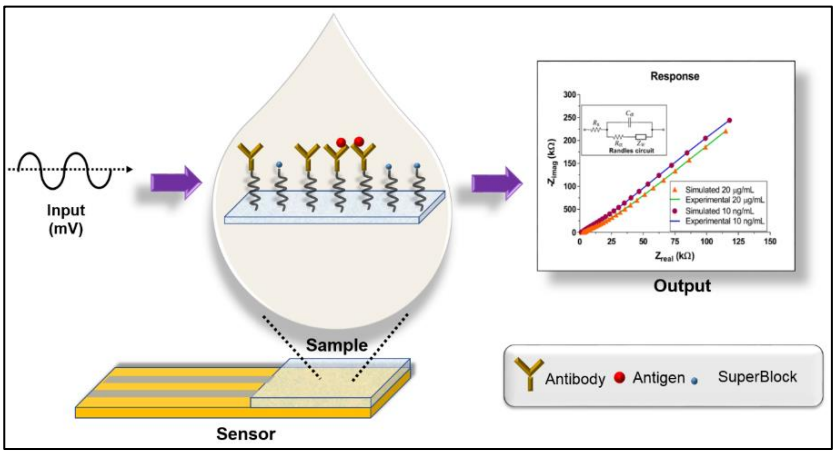

Figure 1.1. Schematic illustrating immunoassay building protocol for point of care biosensor

simultaneously using single drop of fluid. The sensing platform of the biosensor is surface engineered to allow sensitive detection of specific target biomolecules using low volume of undiluted samples. Furthermore, our interdisciplinary approach of designing the POC biosensor allows label-free detection allowing wide range of application in the healthcare field of medicine.

1.4 Overall Approach

A Non-faradaic affinity biosensor is developed on surface engineered electrode surface. The immunoassay is constructed by a series of functionalization protocols that allows successful binding of the target analyte. The sensor surface is functionalized with dithiobis succinimidyl propionate (DSP) cross-linker that allows formation of a self-assembled monolayers using thiol chemistry. DSP is an amine-reactive cross-linker with NHS-ester reactive ends on either arm held by a disulfide bond. NHS esters react with primary amines of antibodies to form stable amide bonds. The capture probe antibody is covalently bound to the electrode surface which

allows target immunoreaction to take place on the biosensing platform. Schematic shown in fig 1.1 illustrates the immunoassay building protocol that aids to capture the binding phenomenon occurring at the electrode interface using electrochemical signals to transduce and provide a measurable signal. EIS is used to measure the binding activity occurring at the sensor surface using a small AC input voltage.

1.4.1 Electrochemical Impedance Spectroscopy (EIS)

Electrochemical biosensors are used in POC applications owing to their excellent properties like rapid response time, capability to translate into a miniaturized device, low cost and high sensitivity [7], [8]. Electrochemical biosensors have electrodes that are functionalized with biological recognition element, selective to the target analyte. The electrodes translate biochemical reaction into electrical signals that quantify the concentration of the interacting analyte. Electrochemical biosensors have eliminated the need for sample preparation while delivering high performance in terms of selectivity, sensitivity, and dynamic range with rapid response time. Out of the many electrochemical techniques, EIS is a powerful technique, attributing to its sensitive detection of binding interactions at the electrode [9], [10]. EIS measures change in impedance owing to the binding interaction between target and capture probe at the electrode–solution interface upon perturbation by a small AC voltage typically less than 10 mV [11]. An important aspect to be considered while developing an electrochemical POC is the ability to achieve sensitivity. Sensitivity depends on several factors including geometry of the sensing material, the resolution of the sensor material, and the surface chemistry used to functionalize the bio-recognition component on the sensing surface.

1.5 Experimental approach

1.5.1 Sensor design strategies for optimum sensing performance

For an electrochemical biosensor, design consideration can help optimize the sensing performance in terms of stability. Maintaining constant potential difference between two points is crucial for the working of a potentiostat. In a three-electrode setup (working electrode, reference electrode and counter electrode), this is achieved between the working and the reference electrode. Positioning of the reference and working electrode is considered to minimize the voltage drop that manifests itself as an error while measuring the potential difference between the electrodes. To minimize the solution resistance of the biosensing system, the position of the electrodes can be altered. Additionally, the shape, size and ratio between the working electrode and reference electrode influences the measuring signal. The general design consideration is that the reference/counter electrode should be larger than the working electrode and positioned symmetrically to ensure constant current density and potential across the sensing area.

For the first application of determining PTH, we considered a three-electrode system on a flexible polyimide surface.

This design consisted of two working electrodes, two counter electrodes and a single reference electrode. Surface area of Working Electrode: Counter Electrode: Reference Electrode was 1:1:4 to ensure optimal binding response. The second application (sepsis) included a two-electrode system with a single reference and seven working electrodes as version 1 (DeTecT Sepsis device) of the sensor. This allowed multiplexed detecting capability to allow multimolecular detection. More advanced application demanding the need for detecting eight biomarkers required an advanced version of the sensor with sixteen independent working and reference electrodes printed

on a single printed circuit board (PCB) capable of multiplexed detection, labelled as DeTecT Sepsis 2.0 device.

1.5.2 Surface modification strategies to achieve enhanced sensitivity

One of the most effective approach to improve the performance characteristics of an electrochemical biosensor is using surface modification strategies. Semiconducting materials like zinc oxide (ZnO) offer remarkable functional and morphological properties that enhances sensitivity for transducing physicochemical changes with biomolecular binding in electrochemical biosensors [12] . ZnO's high isoelectric point (IEP~9.5) enables stable immobilization of biomolecules with lower IEP through electrostatic interaction. This property of ZnO allows the biosensor to retain biological activity on its surface and facilitates bio functionality. Typically, biomolecules have reduced IEP as compared to ZnO at physiological pH which makes them negatively charged. Therefore, biomolecules can be readily immobilized on a positively charged ZnO through a strong electrostatic interaction. Furthermore, the chemical stability of ZnO plays a vital role in maintaining conducive environment for biomolecules in complex body fluids [13], [14]. Additionally, ZnO's crystal structure and surface polarities can be fine-tuned to enhance the electrical transfer properties that makes it suitable for electrochemical biosensing. We adopted the most widely used surface modification strategies to optimize the sensing efficiency of the developed biosensor. A 100 nm thin film of ZnO was deposited on the electrodes using RF-magnetron sputter tool. The ZnO deposited thin film on the electrode surface was characterized using Scanning electron microscope (SEM). Fig. 1.2 represents SEM image of the uniform deposition of ZnO thin film on the sensor platform with a thickness of 120±20 nm.

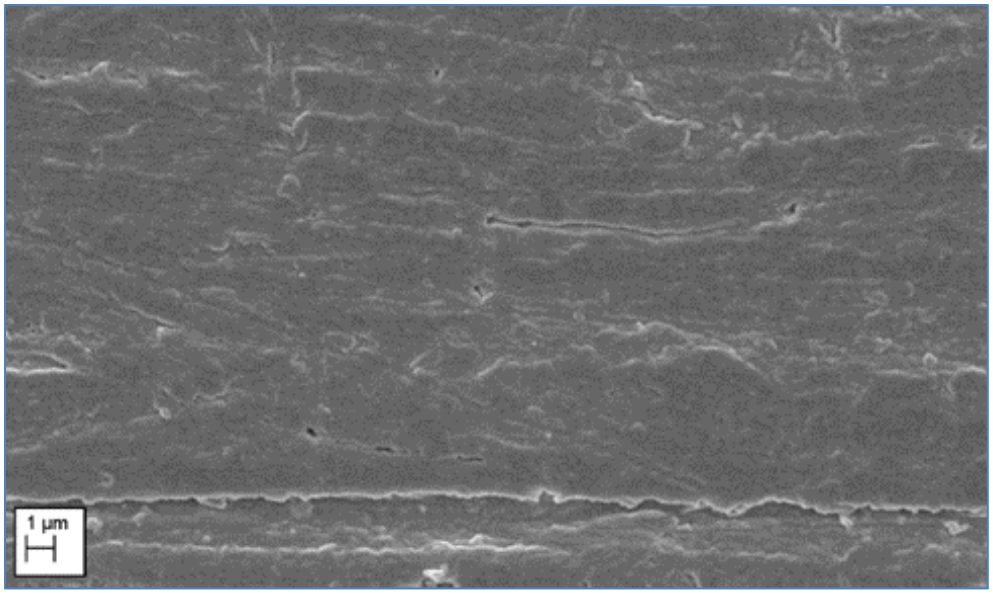

Figure 1.2. SEM image of the uniform deposition of ZnO thin film on the sensor platform

Another commonly used strategy is to integrate ZnO nanostructures to achieve enhanced sensing performance. Incorporation of nanostructures at the electrode surface potentially increases the surface area for increased capture probe immobilization allowing enhanced target biomolecule interaction. Furthermore, nanostructures increase signal amplification; thereby, improving sensitivity, even with complex body fluid matrices.

Figure 1.3 represents an SEM image of the hydrothermally grown ZnO nanostructures aligned vertically in a uniform manner due to pre deposited ZnO thin film. The average height of the hexagonally shaped rod like structure was measured to be 250 ± 20 nm with a diameter of 85 ± 10 nm. The uniform growth distribution of nanostructures increases sensitivity of detection as it controls the mass transport and diffusion of the target analyte at the electrode–electrolyte interface. The nanostructured aspect of the sensor design allows the target confinement, thereby enhancing the signal response.

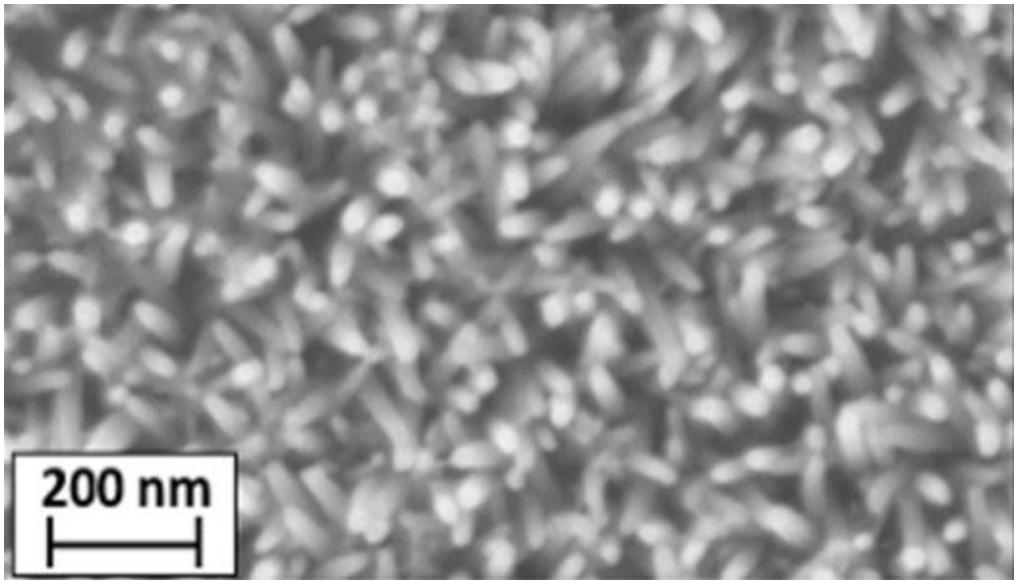

Figure 1.3. SEM image of uniform ZnO nanorods selectively grown on working electrode of the developed biosensor

1.6 Objective

The goal of this research is to develop a multiplexed affinity based electrochemical biosensing platform for small volume detection as a POC biosensor. The designed biosensor is envisioned to be a hand-held device for rapid detection of crucial biomarkers indicative of diseased health status using small volumes of complex biofluids like serum, plasma, and blood. A calibrated dose response will be developed to measure the accurate concentration of each biomolecule. Sensor performance metrics will be evaluated for specificity and further clinical validation will be performed.

This work focuses on leveraging various parameters and aspects involved in developing a POC electrochemical sensing platform to demonstrate single and multi-analyte detection. In chapter 2, we designed a robust POC platform to allow for sensitive and stable detection for a single biomarker. Leveraging the surface modification strategies, we applied this sensor platform to test for PTH as an application in detail. The sensor's capability was tested for clinical

translation by evaluating several assay performances including the features listed in section 1.2 in chapter 3. Chapter 4 introduces sepsis disease and the need to develop a multiplexed POC biosensing system.

Once the sensor was characterized and validated for a single biomarker (PTH detection in chapter 2 and 3), the capability of the sensor was expanded to characterize and validate the performance of the biosensor to test multiple biomarkers in plasma for an intricate infectious disease such as sepsis in chapter 5. In-depth analysis using multi-cohort time points and clinical validation using patient samples from three geographic locations was established in chapter 6. Chapter 7 describes true clinical translational ability by validating and testing the developed POC biosensor in a complex biofluid such as whole blood.

CHAPTER 2

POINT-OF-CARE BIOSENSOR FOR SINGLE MOLECULE DETECTION FOCUSING ON DETECTION OF PARATHROID HORMONE

2.1 Prior publications

Ambalika S. Tanak performed the experiments, data analysis, and wrote the manuscript. Ambalika S. Tanak, Dr. Shalini Prasad, Dr. Sriram Muthukumar, and Dr. Ibrahim A. Hashim co-designed the experiments, and co-wrote the manuscript. Dr. Ibrahim A. Hashim provided the patient samples. This manuscript was published in Bioelectronics in medicine journal in June 2019. This work describes the development and characterization of POC device for detection of affinity based PTH biosensor. The link to the article is https://www.futuremedicine.com/doi/full/10.2217/bem-2019-0011

2.2 Abstract

Novel electrochemical POC biosensing device for rapid assessment of PTH levels has been developed. The analytical nanobiosensor was designed by integrating unique high density semiconducting nanostructured arrays on a flexible sensing surface. Surface modification technique was tailored for enhancing the interaction of nanostructure-biological interface to capture the target PTH level. We demonstrate a rapid nanobiosensor to detect PTH in human serum (HS), plasma, and whole blood (WB) with a limit of detection (LOD) of 1 pg/mL and a clinically relevant dynamic range from 1 to 1000 pg/mL. This is the first demonstration of detecting PTH as a POC device devoid of sample pretreatment suitable in a surgical setting with high specificity to PTH.

2.3 Introduction

Medical and surgical management of endocrine disorders relies on accurate and timely hormone measurements where technology plays central role in the patient outcome. There are number of currently unmet technological needs resulting in hitherto unexplored opportunities for designing analytical biosensors as POC devices towards optimizing the medical and surgical interventions. PTH is a single chain 84 amino acids polypeptide secreted by the parathyroid gland. Its secretion is mainly regulated by extracellular ionized calcium level. In concert with vitamin D and other mediators, it is responsible for regulating body calcium homeostasis [15]. Measurement of circulating PTH levels aids in the investigation of parathyroid gland disorders as well as calcium level.

Primary hyperparathyroidism is the third most common endocrine disorder with its prevalence being one to seven cases per 1000 adults [16]–[19]. In primary hyperparathyroidism, development of benign tumors in one or more of the parathyroid glands causes excessive production of PTH leading to elevated circulating levels. Treatment for primary hyperparathyroidism involves surgical excision of the hyperfunctioning parathyroid gland. Successful resection of the tumor is evident by a 50% drop in peripheral PTH levels [20], [21]. In patients undergoing parathyroidectomy, intra-operative serial PTH measurements provide as a guide to successful resection.

Measurement of intact PTH (1-84 amino acids) is complicated by the presence of several molecular forms of the hormone. Although few clinical assays are termed intact, they also detect the 7-84 fragment which accumulates in patients with renal dysfunction limiting such assays and interpretation[22]–[24]. It is, therefore, important that PTH assays are characterized

in terms of their specificity. During surgery, blood samples collected at pre-incision following anesthesia induction and at 5 - 20 minutes post resection are sent to testing laboratories for analysis. However, the current diagnostic immunoassay techniques may be time-consuming, expensive, require large sample volume, and skilled trained personnel as well [25]–[27]. Additionally, sample transit time to the laboratory adds approximately 20-30 minutes to the analytical time which prolongs effective decision making. To overcome existing drawbacks, it is necessary to develop a sensitive, rapid, low sample volume assay. In this work, we describe the development of a novel POC biosensor intended as a guide to monitor PTH levels to improve effective clinical outcome in patient care.

Electrochemical biosensors are used in POC applications owing to their excellent properties like rapid response time, capability to translate into a miniaturized device, low cost and high sensitivity [7], [8]. Out of the many electrochemical techniques, EIS is a powerful technique, attributing to its sensitive detection of binding interactions at the electrode [10], [28]. EIS measures change in impedance owing to the binding interaction between target and capture probe at the electrode-solution interface upon perturbation by a small AC voltage typically less than 10 mV [11]. One of the most effective approach to improve the performance characteristics of an electrochemical biosensor is using surface modification of the sensing electrode. Incorporation of nanostructures at the electrode surface potentially increases the surface area for increased capture probe immobilization allowing enhanced target biomolecule interaction. Furthermore, nanostructures increase signal amplification thereby, improving sensitivity even with complex body fluid matrices [29]. Amongst various nanostructures, metal

oxide nanostructures have successfully been used by fine-tuning their properties for achieving ultrasensitive detection of affinity-based biosensors [12], [30], [31].

Modulating the surface chemistry of the metal oxide nanostructures allows for the charges in the electrolyte solution to align along the nanostructures to enhance the charge transfer mechanism. Zinc Oxide (ZnO) is one such unique metal oxide semiconductor with exceptional properties including wide band gap (3.367 eV), non-toxic and large excitation binding energy (60 eV) [32]–[34]. Additionally, owing to its high adsorption capability due to its high isoelectric point (~9.5), chemical stability and good electrical conductivity makes it suitable for electrochemical biosensing applications [35], [36]. Chemical stability and biocompatible nature of ZnO nanostructures allows it to be interfaced with several chemical and biological fluids with varying pH levels [37]. Thus, leveraging the unique properties of ZnO nanostructures, we have developed a stable and sensitive electrochemical biosensing device for the detection of PTH.

As previously discussed, the current PTH detection techniques require large sample volume and lack specificity, sensitivity, and quick response time. Hence, our focus is to overcome the technological gap in sensor development for PTH by designing a highly specific sensor for the clinically relevant diagnostic range as a POC device using ZnO nanostructures. The emphasis of this work contributes to the specificity aspect of the nanobiosensor towards validation of the target PTH molecule within complex human biofluids such as serum, plasma, and WB. Subtle biomolecular interactions occurring at the electrode-solution interface is captured by the powerful EIS technique to exemplify the target PTH concentration. In this work, for the first time, we demonstrate rapid and specific PTH screening as a POC device in undiluted HS,

plasma and WB using non-faradaic EIS towards real-time monitoring in a surgical environment using single drop sample (<40 µL).

2.4 Materials and methods

2.4.1 Chemicals and reagents

Hydrothermal growth precursors- zinc nitrate hexahydrate (Zn (NO3)2·6H2O) and hexamethylenetetramine (HMTA) were obtained from Thermo Fisher Scientific (MA, USA) with 99.5% purity. Thiol cross-linker molecule DSP and its solvent dimethyl sulfoxide (DMSO) were procured from Thermo Fisher Scientific (MA, USA) along with SuperBlock (PBS) blocking buffer, used as a blocking agent. Monoclonal PTH antibody and recombinant PTH protein were obtained from Thermo Fisher Scientific (MA, USA). Phosphate buffered saline (PBS) was procured from Thermo Fisher Scientific (MA, USA) and was used to prepare aliquots of stock PTH antibody and target molecule concentrations. Pooled HS, for recombinant PTH dilutions, was purchased from Fisher scientific (MA, USA). Pooled plasma (lithium heparin) was procured from Innovative research (MI, USA). WB was purchased from Carter BloodCare (Bedford, TX) in EDTA-additive tubes. Hormones for cross-reactivity studies were Cortisol, obtained from Abcam (Cambridge, MA, USA), Parathyroid Hormone-like related protein (PTHrp) and Adrenocorticotropic hormone (ACTH) were obtained from Fitzgerald Industries International (Acton, MA, USA). All dilutions were prepared in undiluted HS, plasma and blood for respective calibration dose response experiments.

2.4.2 Sensor assembly and measurement

The sensor was fabricated using thin film fabrication technique on flexible polyimide substrate. The sensors were cleaned with acetone, isopropyl alcohol (IPA) and deionized water (DI) in an ultra-sonic bath and dried under nitrogen to remove any impurities from the surface. Selective deposition of a thin ZnO seed layer (30±20 nm) on a working electrode was performed using RF-Magnetron sputter technique. The seed layer acted as a site for nucleation of ZnO nanostructures growing in a uniform direction following hydrothermal growth technique. The precursors-(Zn (NO3)2·6H2O) and HMTA were dissolved in equal proportions in DI water with optimized parameters as described in the literature [38]. To confine the fluid onto to the sensing region, polydimethylsiloxane (PDMS) encapsulate was attached on the flexible sensor substrate using water resistant silicon adhesive.

2.4.3 ATR-FTIR spectroscopy

ZnO functionalized surface was characterized using attenuated total reflectance Fourier transform infrared (ATIR-FTIR) spectroscopy using 6700 FTIR spectrometer. The spectrometer was equipped with a deuterated, triglycerine sulphate (DTGS) detector with a validation motor and a KBr window. VariGATR sampling stage was fitted with a 65° Germanium ATR crystal, holding the sample with a swivel clamp. Germanium crystal was used for characterization for its highest refractive index. FTIR samples were prepared by sputtering the glass slide with ZnO on a thin film of gold (Au). Prior to use, the sample glass slide was cleaned thoroughly with isopropyl alcohol and deionized water to remove any surface bound impurities. DSP functionalized ZnO samples was rinsed with DMSO, dried with

nitrogen and stored with desiccant beads until measurement. To characterize binding of PTH antibody, the DSP functionalized ZnO surface was washed with PBS and incubated with PTH antibody for two hours at room temperature. PTH antibody functionalized glass slide was dried with nitrogen prior measurement. Each FTIR Spectrum collected for the DSP functionalized ZnO sample and PTH antibody functionalized DSP represents the scan range between 400-4000 cm^{-1} with an average of 256 scans at 4 cm^{-1} resolutions.

2.4.4 Parathyroid hormone sensor calibration

To achieve label-free affinity based biosensing, 40 uL of 10 mM DSP cross-linker molecule was incubated at room temperature for 90 min in the dark. DSP chemi-sorbs on the ZnO surface by forming a strong thiol bond at the electrode surface. The other end of DSP consists of N-hydroxysuccinimide esters (NHS) active group which allows for interaction with primary amines of the target PTH antibody forming a covalent amide bond that results in the release of N-hydroxysuccinimide. The sensor was functionalized by dispensing 40 uL of 10 µg/mL highly specific α-PTH monoclonal antibody prepared in PBS and incubated for 2 hours at room temperature. The monoclonal antibody used is directed towards the N-terminal 1-34 amino acids, which is the active part of the molecule. It can also detect intact 1-84 PTH. To eliminate non-specific binding interactions, the unbound DSP vacant sites were blocked by incubating with SuperBlock for 15 minutes at room temperature. PBS was used to wash the sensor surface to remove excess remaining solution. Blank HS measurement was considered as baseline for further analysis. Aliquots of serially diluted PTH concentration in HS was added post blank measurement starting from lowest concentration (1 pg/mL) to highest (1000 pg/mL), with an incubation period of 15 minutes at room temperature for building the calibration dose response

curve. Excess fluid from the sensing region was removed by performing wash steps after each dose with the HS for the experiment. Identical protocol was followed for detection of PTH in plasma and WB. Dose response experiment for PTH in plasma was performed in the range 10 - 400 pg/mL. A sample volume of 40 uL was used consistently for all the experiments. Gamry Reference potentiostat 600 (Gamry instruments, PA) was used to perform electrochemical measurements over a frequency range of 1 Hz to 1 MHz at 10 mV AC voltage. EIS is a powerful technique used to analyze and decouple complex electrochemical systems as it is sensitive to changes that occur at the electrode-solution interface that provide information on binding events [39]. All EIS experimental data is represented for n=3 replicates unless mentioned specifically.

2.5 Results

This work evaluates the performance of an affinity-based sensing platform for detection of PTH in pooled HS (HS), plasma and WB. DSP cross-linker was used to functionalize capture probe-PTH antibody on ZnO electrode surface. Binding of the PTH antibody with the target PTH analyte was quantified using EIS to capture physicochemical change at the electrode-solution interface. This section focuses on (i) Electrode surface characterization towards establishing a functional surface suitable for PTH sensing through affinity capture mechanisms (ii) Baseline characterization of sensor platform to establish electrode stability (iii) Optimization of PTH antibody concentration and characterization of functionalized assay (iv) Evaluation of sensor performance through calibration dose response and (v) Translatability towards clinical applications.

2.5.1 Electrode surface characterization towards establishing a functional surface suitable for PTH sensing through affinity capture mechanisms

Fig. 2.1 represents a schematic illustration of the immunoassay building process for the affinity-based nanobiosensor. An important characteristic of a biosensor is to establish a stable immunochemistry. Techniques including SEM, Energy Dispersive X-Ray Analysis (EDAX) and FTIR were used to characterize and validate the functional surface suitable for stable biosensing. The active sensing region on the sensor platform is a hybrid composite of nanotextured Au and nanostructured ZnO on a flexible polyimide substrate. Several researchers have shown the effective use of ZnO nanostructures which leverages enhanced sensitivity due to size-based matching with increased surface area particularly for biosensing [12], [40].

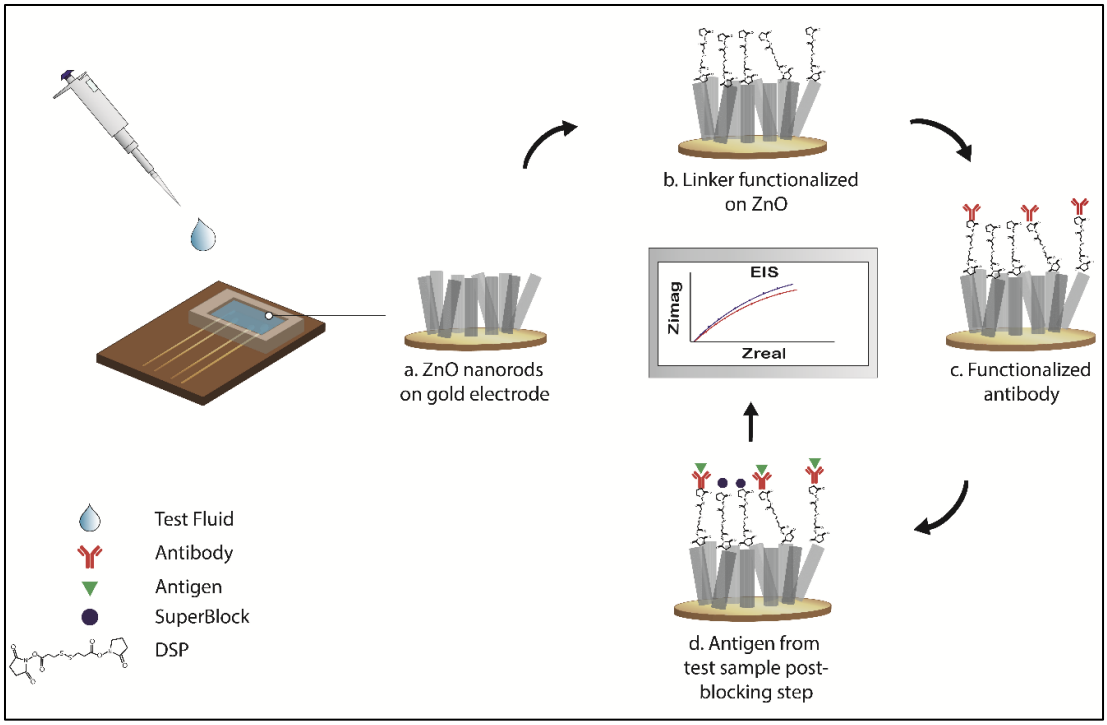

Figure 2.1. Schematic representation of the immunoassay building process for the PTH biosensor. DSP: Dithiobis succinimidyl propionate.

Fig. 2.2 (A) represents an SEM image of the hydrothermally grown ZnO nanostructures aligned vertically in a uniform manner due to pre-seeded ZnO thin film. The average height of the hexagonally shaped rod like structure was measured to be 250±20 nm with a diameter of 85±10 nm. The uniform growth distribution of nanostructures increases sensitivity of detection as it controls the mass transport and diffusion of the target analyte (PTH) at the electrode-electrolyte interface [41]. Fig. 2.2 (B) represents EDAX spectra of the electrode sensing interface shown in the SEM micrograph. The elemental identification of the sensor region is represented with energy level of 8.6 keV corresponding to K shell of ZnO and 9.72 Kev corresponding to L-shell of Au which confirms presence of both ZnO and Au on the electrode substrate.

Fig. 2.2 (C) represents ATR-FTIR spectra of the ZnO modified sensor surface between 1200 cm-1and 1900 cm-1. The results in Fig. 2.2 (C) (i) displays the spectra for the ZnO nanostructure functionalized with DSP crosslinker through thiol chemistry, providing binding sites for antibody immobilization. The first part of the spectrum indicates the presence of symmetric carbonyl stretch of NHS ester in DSP, confirmed by the peak observed at 1785 cm-1 [42]. The peak observed at 1316 cm-1 indicates symmetric C-N-C stretch of DSP. The peak at 1653 cm-1 is observed due to stretching vibration of C=O. Peak observed at 1743 cm-1 indicates free carboxylic acid present in DSP. These results confirm binding of DSP cross-linked with ZnO functionalized surface. In Fig 2.2 (C)(ii) disappearance of the peak at 1743 cm-1 demonstrates cleaving of NHS ester by breaking C-O bond in DSP where the primary amine of PTH antibody is bound through the process of aminolysis [43]. Stability of the antibody conjugation to DSP was confirmed by the shift in peak 1654 cm-1. These results confirm that PTH antibody was bound to DSP functionalized ZnO surface allowing for target PTH sensing through affinity capture mechanism.

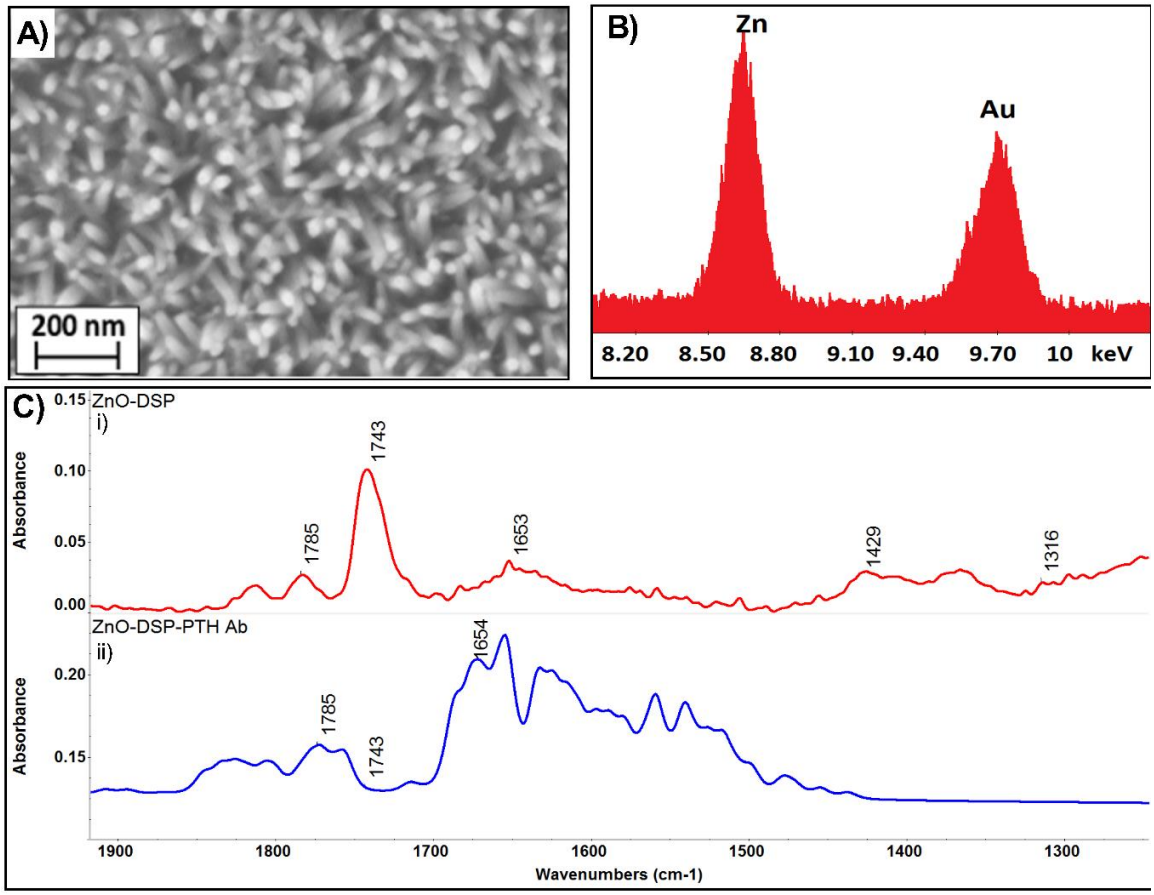

Figure 2.2. (A) SEM image of uniform ZnO nanorods selectively grown on working electrode of the developed biosensor (B) EDAX spectra of the biosensing platform. (C)(i) ATR-FTIR spectra of DSP functionalized ZnO surface (ii) ATR-FTIR spectra of PTH antibody immobilized on DSP. DSP: Dithiobis succinimidyl propionate; PTH: Parathyroid hormone.

2.5.2 Baseline Characterization of Sensor Platform to Establish Electrode Stability

Establishing a stable electrochemical baseline is essential for obtaining robust performance during biosensing. Hence, baseline characterization for the ZnO nanostructured electrochemical sensor was performed using open circuit potential (OCP) and single frequency EIS in the presence of three matrices: PBS, HS, and WB for this study. OCP refers to the potential difference between working and reference electrode in the absence of an input current. This was measured at 10 mV for 1200 s. For PBS buffer, steady state OCP was

measured at -0.02 V, whereas for HS it was at -0.82 V and for WB it was -0.04 V as seen in Fig. 2.3 (A). Negative potential indicates thermodynamic stability where the electrode does not take part in oxidation. Additionally, the presence of ZnO semiconducting material at the electrode interface, induces a negative potential due to variation in charge carrier density [44]. Furthermore, the shift in potential is attributed to the polarities of the constituents of the buffer matrix. In the case of PBS, the presence of the phosphate ions is the key driver for slightly negative potential. An increase in potential is observed in HS to compensate for the highly resistive protein constituents present. The presence of anti-coagulant (Ethylene Diamine Triacetic Acid) in WB minimizes the resistive effects of red blood cells (RBCs) and protein constituents hence, its potential is relatively close to zero at -0.04 V. On addition of a given buffer matrix, the potential reaches a steady state within 1200s. OCP response indicates whether the electrode material is in equilibrium with the electrolyte. A stable OCP response implies that equilibrium has reached between electrode surface and the added buffer (PBS, HS, and WB). Hence, these results indicate the stability of the sensing electrodes in the presence of PBS, HS and WB. Fig. 2.3 (B) represents single frequency EIS at 100 Hz to demonstrate electrochemical characterization of the sensor over time for the given buffer matrix. Frequency of 100 Hz was selected to gain maximum signal response. Single frequency EIS is used to follow changes in electrochemical response against time. A steady-state Zmod impedance (modulus of real and imaginary components of impedance) of 5.7 kΩ was obtained for PBS, whereas 6 kΩ was measured for HS. The impedance value was stable at ~9 kΩ over 1200 s for WB. Steady electrochemical response for all the measured buffer matrices indicates stability of the sensor for biosensing on the ZnO nanostructured surface. Furthermore, these baseline

characterization experiments were performed to understand the inherent nature of the electrode-electrolyte behavior in the absence of target PTH analyte.

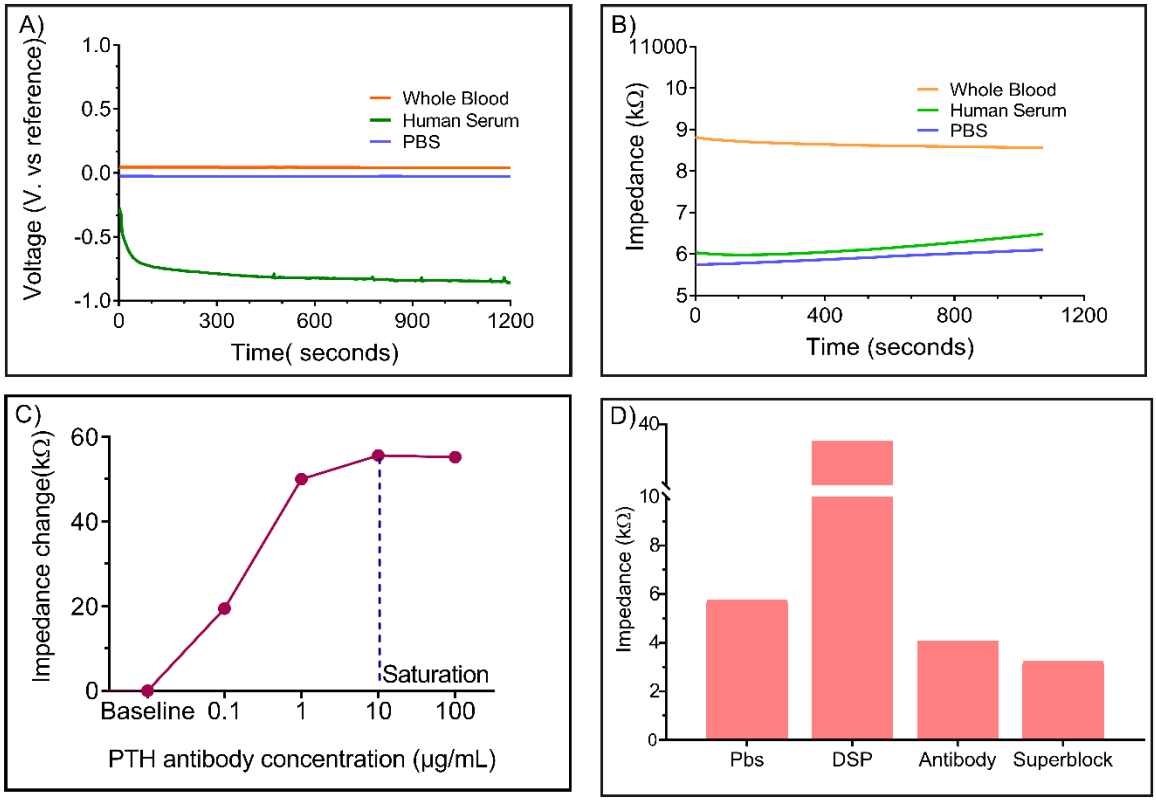

Figure 2.3.(A) Electrochemical characterization of sensing platform by measuring open circuit potential with PBS, HS and WB. (B) Single frequency EIS measurement for PBS, HS and WB. (C) Antibody saturation study on DSP functionalized surface. (D) Impedance response for baseline assay characterization of the immunoassay. DSP: Dithiobis succinimidyl propionate; PBS: Phosphate-buffered saline; PTH: Parathyroid hormone.

2.5.3 Optimization of PTH antibody concentration and characterization of functionalized assay

Antibody saturation study was performed to evaluate the optimal concentration of the antibody required to completely saturate the DSP functionalized ZnO surface. It is essential to saturate the DSP functionalized binding sites to minimize non-specific binding and maximize signal to

noise ratio [45]. The sensor was dosed with increasing antibody concentration starting from 0.1-100 µg/mL. Prior to introducing PTH antibody onto the sensor surface, blank PBS measurement post-DSP functionalization was considered as baseline for analysis. Change in impedance from baseline was measured for each concentration and a dose dependent trend was observed, until the sensor reached saturation as seen in Fig. 2.3 (C). The change in impedance was similar at 10 and 100 µg/mL. This further indicates that any concentration above or equal to 10 µg/mL was sufficient to saturate the available binding sites at the electrode surface. This is because no significant change was observed after 10 µg/mL even with increasing concentrations of antibody until 100 µg/mL. Therefore, 10 µg/mL was chosen as the optimal concentration required to saturate DSP-functionalized sensor surface.

Fig. 2.3 (D) represents the impedance response for each step of the immunoassay functionalization on the sensing platform. Prior to any surface functionalization, blank PBS buffer impedance was 5.7 kΩ. The conducting ions present in PBS contribute to this impedance value. Post functionalization with DSP linker, the impedance response increased to 37 kΩ. The increase in impedance is attributed to the resistive nature of DSP dissolved in an inorganic solvent DMSO. Furthermore, DSP contains thiol functional group that binds to the vacant Zn site, thus forming a Zn-S bond, indicating conjugation on the sensor surface [47]. When PTH antibody is introduced on the sensor platform, the primary amine of the PTH antibody binds to NHS ester of DSP resulting in decrease in impedance to 4.1 kΩ. Confirmation of the antibody conjugation was validated by performing three PBS washes post antibody immobilization and measurements were taken. No significance was observed between PBS

washes, thereby indicating successful chemical conjugation of PTH antibody onto the DSP functionalized electrode surface [46]).

Post-antibody immobilization, further decrease in impedance was measured as superblock was used to block unbound DSP linker sites. The signal contribution of non-specific binding was also minimized by blocking the vacant DSP sites [48]. The impedance response at each step validates the successful functionalization of the immunoassay. Impedance response can further be validated using the simplified Randles circuit [46].

2.5.4 Sensor performance evaluation through calibration response for PTH in HS, plasma, and whole blood

The affinity-based sensor performance was evaluated using non-faradaic EIS for the detection of PTH in HS, plasma and WB. Non-faradaic EIS is an effective technique to capture binding phenomenon occurring at the electrode-solution interface. An electrical double layer (EDL) is formed when a charged electrode surface comes in contact with an electrolyte. Thickness of the EDL (or dielectric permittivity) at the electrode/solution interface is modulated due to binding of the target analyte with the capture probe (PTH antibody) and a capacitive change is induced [49], [50]. This is observed typically in the lower frequency regime <1 kHz [51], [52]. Similarly, when the PTH spiked in HS (or plasma and WB) interacts with the antibody functionalized ZnO semiconducting electrode, it results in modulation of charges within the EDL that contribute towards change in impedance. Fig. 2.4 (A) represents Nyquist plot of real impedance versus imaginary impedance over a frequency range of 1 Hz- 1 MHz for target PTH concentrations from 1 -1000 pg/mL spiked in HS. The region closer to the origin in the graph

represent the impedance in high frequency regime (1 MHz) while the region further away from the origin represent impedance from low frequency regime (1 Hz).

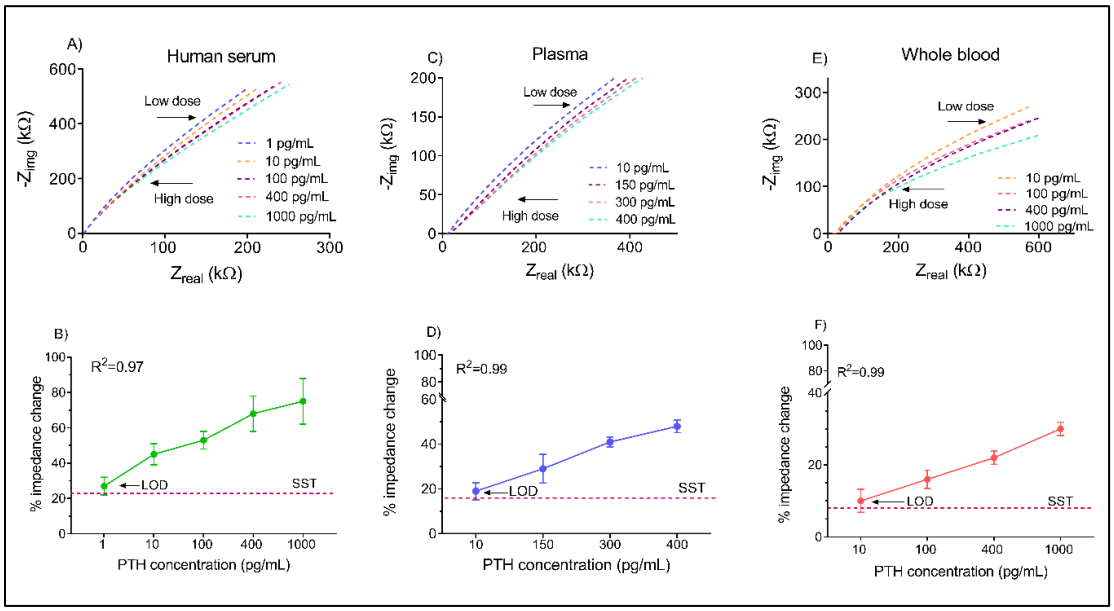

Figure 2.4. EIS response for detecting PTH in various buffers. Nyquist plots representing dose dependent change in impedance indicating binding activity in (A) Human Serum (C) Plasma and (E) Whole blood. Calibration dose response represented as percentage change in impedance for PTH spiked in (B) human serum (D) plasma and (F) whole blood. PTH: Parathyroid hormone.

PTH dose concentrations was introduced serially starting from lowest concentration (1 pg/mL) to the highest concentration (1000 pg/mL) on the PTH antibody functionalized electrode surface. The concentration range was chosen based on physiological range of clinical relevance. Binding events of PTH was characterized based on the changes measured in the output impedance response. The first part of the Nyquist in the high frequency region signifies solution resistance (Rsol) which refers to the resistance offered by the bulk ionic contents in HS. The second part of the Nyquist in the low frequency region resembles a large incomplete semi-circle indicative of a typical non-faradaic system. Typically, the relationship between

impedance and Cdl can be represented as 1/(2π×f×(impedance)). A decrease in imaginary part of impedance (Zimg) is observed with increasing PTH concentrations. This decrease in impedance was quantitatively observed as a function of binding of PTH capture probe and target PTH complex at the electrode interface which results in increased double layer capacitance (Cdl) caused due to charge perturbation within the EDL, typically observed in the low frequency regime. This can further be observed as a shift of incomplete semicircle towards the right in the Nyquist plot of Fig. 2.4 (A) where with increasing dose concentration, the impedance decreases. Furthermore, increase in Cdl is further verified by capacitive phase angle modulations between -60° to -80° in frequency region between 1 Hz to 100 Hz represented in supplementary Fig. 3 [46]. Maximum signal was observed at 100 Hz and hence, 100 Hz was chosen to represent all PTH analyzed data. Similar dose dependent behavior was observed for plasma and WB as seen in Fig. 2.4 (C) & (E).

Calibration dose response (CDR) for PTH in HS, plasma and WB is represented in Fig. 2.4 (B), (D) and (F) respectively as change in impedance response from baseline. The CDR curve is plotted as percent change in impedance for varying PTH concentrations, represented using the equation:

$$\%\ \text{change in}\ impedance = \frac{(Z_{baseline} - Z_{dose})}{(Z_{baseline})} \times 100$$

The percentage change in impedance varied from 27% (±5) to 75% (±13) for the PTH concentration range of 1 pg/mL to 1000 pg/mL in HS as shown in Fig 2.4 (B). Specific signal threshold (SST) also called as the noise threshold was calculated to be 22%. The smallest detectable concentration above the SST is the LOqD. The LOD for PTH in HS was found to

be 1 pg/mL with a linear dynamic range of 1- 1000 pg/mL. A coefficient of determination R^2 = 0.97 was obtained for PTH spiked in HS.

Similarly, sensor performance metrics for PTH in plasma is represented as percent change in impedance from baseline as seen in Fig. 2.4 (D). The change in impedance varied from 19% (±4) to 48% (±3) for varying PTH concentrations spiked in plasma. SST was calculated to be 13% and signal was established well above the noise threshold. The LOD for PTH in plasma was 10 pg/mL with a linear dynamic range of 10-400 pg/mL. A R^2 value of 0.99 was obtained for PTH spiked in plasma. To show proof-of-feasibility towards clinical translation, performance of the nanobiosensor was also evaluated in WB. Fig. 2.4 (F) represents CDR of the sensor for PTH spiked in WB. A total change in impedance of 30% was obtained from baseline for PTH ranging from 10 -1000 pg/mL. SST was obtained to be 8% with the LOD being 10 pg/mL for PTH spiked in WB. An R^2 value of 0.99 was obtained for PTH spiked in WB. The sensor performance metrics computed for PTH calibration in HS, plasma and WB is shown in supplementary Table S2 [46].

As observed from these results, a dose dependent increase in impedance change is indicative of binding of target PTH to the antibody immobilized surface within the electrical double layer. Charge distribution at the EDL is perturbed due to this binding phenomenon, which is reflected in Zimg of EIS response. These impedance changes can be attributed as double layer capacitance modulation since the phase angle is capacitive in the low frequency region (1-500 Hz) as shown in bode phase plot (supplementary Fig. S3 [46]).

This impedance behavior is comparable across all the three biological sample matrices, thereby retaining the performance metric of the nanobiosensor. The LOD of HS is 1 pg/mL

and 10 pg/mL for plasma and WB. We hypothesize the LOD for plasma & WB is pushed to 10 pg/mL due to the interference of anti-coagulants. However, this does not limit the sensing performance as the reported LOD for all three buffers is in agreement with Clinical and Laboratory Standards Institute (CLSI) guidelines [53]. Supplementary table S1 [46] compares the present work with other biosensors for the detection of PTH. It is observed that incorporating ZnO modified nanostructures on the sensing electrode surface enhances the sensing metrics of the target PTH biomolecule.

The ability of a biosensor to detect specific signal response is crucial in validating its reliable performance. Once the sensitivity metrics of the nanobiosensor was characterized, the sensor was challenged to test for specificity. This was evaluated by testing the PTH capture probe immobilized sensor surface against reactive non-specific molecules such as cortisol, PTHrp and ACTH spiked in HS at a very high concentration of 1000 pg/mL. These hormones were chosen for their anatomical and clinical implications. High cortisol and ACTH levels increase as a part of the body's response to surgical trauma, whereas PTHrp is elevated in patients with malignancy associated hypercalcemia and for its structural homology with PTH. The impedance response of the non-specific cross-reactive molecules was compared with dose response of PTH as represented in Fig. 2.5 (A). The starting impedance value (baseline) for specific (PTH) and non-specific (PTHrp, ACTH and Cortsiol) biomolecules was about ~4278±200 Ω. The percent impedance for all the tested biomolecules were calculated with respect to this baseline impedance value. Cortisol showed a maximum change of 25% while ACTH showed a maximum change of 19%. Impedance response for PTHrp was measured to be 31%. The structural similarity of PTHrp to the PTH biomolecule could contribute towards

a slightly high signal. However, even with such high concentration of the cross-reacting molecules, the maximum change in impedance was less than impedance change for specific PTH molecule with 10 pg/mL (low concentration). The impedance change measured for all the non-specific biomolecules was about 18-31%. Whereas the specific PTH signal associated with binding caused a significant change in impedance of 45-75%. Therefore, the impedance change caused due to the non-specific molecules (ACTHT, PTHrp and Cortisol) is much lower than the specific PTH. Since, the starting baseline impedances are in the similar range for both specific and non-specific molecules, the percent impedance change has been used as a quantifiable metric. Furthermore, it can be observed that the impedance response for the non-specific biomolecule is below the noise threshold. While for specific PTH signal (≥10 pg/mL) is well above the calculated noise threshold. Therefore, the impedance change caused due to the non-specific biomolecules is insignificant as compared to specific PTH signal. This confirms, the developed sensor platform is specific to target PTH molecule and can be detected reliably in complex biological medium using non-faradaic EIS with minimum interference from other non-specific biomolecules tested in this study.

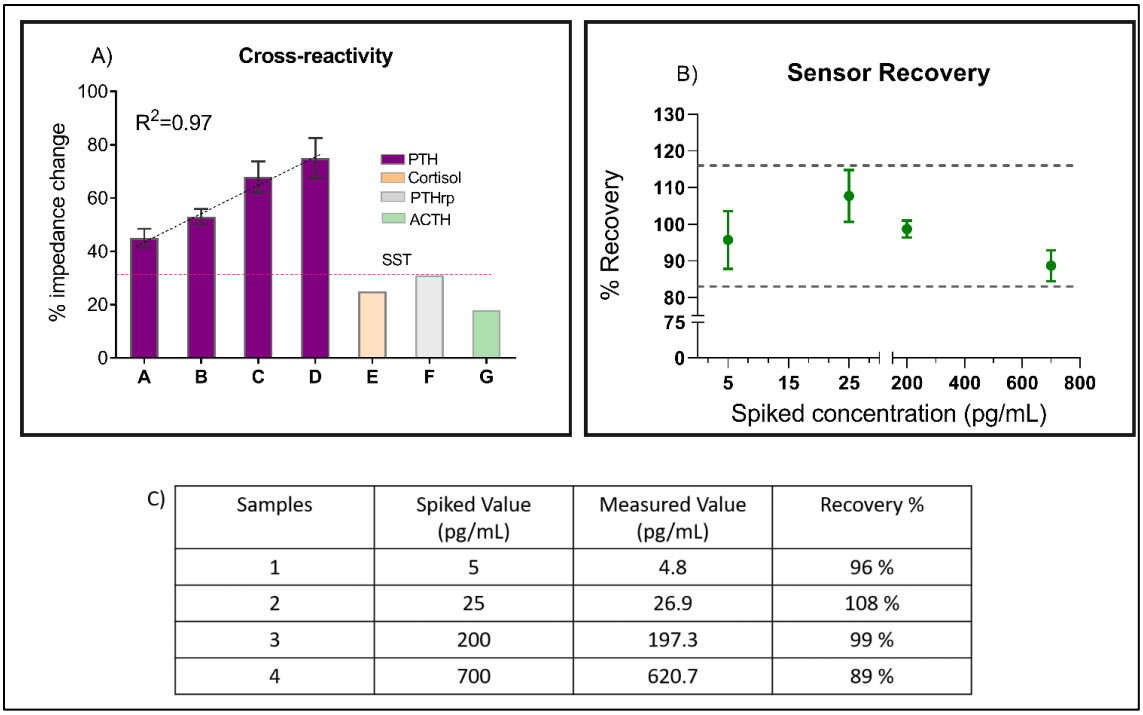

C)

Samples	Spiked Value (pg/mL)	Measured Value (pg/mL)	Recovery %
1	5	4.8	96 %
2	25	26.9	108 %
3	200	197.3	99 %
4	700	620.7	89 %

Figure 2.5. (A) Selectivity of biosensor evaluated with cross-reactivity study represented as percentage change in impedance. Calibration dose response for PTH indicated on the x-axis (A=10 pg/mL, B= 100 pg/mL, C=400 pg/mL and D= 1000 pg/mL). Cross reactivity tested on PTH immobilized surface for E= Cortisol, F=PTHrp and G=ACTH. Each at 1000 pg/mL concentration (B) Sensor recovery measured for four PTH samples spiked in Human Serum (C) Table indicating percentage recovery for PTH in Human Serum. ACTH: Adrenocorticotropic hormone; PTH: Parathyroid hormone.

2.5.5 Sensor performance evaluation towards translating for clinical application

To establish efficacy and proof of feasibility towards clinical translation as a POC device, the nanobiosensor was evaluated for (i) sensor recovery analysis and (ii) patient plasma sample evaluation. Four random concentrations were spiked in HS and the results were compared with the previously established calibration curve. Results in Fig. 2.5 (B) demonstrates the sensor recovery rate between 89- 108%. The recovery of each sample is similar to the added concentration of PTH in HS. This confirms the ability of the biosensor to reliably determine PTH in HS samples.

After establishing accuracy of the nanobiosensor, four unknown patient plasma samples were tested to validate the performance of the sensor against Roche-lab standard PTH analyzer. Unknown patient samples were dispensed directly on the functionalized sensor without dilution and concentrations were determined from the developed calibration curve. Regression analysis was used to correlate the concentrations reported by both nanobiosensor and the Roche analyzer. As represented in Fig. 2.6 (A), a linear relationship between nanobiosensor and Roche analyzer was obtained, with the regression equation being y=0.0763x+31.96. The coefficient of determination, R^2= 0.99 was achieved for the regression analysis. Additionally, Bland-Altman analysis was performed to evaluate the agreement between the nanobiosensor and the Roche analyzer in determining the PTH concentration in patient samples. Fig. 2.6 (B) shows the percentage mean difference between Roche analyzer and the nanobiosensor vs mean concentrations of Roche analyzer and nanobiosensor. In a Bland-Altman plot, the two test methods are said to be in good agreement when the mean difference for the measured samples lie within ±1.96 SD. The mean bias value of 1.736 % or 11.4 pg/mL indicates no significant difference between the two test methods. The mean difference at lower concentrations (~30 pg/mL) varied by ~14% while the mean difference at higher concentrations (~ 365 pg/mL) was ~5%. The range of mean difference values between the two methods obtained for various concentrations are in acceptable range as per Clinical and Laboratory Standards Institute (CLSI) guidelines [53]. As observed in the plot, all measurements except one data point lie within ±1.96 SD of the mean bias. This confirms that the developed nanobiosensor is comparable with and in good agreement with the standard Roche analyzer. Fig. 2.6 (C) summarizes the PTH concentrations obtained from Roche analyzer and the nanobiosensor for

the patient samples. It is observed that the concentrations are similar between the two methods with a coefficient of variation (CV) ≤10 % between the two methods, thereby confirming the ability of the nanobiosensor to reliably detect patient samples comparable to that of the current lab standard.

These preliminary results demonstrate comparable performance of the nanobiosensor to the lab standard Roche analyzer. The advantage of the nanobiosensor is that it uses a single drop of sample (<40 µL) without any pretreatment and has a response measurement time of 5min as compared to larger samples volume (>200 ul), pre-analytical sample processing and analytical time of 20 minutes for the clinical laboratory based PTH analyzer.

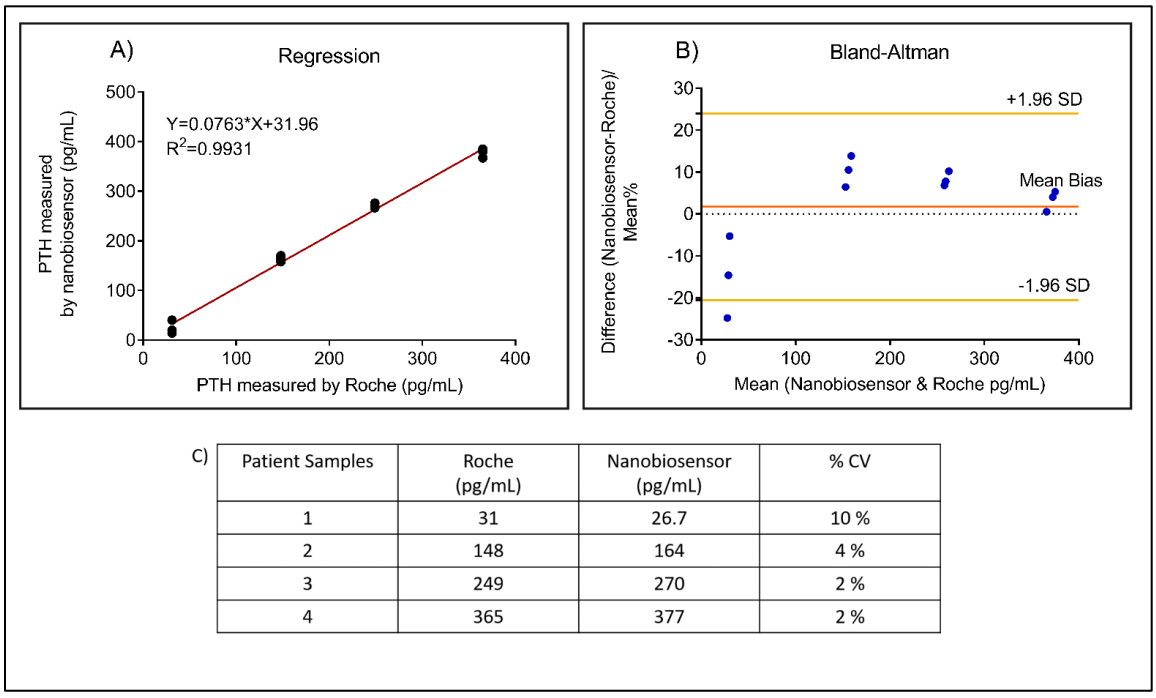

C)

Patient Samples	Roche (pg/mL)	Nanobiosensor (pg/mL)	% CV
1	31	26.7	10 %
2	148	164	4 %
3	249	270	2 %
4	365	377	2 %

Figure 2.6. (A) Regression analysis representing comparison of Roche and developed biosensor for PTH detection using four patient samples (B) Comparison of Roche and developed biosensor using Bland-Altman analysis for four patient samples (C) Table summarizing measured values of PTH concentrations obtained from Roche analyzer and the nanobiosensor for the patient samples. PTH: Parathyroid hormone.

2.6 Discussion

The current methods to detect PTH include chemiluminescence, electrochemiluminescence, time resolved florescence assays, and ELISA based assays. However, these laboratory-based methods require large sample volume, sample preprocessing, and are time consuming. To over these short-comings, we have engineered a robust sensing platform by leveraging the properties of nanostructured ZnO in combination with non-faradaic impedance spectroscopy for developing a rapid, low-sample POC affinity-based PTH biosensor.

Bimolecular detection has been revolutionized using nano-engineered biosensors allowing for highly selective and sensitive detection. Smart engineering techniques permit nanomaterial functionalities to be optimized by designing distinctive features that are significantly different from their inherent bulk properties. Nanoscale aspect allows distinct biomolecular interactions to unwind due to size-based matching. Furthermore, surface modification with nanostructures provides an opportunity to fine-tune the performance characteristics thereby eliminating non-specific interaction, and bio-fouling. Thus, improving the signal to noise ratio.

ZnO has exceptional properties that makes it an ideal semiconducting material for biosensing application. ZnO has a high isoelectric point (IEP) of ~9.5 inducing pH stability at the interface, thereby, creating a conducive environment for biomolecules in any biological fluids.

ZnO nanostructures facilitate enhanced charge transfer mechanism coupled with steady state diffusion. Here in, confinement of PTH molecule on ZnO nanorods prevents steric hindrance. This facilitates charge buildup at the ZnO interface and thus, enhances the signal response. Additionally, mass transport and diffusion of the PTH biomolecule from the bulk solution to the electrode substrate determines the sensitivity of the electrochemical detection system. ZnO

nanostructures with uniform height and density are grown in a highly ordered crystalline orientation as represented in Fig.2.2 (A). This surface modification increases the effective surface area suitable for active functionalization of specific capture probes that enhances sensitivity.

ZnO nanorods were selectively functionalized with highly specific PTH capture probes via a thiol based cross-linker for achieving specific signal response. This strategy reduces signal response from any non-specific physi-adsorption on the nanoengineered biosensing platform. Considering the physico-chemical properties of ZnO nanostructures for electrochemical biosensing, when an electric field is applied, distribution of charges occurs at the ZnO-solution interface to form an electrical double layer. Typically, the binding interactions between the capture probe and target analyte occur within the EDL. The target PTH- capture probe antibody interaction results in subtle changes within the EDL that can be reliably captured using non-faradaic EIS. The modulation of the EDL interface captured by impedance change using EIS is typically modeled as a Randles equivalent circuit (Supplementary Fig. S2 [46]) which is a combination of capacitive and resistive elements.

Non-faradaic EIS is an effective technique that can characterize and differentiate target binding interactions at the surface from bulk solution. Bulk resistance offered by the buffer is represented as the solution resistance (Rs) in the Randles circuit. Due to nanoscale aspect of the sensor, the bulk solution resistance does not have any effect on the electrochemical response at the ZnO electrode- buffer interface. Using non-faradaic EIS, the modulation of the electrical double layer due to binding interactions are captured as a change in the double layer capacitance (Cdl). These binding interactions result in an accumulation of charge at the

interface. The Cdl increases with increase in dose concentrations of the target PTH. Additionally, non-faradaic EIS can capture subtle binding interactions through impedance changes, making it highly sensitive without the need of any sample pretreatment for complex biofluids such as plasma and WB. Furthermore, it is label-free technique that can directly quantify the target PTH concentrations without the use of a redox label. The combination of non-faradaic EIS and ZnO nanostructures can be extremely effective in developing highly specific POC biosensing systems as demonstrated in Fig.2.4 A. This study is the first demonstration of a single drop, label free POC device for specific detection of PTH biomolecule that can aid in surgical screening. The validation of the developed PTH sensor system with Roche lab standard analyzer on a 5 patient samples demonstrates promising results for translation as a POC device for clinical utility.

2.7 Conclusion

This is the first study to our knowledge for detecting PTH as a POC device devoid of sample pretreatment potentially suitable in a surgical setting for reducing delays during surgery hence, improving patient care. We have demonstrated reliable detection of PTH in undiluted HS, plasma and WB using non-faradaic electrochemical biosensing platform. EIS captures binding phenomenon between PTH antibody-target complex at the electrode- solution interface. In comparison to previously reported PTH biosensors [54], [55], the developed sensor demonstrates better performance metrics with LOD of 1 pg/mL in a clinically relevant dynamic range of 1- 1000 pg/mL. Enhanced sensor metrics was achieved by leveraging the unique ZnO nanostructure properties. Selectivity and specificity of the nanobiosensor was validated by evaluating cross-reactive response to cortisol, PTHrp and ACTH. The sensor exhibits 97%

recovery for spiked samples and an R^2 value of 0.99 when validated with patient samples using a clinical laboratory-based analyzer. Further clinical validation with more patient samples is underway to determine the feasibility of the device for a clinical setting. The novelty of the engineered nanobiosensor is its unique combination of incorporating ZnO nanostructures specifically tailored for detecting target PTH molecule with non-faradaic EIS to directly measure in body fluids with a turnaround time of less than 5min using single drop sample volume.

2.8 Future Perspective

The developed POC nanobiosensor unveils the potential as an effective detection modality during parathyroidectomy surgeries. The response time of the developed nanobiosensor is less than 5 min and requires no sample pre-processing. This would significantly reduce the pre-analytical delays caused due to sample transport and preparation as compared to the current central laboratory techniques, enabling it for effective clinical implementation. The results demonstrated in this work provide foundation for future work towards translation in a clinical setting. Further studies with additional patient samples with different clinical scenarios (e.g., Renal dysfunction) in continuation to this work is underway for an in-depth validation towards clinical utility. Furthermore, the intended future purpose of the assay is to examine relative changes in serial samples over a short period of time which may ameliorate unforeseen cross-reactivities.

CHAPTER 3

CLINICAL VALIDATION OF PARATHYROID HORMONE

3.1 Prior publication

Ambalika S. Tanak performed experiments, carried data analysis and data interpretations, and wrote the manuscript. Ambalika S. Tanak, Dr. Shalini Prasad, Dr. Sriram Muthukumar and Dr. Ibrahim A. Hashim co-designed the experiments, and co-wrote the manuscript. Dr. Ibrahim A. Hashim provided the patient samples and provided guidance on experimental designs for assay validation.

This manuscript was published in Scientific Reports Journal in November 2020. The primary goal of this work was to clinically validate the performance of the developed sensor using patient samples for smooth clinical translation. This article is reproduced here by the permission of the Nature Publishing Group. Link to the paper: https://doi.org/10.1038/s41598-020-75856-2

3.2 Abstract

Measuring the PTH levels assists in the investigation and management of patients with parathyroid disorders. Rapid PTH monitoring is a valid tool for accurate assessment intraoperatively. Rapid Electro-Analytical Device (READ) is a POC device that uses impedance change between target and capture probe to assess the PTH concentration in undiluted patient plasma samples. The aim of this work focuses on evaluating the analytical performance of READ platform to Roche analyzer as a prospective clinical validation method. The CV for intra-assay imprecision was <5% and inter-assay imprecision CV was <10% for high (942 pg/mL) and low (38.2 pg/mL) PTH concentration. Functional sensitivity defined at

15% CV was 1.9 pg/mL. Results obtained from READ platform correlated well (r=0.99) with commercially available clinical laboratory method (Roche Diagnostics) to measure PTH concentrations with a turn-around time of less than 15 min. Furthermore, the mean bias of 7.6 pg/mL determined by Bland-Altman analysis, showed good agreement between the two methods. We envision such a sensing system would allow medical practitioners to facilitate targeted interventions, thereby, offering an immediate prognostic approach as the cornerstone to delivering successful treatment for patients suffering from primary hyperparathyroidism.

3.3 Introduction

PTH measurement is essential for the assessment and management of patients with parathyroid gland dysfunction with primary hyperparathyroidism (PHPT), being the third most common endocrine disorder [56]. While most primary hyper parathyroid patients have a single abnormal gland up to 20% of patients will either have multiple adenomas or hyperplasia of all four glands [57]. Surgery is the only curative treatment for PHPT, [58]. PHPT surgical procedures can be challenging and carries ambiguity regarding the presence or absence of the disease in a single or multiple hyperplastic glands [59].

Several imaging techniques provide information about the location of the adenoma as a pre-operative study prior surgery but may not be sensitive to detect multiglandular hyperplasia [60]. Measurement of circulating PTH levels additionally aids in the investigation of calcium disorders [61]. PTH is a single chain 84 amino acids polypeptide produced by the parathyroid gland and in concert with vitamin D and other mediators is responsible for regulating body calcium homeostasis [62], [63]. In addition to diagnosis and management, PTH measurement is essential to guide surgical interventions where due to its short half-life (1-3 minutes) an

intraoperative decline in circulating levels indicates successful surgical resection of a hyperfunctioning adenoma [64]. Laboratory-based assays at best take up to 60 minutes to deliver results from the time sample is received in the central laboratory [25] . During this time, the patient is kept in the operating room while the surgeon waits for results [65]. Additionally, in patients with failed initial surgery, surgical selective thyroid venous catheterization is performed, and resection surgery is repeated several weeks later once laboratory PTH result is available. This highlights the need for a rapid and reliable technique to measure PTH which facilitates point of surgery testing (POST). In addition to the rapid turnaround time, the device must afford specificity for PTH since, the measurement of PTH is complicated by the presence of several molecular forms of the hormone. The intact form being 1-84 amino acids, a mid-molecular form (7-84 amino acid), and a N-truncated form.

Although some assays are termed intact, they also detect the 7-84 fragment, which accumulates in patients with renal dysfunction and thus limits such assays and interpretation. Our previous work established reliable PTH detection in undiluted HS, plasma and WB with a rapid response time [66]. The physicochemical properties of the READ sensor platform captures specific target PTH interaction using EIS as the detection modality. EIS has been incorporated in many POC sensor applications owing to its label-free approach with the least procedural complexity to acquire results [9], [67]–[70]. A major advantage of using EIS technique is its ability to capture subtle electrochemical changes by optimizing input parameters. Impedance sensing has already paved its way into clinical entourage such as blood impedance analysis [71], electrical impedance topography [72] and electrical impedance myography [73].

This work focuses on expanding the previously established scope of research for its use as a clinical utility by validating its results with a standard laboratory analyzer (Roche diagnostic) with 40 patient samples [46]. Our aim is to allow surgeons along with their surgical staff to conduct dynamic PTH measurements during resection of the hyperfunctioning gland procedure without the need for a laboratory technician in a convenient and effective manner to facilitate improved patient outcome.

3.4 Materials and Methods

3.4.1 Analytical Validation

Chemicals & Reagents

DSP was procured for Pierce Biotechnology. DMSO solvent, PBS, SuperBlock along with specific PTH antibody and antigen was obtained from Thermo fisher Scientific. Cortisol for cross reactivity study was procured from Abcam, whereas PTHrp and ACTH were obtained from Fitzgerald Industries.

Sample collection and preparation

Leftover, de-identified discard samples (heparinized plasma) (n=40) were obtained from Clements University Hospital (CUH) and Parkland Memorial Hospital (PMH) from patients being investigated for thyroid dysfunction and undergoing parathyroid surgery between September 2018 & July 2019. The study design and experimental protocols were approved by the University of Texas Southwestern Medical Center Institution Review Board (IRB) number 2020-0373 under which, the requirement for patient consent was waived. All the methods were carried out in accordance with clinical guidelines and regulations. The samples were stored at -20°C until further use. Samples did not undergo >2 freeze/thaw cycles

prior measurement. PTH levels were measured using both Roche diagnostic Cobas analyzer (reference standard) and READ platform.

Rapid Electro-Analytical Device (READ)

The READ POC platform includes a disposable sensor mounted on a handheld electronic reader as explained in detail previously from our group [74]. The sensor surface comprises of a zinc oxide semiconducting layer deposited onto gold electrodes. Fluid confinement on the sensing platform was achieved by fabricating a waterproof silicone barrier using Loctite clear silicone sealant along boundaries of the sensor platform. The assay protocol followed was similar to our previous [46]. Briefly, immunoassay was built on the sensing surface by functionalizing 40 µL of 10 mM DSP (which is a thiol crosslinker) incubated for 90 min in dark at room temperature. Specific monoclonal PTH antibody and antigen (Thermo fisher) was used to build the calibration curve for the sensor. 40 µL of 10 µg/mL PTH antibody was incubated for 120 min at room temperature. Post antibody immobilization, the sensor was incubated with SuperBlock for 15 min to avoid nonspecific binding interaction. PBS wash was used to remove the unbound molecules and baseline measurement was taken. The sensor was functionalized in the same manner until this assay step followed by the validation experiments as explained in the following sections. READ platform measures the impedance change at the electrode-solution interface when the target PTH binds to immobilized capture antibody by EIS technique when a small input voltage (10mV) is applied to the electrode surface.

Assay Performance characteristics

READ platform performance was assessed with laboratory-based analyzer for functional sensitivity, accuracy, precision, specificity, interference, and correlation as follows:

Functional Sensitivity:

Sensitivity was determined following serial dilution of a patient sample with PTH concentration of 493 pg/mL. Doubling dilutions were prepared using pooled plasma as a diluent. Samples were measured in triplicate. Functional sensitivity was determined as the lowest PTH concentration that can be measured with an imprecision of less than 20%.

Accuracy:

Recovery experiments were conducted to determine the accuracy of the assay. Plasma sample procured from innovative research was spiked with PTH concentrations at 50, 250, 500 and 1000 pg/mL. Prepared samples were measured in triplicates.

Precision:

Inter-assay and intra-assay imprecision for READ platform for the PTH analyte in plasma was evaluated using low (38.2pg/mL) and high (942 pg/mL) levels. Each level was analyzed in duplicates with READ platform for a total of 5 days, with a total of 20 samples. Intra-assay, Inter-assay and total imprecision was calculated to identify READ platform precision.

Specificity:

Effect of interferants in plasma was performed to measure specificity of READ platform. Cross-reactive mixture includes cortisol, PTHrp, and ACTH spiked in plasma with varying concentrations in three different ranges (i) low (200 pg/mL per molecule) represented as D in fig 3.7 B, (ii) medium (400 pg/mL per molecule) represented as E in fig 3.7 B and (iii) high (1000 pg/mL per molecule) represented as F in fig 3.7 B. A schematic representation has been included for better visualization in Fig 3.7 B.

3.4.2 Statistical analysis

The data was analyzed and graphed using GraphPad Prism 7(GraphPad Software, Inc.) and Origin. Statistical analysis includes correlation, linear regression, and Bland-Altman analysis.

3.5 Results

A use case scenario is illustrated as a schematic diagram in fig 3.1. Top half of the figure represents the current method used during parathyroidectomy surgery where significant time is expended in sample transit and receiving results to confirm PTH levels determining successful operation. The proposed method specified in the lower half of fig 3.1 reveals an enhanced technique that would assist surgeons to determine complete removal of hyperfunctioning parathyroid tissue from the patient during surgery by assessing PTH concentration within 15 minutes using READ platform.

We had previously demonstrated reliable detection of PTH in undiluted HS, plasma, and WB as a point of care biosensor using EIS. Binding interaction between the target PTH and specific capture probe causes change in impedance occurring at the sensor's electrode interface. The dose dependent change in impedance quantifies the amount of PTH bound to the specific capture probe. Results demonstrated in the previous work provide foundation for the current work to enable effective validation for clinical implementation. This work extends the scope of READ platform to be established for clinical application.

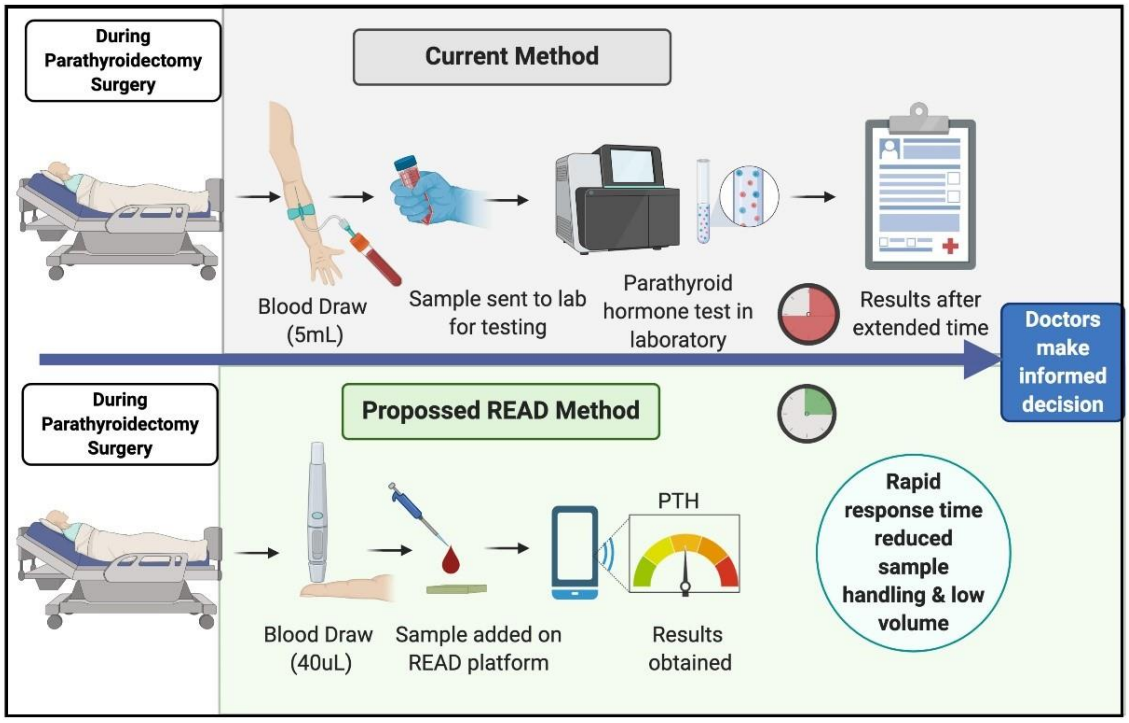

Figure 3.1. Schematic illustration of use case scenario during parathyroidectomy demonstrating ease of use with READ (represented in lower half) as a point of surgery testing (POST) device. Figure created with BioRender.com

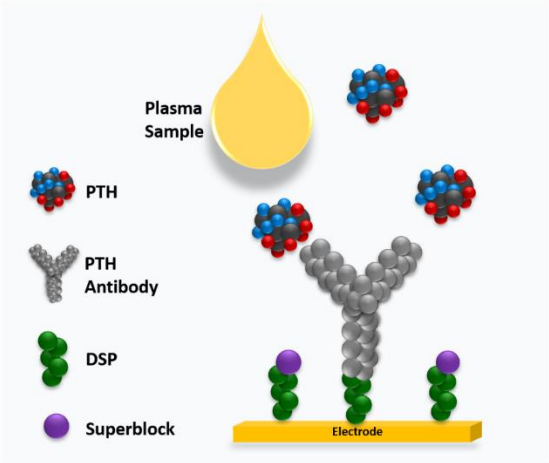

Figure 3.2. Schematic representation of the Immunoassay built on READ platform.

Fig 3.2 illustrates the schematic representation of the immunoassay developed on READ sensor platform using thiol crosslinker chemistry followed by conjugating specific monoclonal

PTH antibody. Calibrated dose response was established for READ platform with varying PTH doses spiked in human plasma.

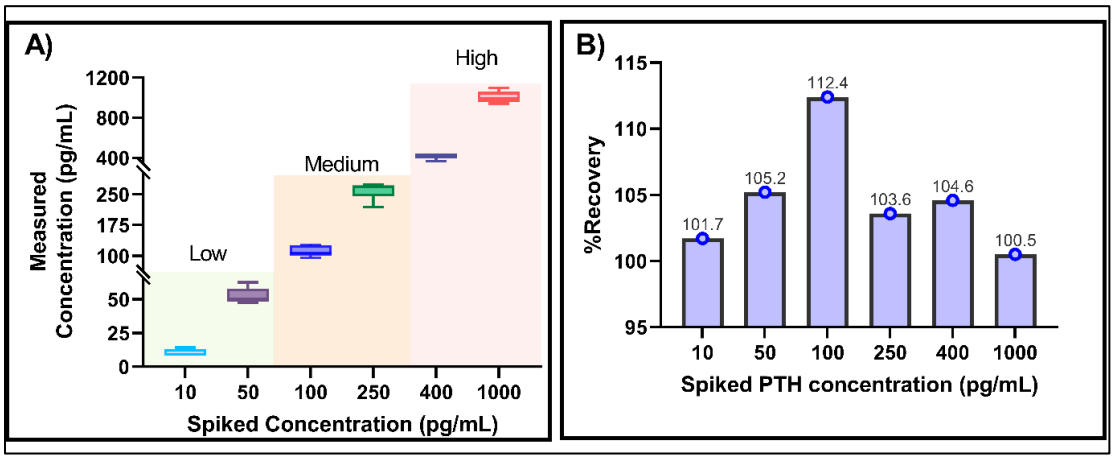

Figure 3.3. A) Varying PTH concentration (Low, medium & high) spiked in plasma samples plotted against measured PTH concentration. B) Recovery analysis for READ platform

Fig 3.3 A represents the dose response of PTH across a wide dynamic range from 10 pg/mL to 1000 pg/mL in human plasma samples. Non-overlapping interquartile ranges for each concentration in the box plots portrays the accuracy of the recovered concentrations with respect to its spiked concentrations, indicating minimum variation among replicates. Analysis of variance (ANOVA) showed statistically significant differences between means across low, medium and high concentrations with p value <0.0001 and an R squared of 0.9940. Recovery percentage for each PTH concentration can be seen in figure 3.3 B across 6 replicates. PTH concentration recovery ranged from 100-112%, with an average recovery of 104.7% ± 4.1, which lies within the acceptable recovery range (80-120% of the expected concentration) as per the Clinical laboratory Standards Institute [75] (CLSI). Furthermore, highest CV percentage achieved was 11.7 %, plotted for each PTH concentration revealed good precision with minimal variation among replicates for READ platform which can be seen in

supplementary figure 1 [76]. Spike and recovered concentrations for PTH have been tabulated in supplementary table 1 [76]. Recovery analysis confirms the ability of READ platform to reliably measure multiple PTH concentrations in spiked plasma samples. READ platform demonstrated a LOD of 1 pg/mL with a clinically relevant dynamic range of 1-1000 pg/mL as previous established in our work [46]. The major focus of this study is to analytically validate the performance of READ platform with the Roche lab analyzer. With that reliable READ sensor performance established, analytical validation was evaluated by following the design of experiments illustrated in fig 3.4 for accuracy and reliability to be useful for effective clinical decision making.

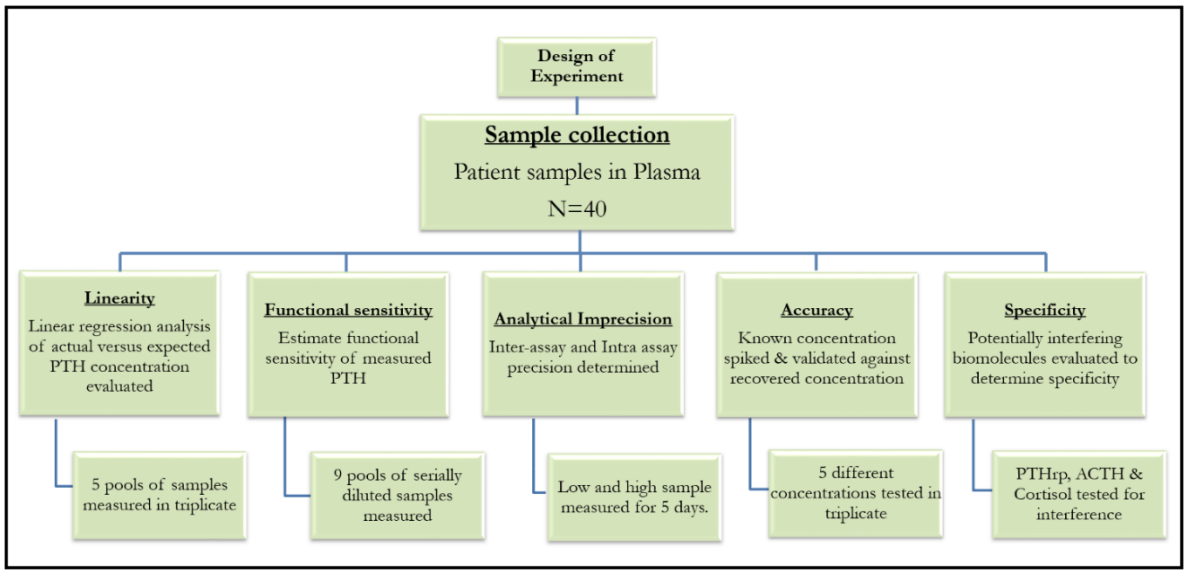

Figure 3.4. Flow chart describing the design of experiment.

3.5.1 Analytical Validation

Method Comparison

The primary goal of method validation is to ensure accuracy of READ platform for the reported results. To clinically validate the performance of READ, PTH concentration was measured in 40 patient samples using Roche analyzer (laboratory standard) and READ platform covering a range from 1 pg/mL to 1050 pg/mL, as represented in fig 3.5 A. Correlation along with linear regression analysis for patient plasma samples compared by the two methods had an intercept of 0.0209, 95% confidence interval (CI), 0.91 to 1.007; slope of 0.96, 95% CI, -15.74 ,15.79 and a Pearson's r of 0.99. Correlation analysis quantified the degree to which PTH measured by both methods were related with a linear relationship. High correlation does not necessarily imply a good agreement between the two methods, thus, Bland-Altman analysis was performed, as seen in fig 3.5 B. In this residual method, difference between two paired measurements was plotted against mean of the two methods. The resulting graph was a scatter plot with x axis represented as the measured mean PTH concentration, while y axis showed difference between the PTH measured using Roche analyzer and READ platform. The bias indicated how series of measurements agreed with the comparative measuring technique. The mean bias between Roche analyzer and READ platform was 7.6 pg/mL. All the sample points were well within the 95% CI (±1.96 SD) except for 4 points. Bland-Altman analysis confirmed overall agreement between the Roche analyzer and the developed READ platform.

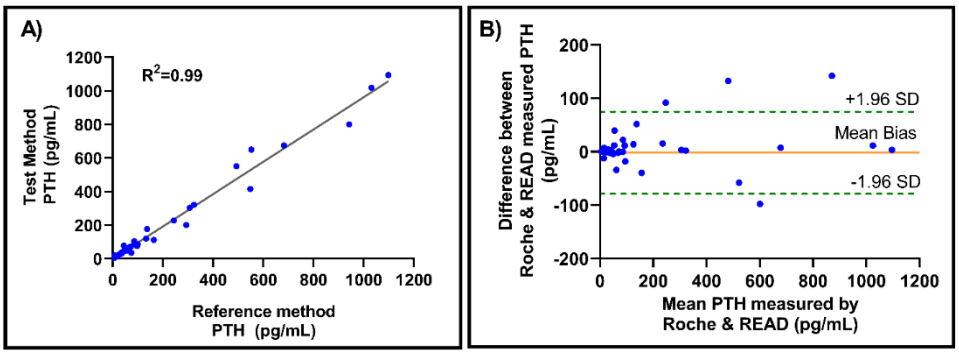

Figure 3.5. A) Reference method (Roche analyzer) compared with Test method (READ platform) using 40 patient plasma samples with a Pearson's r= 0.99. B) Bland-Altman plot compares PTH measured by Roche analyzer and READ platform for 40 patient plasma samples. Orange solid line represents mean bias of 7.6 pg/mL. 1.96 SD is represented as green dotted lines computed at 88.07 pg/mL and -72.77 pg/mL respectively.

Imprecision

Precision was determined by assessing multiple measurements with two patient samples (low and high) within the same day and across 5 days. Precision for READ platform was established in terms of repeatability (intra-assay imprecision) and reproducibility (inter-assay imprecision). The intra-assay and inter-assay imprecision represented as CV for READ was 3% and 8 % for low PTH level (38.2 pg/mL) whereas intra-assay and inter-assay imprecision CV for high PTH level (942 pg/mL) was 3% and 10.5% respectively, as seen in table 3.1. The CV for both low and high level of PTH samples lie well within the clinical standard practice (<20%) as per the Clinical and laboratory standards institute guidelines [77], [78].

Table 3.1. representing the inter-assay and intra-assay variability as measured by READ platform.

Sample	Reported Concentration (pg/mL)	Intra-assay CV%	Inter-assay CV%
Low	38.3	3%	8%
High	942	3%	10%

Functional Sensitivity

Functional sensitivity determines the lowest concentration representing clinical usefulness for a given assay. In this work, the functional sensitivity for PTH was defined at 15% CV with a concentration of 1.9 pg/mL as seen in the precision profile represented in fig 3.6 A. A CV of 20% is widely accepted for being clinically useful according to CLIA requirements [79]. Consequently, a LOD of 1.9 pg/mL was achieved for the PTH assay when measured by READ platform. The outcomes of the pre-clinical validations suggest the ability of READ platform to identify low PTH concentrations directly from undiluted patient blood plasma samples, as a POST device with results acquired under 15 minutes of sampling time.

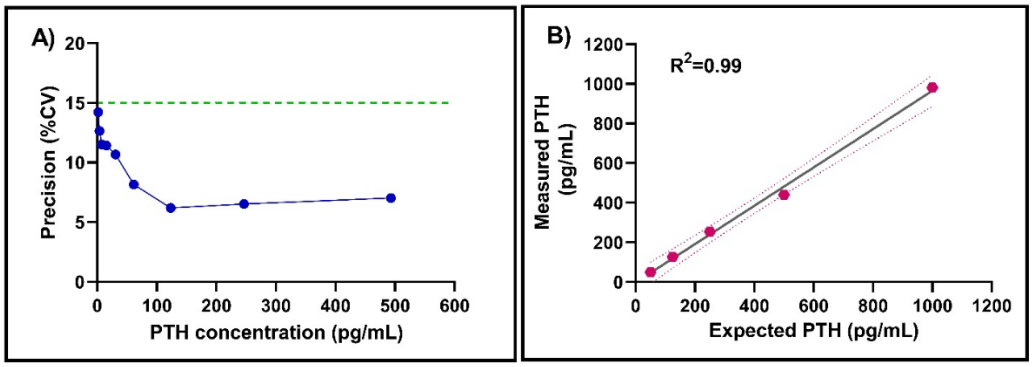

Figure 3.6. A) Functional sensitivity of READ platform. CV defined at 15% and was 1.96 pg/mL. B) Dilution linearity across 5 PTH concentrations were analyzed with an R2 of 0.99 measured with the READ platform.

Linearity

Linearity of the READ platform was assessed to evaluate the accuracy across PTH working range. Linearity of READ platform was achieved when measured PTH results were directly proportional to the PTH concentration in the test analyte. Furthermore, READ platform

demonstrated a linear response for the concentrations tested from 50 pg/mL to 1000 pg/mL as shown in fig 3.6 B with an r2=0.99.

Repeatability

Repeatability study evaluated the closeness of agreement with multiple measures obtained with READ platform. Fig 3.7 A demonstrates the repeatability performance of READ sensor platform by measuring five patient samples across the quantifiable detection range with 13 measurements performed under similar conditions. The repeatability (%CV) for READ platform with patient samples ranged from 11.7 % to 2.6 % for 50 pg/mL and 1000 pg/mL of PTH patient concentration in plasma respectively. This showed that results obtained using READ platform were reliable and repeatable.

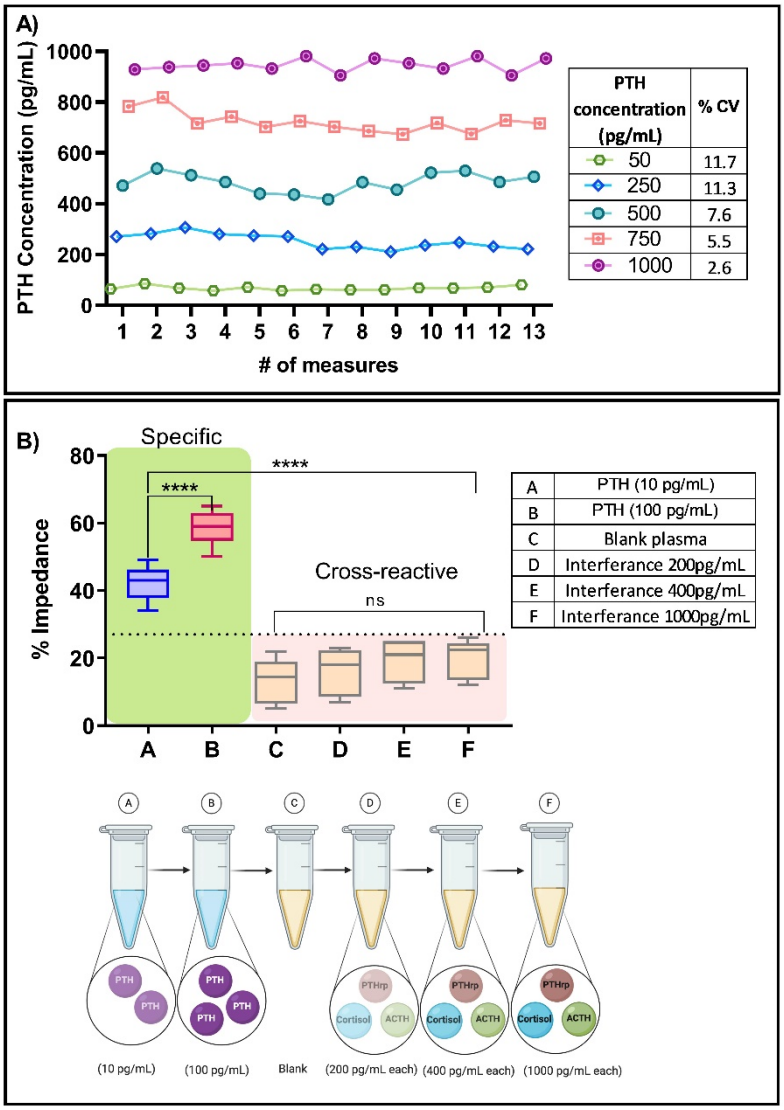

Figure 3.7. A) Repeatability of READ validated across 13 measurements for 5 patient plasma sample. B) Specificity of READ platform where A represents low (10 pg/mL) concentration of PTH, B represents high (1000 pg/mL) concentration of PTH, C represents blank plasma. D, E and F represents cross-reactive mixture of cortisol, Parathyroid hormone related protein (PTHrp) and Adrenocorticotropic hormone (ACTH) biomolecules in low (200pg/mL per molecule), medium (400 pg/mL per molecule) and high (1000 pg/mL per molecule) concentrations respectively. Dotted line represents signal threshold. The pictographic representation of cross-reactive mixtures vials is created in BioRender.com.

Interference

To evaluate selectivity of READ platform towards PTH in the presence of common cross-reacting biomolecules, interreference study was conducted with highest concentration of non-specific molecules like Cortisol, ACTH, and PTHrp. The interference measured from varying non-specific molecules showed no significance when compared with specific PTH dose response. Fig 3.7 B displays specific PTH signal response (A and B) and non-specific response (C, D, E and F) as percentage change in impedance. Specific PTH signal response for the median value as seen in bar A contributes to 43% which is approximately ~1.6 times greater than the non-specific response seen in the highest concentration (1000 pg/mL) of the cross-reactive mixture in F that accounts for 26% impedance change. Furthermore, all the remaining cross-reactive mixtures (C, D, E and F) of varying concentrations lie well within the established signal threshold as indicated by the dotted line and hence can be considered as noise. READ platform was able to significantly distinguish specific PTH concentration from cross-reacting molecules of cortisol, PTHrp and ACTH despite being spiked with high concentration of 1000 pg/mL each.

3.6 Discussion

The utility of intraoperative PTH has significantly improved outcomes, although the success of surgical interventions depends on the surgeon's experience. Typically, during parathyroidectomy, peripheral blood samples collected prior to incision, at incision and 5, 10 and 15-minutes post incision where a 50% decline in PTH indicates successful adenoma resection. Conventionally, results for samples sent to the clinical laboratory are not usually available before all samples are collected and often take up to 60 minutes from the initial

collection. During this time the patient is on the operating table and surgical team awaiting the outcome of the PTH tests. Therefore, availability of PTH results at the point of surgery with a rapid turn-around time for each sample collection will allow surgeons to make immediate informed decisions. This technology has the potential of significantly reducing surgery and anesthesia exposure times. Additionally, a reliable method of PTH measurement is key for the detection of patients with hyperparathyroidism along with successive follow-up monitoring of medical interventions. READ platform fits perfectly in the clinical workflow to allow surgeons to make decisions regarding the success of the surgery using low sample volume without waiting for time consuming results from the laboratory. Therefore, READ platform is designed to report rapid, accurate, and sensitive PTH results addressing the shifting needs and trends of parathyroid surgery in a clinically feasible manner. With an intention to aid surgeons in making rapid informed decisions, an electrochemical READ platform to measure PTH was developed and validated with clinical rigor. This work evinces the importance of determining concordance between laboratory obtained values to READ platform measurements. Moreover, some of the major advantages of READ platform over existing laboratory techniques are as follows (i) READ platform's small form factor diminishes the need for large operational space and reduces storage requirement. (ii) Portable feature of READ platform enhances efficiency as testing can be conducted flexibly at bedside or near the location of patient care. (ii) READ platform eliminates the need for complicated assay preparation steps prior to testing compared to the Roche analyzer making it a lean process (iii) READ platform provides rapid test results with the propensity to expedite clinical decision-making process (iv) As most POC testing with

READ platform can be initiated at patient bedside and conducted quickly, the potential for sample deterioration can be reduced drastically.

PTH levels from 40 patient samples were compared between READ platform and commercially available reference standard (Roche analyzer). The READ platform demonstrated good correlation (r=0.99) with Roche analyzer than the previously reported study (r=0.93) [80]. Bland Altman analysis showed a good overall agreement between the two methods with a mean bias of 7.6 pg/mL. PTH assays for clinical use have to offer wide dynamic range to encompass the entire physiological range. For instance, PTH levels rise above ~500 pg/mL during hyperfunctioning adenoma while post-surgical excision of the hyperfunctioning gland, PTH levels may drop upto ~ 20 pg/mL. The READ platform demonstrates a wide dynamic range from 1-1000 pg/mL which accommodates the diverse PTH levels across patients. Additionally, an important consideration when measuring PTH is the presence of cross-reacting fragments and other hormones with molecular similarities [81]. Successful PTH assay should possess least cross reactivity to minimize the chances of false positive results. Previous studies have shown variability amongst several commercially available PTH assays that demonstrated varying outcomes [82], [83]. This can be attributed to the presence of varying PTH fragments and the presence of structurally similar molecules such as PTHrp in circulation. Predominantly, the liver metabolizes and cleaves most of the (1-84) PTH between amino acid 33 and 36 [84]. Once PTH is metabolized, only the quiescent C-terminal segment of PTH (cPTH), consisting of 35 to 84 amino acids, are released back into circulation [85]. Since, the kidney is responsible to clear the inactive cPTH, patients with kidney dysfunction have elevated cPTH fragments [86], [87]. This may result in inaccurate results for assays that

detect (1-84) PTH. Biological activity is retained by the N-terminal products of PTH metabolism which comprises of first 34 amino acids. To minimize interference from other PTH fragments, we used a highly specific monoclonal antibody directed against the 1-34 bioactive fragment of the PTH molecule. The capture probe functionalized on READ platform is specific to the first 34 amino acid sequence on the amino-terminal end of PTH molecule and does not react with amino-truncated fragments. Furthermore, READ platform was evaluated for interference with PTHrp, Cortisol and ACTH that either have similar structural homology or they are likely to be significantly elevated intraoperatively. The assay showed no cross reactivity (Fig 3.7 B) with PTHrp nor ACTH, or cortisol. The assay can be linearly operated from 50 pg/mL to 500 pg/mL. Additionally, high degree of precision was achieved to facilitate reliable treatment following tumor resection. Imprecision studies confirmed the reproducibility of the assay with a variability (%CV) <10.5%. This level of precision facilitates reliable detection to capture the decline within high PTH levels intraoperatively post tumor resection. The developed READ platform demonstrates rapid results (<15 minutes), a feature that is important when being used intraoperatively. READ does not require any sample dilution thereby, reducing sample processing and handling time. READ is a simple-to-use, handheld electrochemical sensing platform that makes it suitable for intra-operative use. It also allows for immediate further exploration of the resection site if the PTH results did not decline appropriately.

In conclusion, the developed READ platform for the measurement of PTH was evaluated for clinical utility. The wide dynamic range detection capability of READ to report significantly elevated PTH levels seen in patients suspected of hyperparathyroidism can be categorized as

candidates for parathyroid surgery. READ also exhibited good precision across the measurement range and had good accuracy performance which can help to capture low PTH levels post-surgical excision as an effective POST device. Developing rapid POST devices is not aimed to replace clinical laboratory services but supplement them.

CHAPTER 4

SEPSIS

4.1 Prior publication

Ambalika S.Tanak, Badrinath Jagannath and Yashaswee Tamrakar performed literature review, performed experiments and wrote the manuscript. Dr. Sriram Muthukuma rand Dr. Shalini Prasad reviewed and modified the manuscript.

This work was published in Analytica Chimica Acta X in October 2019. Parts of the manuscript has been used in this chapter with appropriate permission form Elesevier. This chapter will discuss the background on sepsis and the need for developing POC device for detection of sepsis. The link to this journal article is https://doi.org/10.1016/j.acax.2019.100029

4.2 Introduction to sepsis

Infectious disorders in human have been described in the medical records dating all the way back to 1000 BC, and pathogenic infection remains the major risk factor of illness and death even today[88]. Sepsis has been known in some form or another in the early years, when it was initially characterized as decomposition of blood and tissues which was indicated by arrival of fever by the Islamic philosopher known as Avicenna. Due to its complicated pathophysiology, sepsis and its treatments have perplexed experts for almost 3000 years, as documented in ancient literature. Previously, it was thought that the predominant source of infection was the gut microbiota[89]. With advanced research findings, Pseudomonas sp. which colonizes and develops infection especially in the respiratory tracts, was identified to be the most linked infection with sepsis[90]. We now know that sepsis is a disease that is remarkably diverse in both its etiology and progression. For instance, sepsis can be triggered by a variety of

organisms, including bacteria, parasites, and fungi. Astonishingly, an invading pathogen is not apparent in around a third of the patients which may include trauma or burn patients that do not have the pathogen in their blood but showed indication of sepsis [91]. Finally, in 1992, during a consensus conference in Chicago, physicians were made to reconsider the diagnostic criteria for sepsis, as a result of such discrepancies[92]. The new sepsis guidelines revealed that infection was not exclusive to bacteria, and the new term was designated as System inflammatory response syndrome (SIRS). Even though the clinical diagnostic criteria were revised from time-to-time, one key element of sepsis captivated researcher's interest and remained consistent: the prevalence of inflammation throughout sepsis.

4.3 Sepsis epidemiology

Globally, sepsis is still one of the leading causes of morbidity and mortality. The overall burden of the disease is projected to be more than 50 million cases each year [93] and more as indicated in chapter 5,6 and 7. In the last two decades, sepsis has become more common not just in underdeveloped countries, but also in the United States and other Western countries [94]. Sepsis affects 2% of all hospitalizations in affluent nations, and the condition is significantly worse in underdeveloped countries with an occurrence of 6-30% for all ICU patients [95]. Although increased awareness, early detection and proper antibiotic supportive treatment have improved outcomes of sepsis, fatality rates remain high. This is because the improved sepsis outcomes are presumably attributed in part to volume change from the increased number of cases reported [95]. Based on the source of infection, features of the pathogen affected, such as microbial count and virulence, along with immune status of the host such as underlying health state, age, genetic composition and medication, patients with sepsis can have a wide

range of clinical symptoms [96]. High body temperature or hypothermia, increased heart rate, hyperventilation, leukocytosis, low blood pressure, and impaired mental status are some of common symptoms [97]. However, these symptoms can be minimal in very young, elderly, or immunocompromised individuals.

The most prominent infection that causes sepsis is pneumonia accounting for half of all the cases. Intraabdominal and urinary tract infections are the next most common sources of infection. According to new findings, the initial site of infection affects the risk of mortality, with intraabdominal infections holding the greatest risk and urinary tract infection with the lowest risk for in-hospital fatality post sepsis [98]. Although the crucial factor in sepsis may be the pathogen that causes the infection, no microorganisms can be grown from any region within the body in 30% of all septic incidences[99].

4.4 Sepsis pathophysiology and role of inflammation

Sepsis is primarily an inflammatory disease triggered by the immune system of the host. The initiation of pattern recognition receptors (PRP) during early stages of sepsis promotes the innate immune response. Pathogen -associated molecular patterns (PAMPs) and/or damage-associated molecular pattern (DAMPs) such as mitochondria produced from damaged tissues, can both evoke the receptor response[100], [101]. Poorly regulated hyperinflammation can cause a variety of symptoms in the early stages of sepsis, including disseminated intravascular coagulation (DIC) and subsequent multi-organ dysfunction syndrome (MODS), inflammation-coagulation caused by abnormal platelet activation, peripheral vasodilation resulting in low blood pressure, hypoperfusion of the kidney, and renal failure[102], [103]. As a result, sepsis

is a complicated disease characterized by endocrine dysfunction, coagulopathy, neurological dysfunction, all of which are mediated by epigenetic inflammation.

Inflammatory response is a critical stage in signaling the immune system to the presence of infection, enabling the host's white blood cells to find and kill the pathogen promptly. This is usually well-controlled, with inflammation subsiding once the infection has been cleared, and the host's white blood cells returning to normal levels. Severe inflammation and immune cell proliferation are prevented when equilibrium is maintained, and the immune system prepares itself for appropriate strategies to respond to future infections.

Most infections can be combated by the immune system when it is working properly, with only a slight degree of inflammation emerging before the pathogens are eliminated from the body. The effective management of cytokines is essential, for overcoming most infections quickly with minimal impairment to the host. During sepsis, this normal response is altered substantially resulting in a cytokine storm triggered by the overstimulation of the innate and adaptive immune activity as cytokines play a crucial role in triggering and amplifying both innate and adaptive immune response in the host.

4.5 Need for effective identification and management of sepsis

Over the last decade, despite significant medical advancements in prevention, diagnosis, and treatment, infectious diseases remain amongst the top three causes of death worldwide according to the World Health Organization (WHO). For sepsis, every hour of delayed treatment increases the rate of mortality by 8% [104]. Timely diagnosis with rapid treatment methodology has been reported to improve the chances of preventing adverse complications, and thus, reduce mortality rate [105]. The clinical appearance of an infectious disease mirrors

the interaction between the host and the microorganism [106]. An effective method to scan for infection is by monitoring biomarkers responsible for host immune response, which unveils the severity of sepsis. However, relying on a single biomarker to determine sepsis can lead to misdiagnosis, as sepsis is a result of multiple complication of an infection[107]. In response to an infection, the body releases multiple triggers, which impairs regular blood flow and leads to blood clots and leaky blood vessels. This deprives the organ from necessary nutrients and results in organ damage. In severe cases, blood pressure drops drastically, heart weakens and patient spirals into septic shock. The patient requires immediate and accurate diagnosis at this crucial stage. An approach for successful prognosis includes integrating a combination of an early and a late onset biomarker for achieving a patient's comprehensive sepsis profile.

CHAPTER 5

MULTIPLEXED CYTOKINE DETECTION USING ELECTROCHEMICAL POC SENSING DEVICE TOWARDS RAPID SEPSIS ENDOTYPING

5.1 Prior publication

Ambalika S. Tanak, Dr. Sriram Muthukumar, and Dr. Prasad co-designed the study. All three contributed towards experimental design, data interpretation, and wrote the manuscript. Ambalika S.Tanak performed experiments, fabricated the sensors, and performed data analysis. Subramaniam Krishnan, Kevin L.Schully, and Danielle V. Clark provided patient sample resources, reviewed and edited the manuscript. Published in Biosensors and Bioelectronics journal in October 2020, this article focuses on demonstrating simultaneous detection of five host response biomarkers in plasma for detection of sepsis. The link to the journal article is https://doi.org/10.1016/j.bios.2020.112726.

5.2 Abstract

The implementation of endotype-driven effective intervention strategies is now considered as an essential component for sepsis management. Rapid screening and frequent monitoring of immune responses are critical for evidence-based informed decisions in the early hours of patient arrival. Current technologies focus on pathogen identification that lacks rapid testing of the patient immune response, impeding clinicians from providing appropriate sepsis treatment. Herein, we demonstrate a first-of-its-kind novel POC device that uses a unique approach by directly monitoring a panel of five cytokine biomarkers (IL-6, IL-8, IL-10, TRAIL & IP-10), that is attributed as a sign of the body's host immune response to sepsis. The

developed POC device encompasses a disposable sensor cartridge attached to an electrochemical reader. High sensitivity is achieved owing to the unique sensor design with an array of nanofilm semiconducting/metal electrode interface that is functionalized with specific capture probes to measure target biomarkers simultaneously using non-faradaic EIS. The sensor has a detection limit of ~1 pg/mL and provides results in less than 5 minutes from a single drop of an undiluted plasma sample. Furthermore, the sensor demonstrates an excellent correlation (Pearson's r>0.90) with the reference method for a total n= 40 clinical samples, and the sensor's performance is ~30 times faster compared to the standard reference technique. We have demonstrated the sensor's effectiveness to enhance diagnosis with a mechanistic biomarker-guided approach which can be helpful towards disease endotypying for effective clinical management of sepsis at the patient bedside.

5.3 Introduction

Endotypes are biological subtypes characterized by distinct pathophysiological functions, described by specific biomarkers. The interpretation and verification of sepsis endotypes can save lives, by encouraging early identification of patient groups for accurate therapy. Sepsis endotyping enables physicians to provide critical care and precision medicine as it showcases the patient’s immune and treatment response to sepsis. Thus, there has been a promising transition from predicting the outcome to pathobiology driven understanding of host response heterogeneity to sepsis, leveraging innovative high-performance translational techniques and analytical methods to identify distinct biomarker subgroups of the host response. Medical communities have further acknowledged the value of biological markers as they continue to enhance sepsis diagnosis, which allows the classification of patients within the specific clinical

category [108], [109]. Sepsis is recognized as a global health crisis affecting more than 49 million people every year[110]. It is a life-threatening condition that represents the systemic immunological reaction of the body to an infectious incident that leads to death [111]. It is well known that sepsis-related fatality is not directly caused by the invading pathogen; rather, the clinical complexity is triggered by the dysregulated host immune response that leads to multiple organ dysfunction [112]. The pathogen or the causative agent triggering sepsis may differ the host's immune response being a key indicator in assessing fatality and the need for complex medical treatments. Ultimately, the combination of pathogen load, infection site, and host susceptibility leads to clinical presentation and course of the disease. Sepsis may be caused by any form of infection; the most common cause is a bacterial infection (pneumonia or urinary tract infection) that affects the body and triggers bacterial sepsis. Whereas, viral sepsis is caused by a viral infection (flu), and more cases of viral sepsis are triggered by COVID-19, which has caused a pandemic in 2020. Additionally, recent studies have reported mortality in COVID-19 patients triggered by sepsis, especially for elderly patients with pre-existing chronic illness [113]–[116].

Currently, rapid diagnostics exist mainly for pathogen identification, such as those highlighted in supplementary (table S1[117]) while a traditional clinical workflow is illustrated in Fig 5.1A. Briefly, technologies such as SeptiFast (Roche) identifies multiple pathogens in six hours, HYPLEX (BAG) relies on the Polymerase chain reaction (PCR) technique to recognize relevant pathogens within three hours, and the Film Array device (BioFire) requires an hour for pathogen detection. These commercially available and those in development focus solely on detecting sepsis based on the pathogen. However, it is crucial to understand the nature of

sepsis and its form of representation in the patient by tracking the host immune response. As sepsis initiates, both pro-inflammatory and anti-inflammatory mechanisms start promptly with a predominant initial hyper-inflammatory phase, as shown in Fig 5.1B. In most of the cases, the innate immune response destroys the invading pathogen, but occasionally the pathogen prevails, and the host response may become unbalanced and destructive. The increased production of cytokines and chemokines is attributed to the severity and prevalence in sepsis, implying that a chain of unregulated inflammation has initiated displaying signs of both excessive inflammations as well as immune suppression, the severity of which varies from patient to patient. This perplexing phenomenon of the host immune response has been thought to be a race to the death between the invading microbes and the host immune response. The pathogens seek and benefit by suppressing various facets of host immunity, according to Hotchkiss and coworkers [90]. Therefore, monitoring cytokine biomarkers can assist in clinical decision-making and forecast sepsis-related outcomes to treatments [91]. For instance, measuring the cytokines levels near-patient at different time points would help in administering specific types of drugs, where immunosuppressants may be prescribed early in the disease etiology addressing the hyperimmune state of the patient and immunomodulators at a later stage in conjunction with antimicrobial therapy. Hence, it is critical to additionally track immune response imbalance triggered by inflammatory & anti-inflammatory cytokine immune response to channelize appropriate treatment strategy. As a POC treatment option, to date, no molecular host biomarker panel is available which makes an informed decision on the specific intervention based on the diagnosis of the immune response or the ability to detect improvements in the status of patients with sepsis[92], [93]. This gives rise to a major

diagnostic gap in near-patient testing capabilities. To address this technological gap this work demonstrates first-of-a-kind near-patient testing ‘DETecT Sepsis’ (Direct Electrochemical Technique Targeting Sepsis) sensor, which directly measures a panel of five host immune biomarkers in <5 minutes to guide the physician with active feedback on patient immune status for better therapeutic administration. DETecT sepsis sensor enables a mechanistic approach for sepsis stratification by leveraging the use of endotypes as defined by specific biomarkers to classify based on pathophysiological process rather than the clinical representation of sepsis which is a step towards precision medicine. Electrochemical sensing modality in conjunction with affinity-based capture probes, specifically quantifies levels of pro- and anti-inflammatory biomarkers (IL-6, IL-8, IL-10, TRAIL, and IP-10) using minimally acquired blood plasma samples.

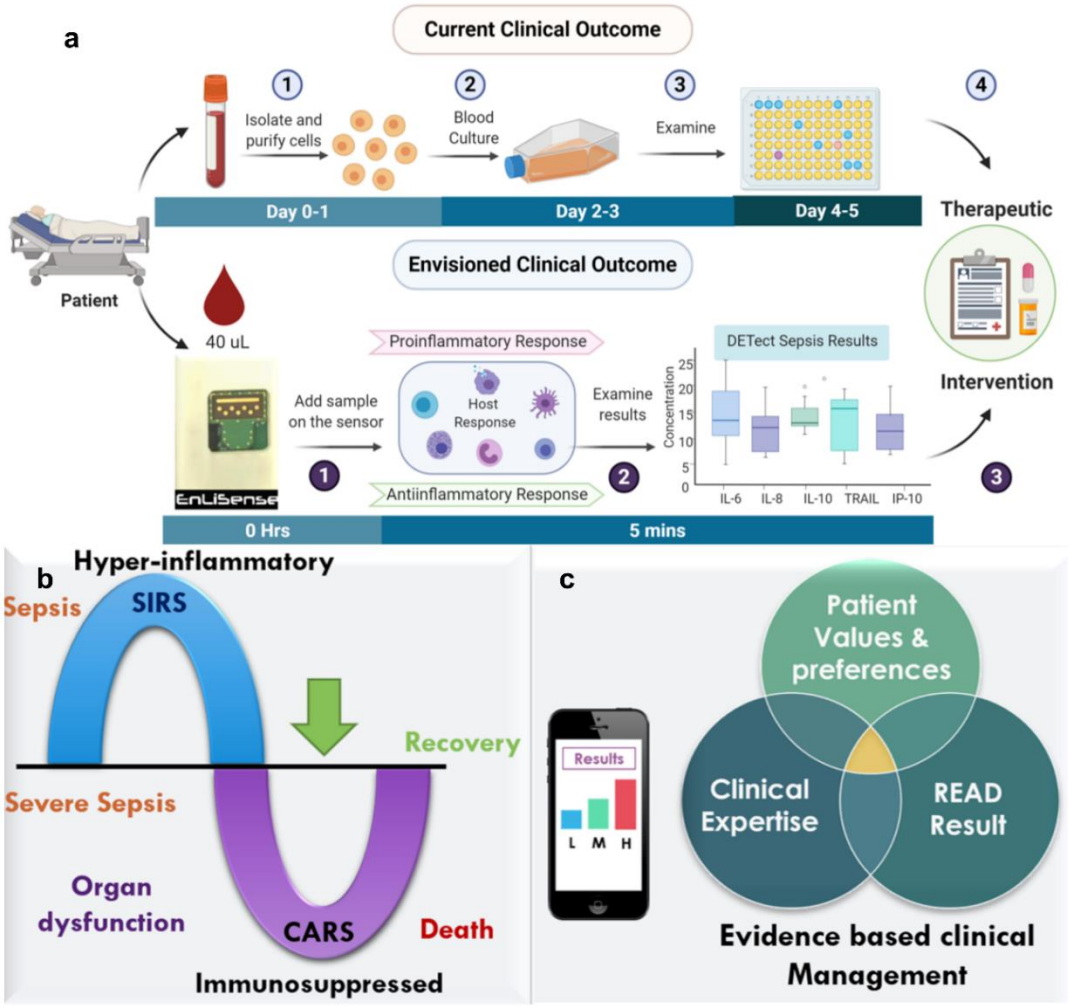

Figure 5.1.a) Illustration of the current clinical timeline vs. DETecT Sepsis approach as rapid near-patient testing for disease severity screening based on biomarker levels. Image is created with Biorender.com b) Hyper-inflammatory and Immunosuppressed phase of Sepsis hypothesis c) Proof of feasibility towards establishing evidence-based clinical management approach using n=40 patient samples.

Fig 5.1 a illustrates the current clinical workflow, and fig 5.1b represents the opportunity the developed sensor offers for detecting sepsis and tracking the host immune response allowing evidence-based clinical management (fig 5.1c). Our point-of-treatment technology allows rapid detection of multiple host-immune response sepsis cytokine biomarkers with ease of sample handling coupled with low sample volume (~40 µL) to facilitate near-patient bedside

monitoring towards enabling biomarker-guided patient stratification, endotyping, and improving treatment response within the critical golden hour post sepsis detection. The advantages of the DETecT Sepsis sensor over existing POC tests are: (i) direct hassle-free measurement from a single drop of undiluted blood plasma; (ii) allows sepsis stratification based on the body's hyper and hypo immune response; (iii) specifically surface engineered sensor design facilitates high sensitivity and specificity; (iv) portable hand-held format enables multi-measure capabilities at near-patient testing. Such a POC-testing device would allow clinicians to make an evidence-based decision on immune-modulating treatments customized to the patient's inflammatory response within the "golden hour" as illustrated in Fig 5.1c.

5.4 Materials and Methods

5.4.1 Experimental design

DETecT Sepsis sensor uses EnLiSense's READ platform for the detection of sepsis. The sensor was designed to allow simultaneous detection of cytokine biomarker panel using minimal sample fluid (<40 uL) in human blood plasma. Sensor performance metrics (sensitivity, specificity, dynamic range, detection limit, precision, and accuracy) were tested for IL-6, IL-8, IL-10, TRAIL & IP-10 in plasma. DETect Sepsis sensor was further validated for clinical translation by testing 20 patient samples tested positive for sepsis at the time of admission compared to the 20 healthy cohorts. The performance of the developed sensor was compared with the Luminex standard as a reference method.

5.4.2 Reagents

DSP and the DMSO solvent were purchased from Thermo fisher scientific (USA) along with the PBS and SuperBlock. The antibodies and their specific antigens for IL-6, IL-8, IL-10, TRAIL, and IP-10 were purchased from Abcam. Pooled human plasma was obtained from Innovative Research, Inc. (USA) for sensor characteristic studies. Plasma from sepsis patients was obtained from the Austere-environments Consortium for Enhanced Sepsis Outcomes (ACESO), a consortium consisting of US Government, non-profit, academic, and industry partners. All the stock proteins and patient samples were stored at -20°C or according to their storage conditions until further use. None of the proteins underwent more than 3 freeze-thaw cycles to avoid denaturing of the proteins. The antibodies were diluted in PBS to bring them to their optimized concentration while their respective antigens were spiked in pooled human plasma in varying concentrations to perform calibrated response curves for each target biomarker.

5.4.3 Direct Electrochemical Technique Targeting Sepsis sensor on EnLiSense's READ platform

The DETecT (Direct Electrochemical Technique Targeting Sepsis) sensor uses EnLiSense's READ platform that comprises of the following: (1) A disposable, single-use sensor cartridge with an array of sensing electrodes that are individually configured to detect multiple biomarkers simultaneously from the sample specimen in real-time. (2) A handheld, palm-sized form-factor electronic reader onto which the sensor is mounted, which transduces the electrical outputs resulting from the sample specimen to other electronic devices/data server through a

software interface (configurable to support both wired and wireless communication). The subtle changes between antibody-antigen affinity interaction result in an electrochemical impedance signal response. Briefly, the detection mechanism is based on non-faradaic EIS. Herein, a small input voltage (10 mV) is applied to the sensor over a frequency range and the resulting impedance response is measured by the portable electronic device. The functioning of the electronic reader has been previously demonstrated elsewhere by our group [74]. EIS is a powerful technique that captures subtle interaction at the functionalized electrode surface. When a sample is introduced on the electrode surface and the electrode is polarized, the rearrangement of charges occurs at the electrode-solution interface. This results in a local built-up of excessive ions of opposite charge. The extent to which the exponential charge built-up decays form the electrical double layer (or double-layer capacitance). The target analyte binds to the specific capture probe antibody within this double layer leveraging the antibody-antigen affinity mechanism across each working electrode and impedance is measured [37], [94], [95]. Advantages of non-faradaic EIS over faradaic method includes (i) label-free technique that can directly measure the subtle binding interactions without the need for a redox label for the measuring impedance response, thus, making non-faradaic EIS considerably more compatible in POC applications (ii) non-faradaic impedance measurement eliminates the need for a DC potential; thus, it does not denature the biomolecules immobilized on the sensing electrode surface. The sensing layer was surface engineered through a standard sputter fabrication technique using RF magnetron to deposit a 200 nm thickness of semiconducting thin film on the gold electrodes. Before deposition, a solvent cleaning strategy was applied where the surface was thoroughly cleaned with isopropyl alcohol (IPA), acetone, and DI water to

eliminate any impurities. Modulating the metal oxide layer's surface chemistry helps to improve the rearrangement of charges near the electrode-solution interface. Furthermore, Zinc oxide semiconductor has unique properties, including a large bandgap (3.367 eV), is non-toxic, and has high excitation binding energy (60 eV) that helps increase overall sensitivity. Additionally, due to its high adsorption capability owing to its high isoelectric point (~9.5), chemical stability and good electrical conductivity enhance its use for sensitive electrochemical biosensing applications [95]. Nanoscale dimensions of the semiconducting thin film allow size-based matching to the target analyte, which effectively increases surface area to volume ratio. Additionally, the structural morphology of the nanofilm offers selective biomolecular binding for the functionalized capture probes. With the increase in the surface-to-volume ratio, the surface structures of nanofilms can significantly modulate the charge carrier densities within the material and increase band bending [96], [97]. Previously, our group has experimentally demonstrated a three-fold increase in sensitivity for the nanofilm as compared to planar nontextured microelectrodes [98]. Thus, leveraging the unique properties of the ZnO nanofilm surface engineered layer, we have demonstrated sensitive electrochemical biosensing for the detection of multiplexed biomarkers.

5.4.4 Immunoassay development

The sensor surface was immobilized with 10mM DSP dissolved in DMSO and incubated in the dark at room temperature. Specific capture antibodies (IL-6, IL-8, IL-10, TRAIL, and IP-10, 10 µg/mL each) were individually functionalized on each working electrode of the sensors. Superblock was used to hydrolyze unbound linker sites to avoid non-specific interaction. A calibrated response was established for each of the pentaplex biomarkers against varying dose

concentrations spiked in pooled human plasma. Data were represented as a percentage change in impedance with respect to baseline (plasma blank without the target biomarkers), using the equation S1 (supplementary information [117]). Cross-reactive study was tested by preparing a cocktail of non-specific biomolecules in low (10 pg/mL) and high concentrations (1000 pg/mL) with the absence of the target biomarker. Individual response for the cross-reacting molecules was measured for each sensor functionalized with the target capture antibody. To test the specificity of the sensor in the presence of interfering biomarkers, the target biomolecule was spiked to the previously prepared cocktail solution, and the response was measured for each of the pentaplex biomarkers. All the data represented is measured from n=3 replicates. The LOD described as the lowest measured concentration was calculated as 3 times SD of blank plasma.

5.4.5 Patient sample acquisition

Plasma samples were collected under written informed consent as part of an ongoing observational trial of sepsis in resource-limited settings conducted by ACESO [99], [100]. Briefly, patients presenting to the emergency department of a participating hospital with at least two SIRS features and a suspected infection (SEPSIS-2 criteria) were eligible for enrollment. For this work, plasma samples collected 24 hours after enrollment from sepsis patients were used. Samples were provided stripped of all identifiers by ACESO to Biomedical Microdevices and Nanotechnology Laboratory, UT Dallas following the Material Transfer Agreement (MTA), approved by the Institutional Review Board (IRB# 19MRO151) at the University of Texas at Dallas. The samples were stored at -20°C immediately on arrival until further use and did not undergo more than two freeze-thaw cycles.

5.4.6 Statistical Analysis

Statistical analysis was performed using GraphPad Prism Software (GraphPad Software Inc., La Jolla, CA). ns: non-significant, *P<0.05, **P<0.01, ***P<0.001, ****P<0.0001. Data represented as mean ±SEM for n=3 replicates unless stated otherwise. One-way analysis of variance (ANOVA) was used for the comparison between three or more groups. T-test was used to compare significance for specific signal against non-specific interferons in the cross-reactive study. Differences between healthy and septic cohort were assessed using non-parametric (unpaired Mann-Whitney tests).

5.5 Results

5.5.1 DETecT Sepsis sensor evaluation for multiplexed quantification of immune biomarkers

There is an immense unmet need for a rapid diagnostic to enable patient stratification in sepsis towards effective disease management. Therefore, the POC-tests should be highly sensitive with a wide dynamic range for a panel of host response biomarkers, that can be leveraged for assessing the patient's immune state towards stratification and disease management. Based on the wide body of scientific literature, and clinical evidence, our approach was to target a combination of pro and anti-inflammatory cytokines in conjunction with cell apoptosis monitoring protein. Therefore, we selected IL-6, IL-8, IP-10, IL-10, and TRAIL for this study as the levels of these biomarkers provide a composite snapshot into a patient's immune response state towards establishing disease severity and mortality risk in the patient. TRAIL and IP-10 were included for discriminating between the viral and bacterial loadings on the host

[101]. DETecT sensor device was calibrated for each of the pentaplex biomarker panels in pooled human plasma (control set with no infections). Herein, varying dose concentrations were measured for specific analytes to establish a calibrated dose-response on the multiplexed affinity capture probe functionalized sensor array. Signal impedance response between antibody and the target analyte was captured using EIS and represented as a percentage change in impedance with respect to the baseline (described in the methods section) in pooled plasma as shown in fig 5.2(a-e).

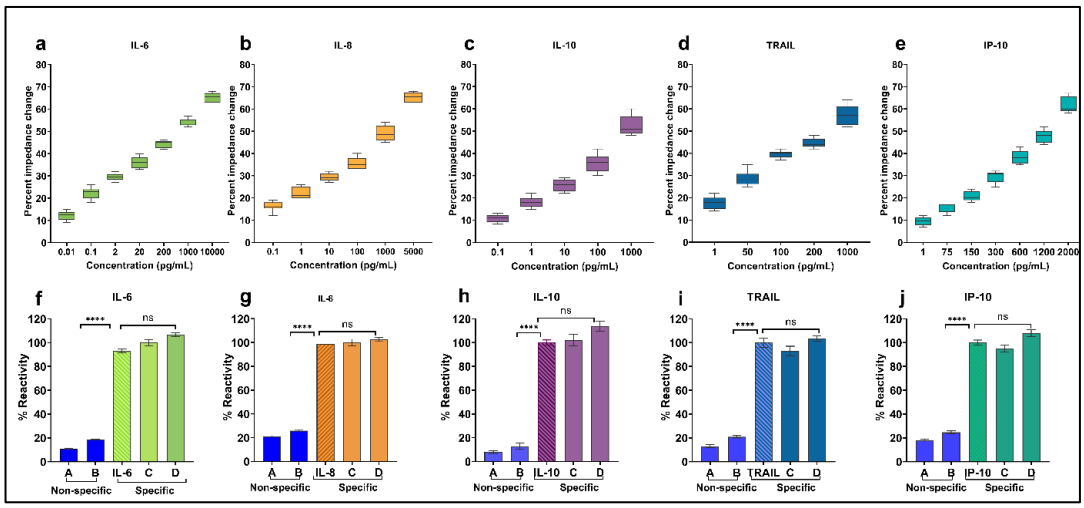

Figure 5.2. (a-e) Calibrated dose-response for IL-6, IL-8, IL-10, TRAIL, and IP-10 in pooled human blood plasma with a clinically relevant dynamic range. (f-j) The cross-reactive study demonstrating the specificity of DETecT Sepsis sensor for each of the target biomarker. A; Low concentration of non-specific biomarker mixture, B; High Concentration of non-specific biomarker mixture, C; Target marker along with a low concentration of non-specific biomarker mixture, D; Target marker along with a high concentration of non-specific biomarker mixture.

A dose-dependent increasing trend in impedance signal response was observed for all the biomarkers. The dynamic range for each biomarker was aimed to capture the healthy as well as a diseased state within the physiologically relevant range of clinical samples. IL-6 demonstrated a wide dynamic range of 0.01 pg/mL to 10 ng/mL with a LOD of 0.1 pg/mL in spiked plasma samples (fig 5.2b). The box plots for each biomarker display no overlapping

inter-quartile ranges with a minimum variation for each concentration, indicating good repeatability with the least variance. The signal impedance response is reflective of the affinity binding mechanism between the specific capture probe and the target analyte that indicates the biomarker concentration in pooled plasma. The unique multiplexed sensor design coupled with specific surface functionalization augments the signal response and has previously been described elsewhere [95], [102]. IL-8 demonstrated a dynamic range of 0.1 pg/mL to 5 ng/mL with a detection limit of 0.1 pg/mL (Fig 5.2c). IL-6 and IL-8 are known to be major mediators of an inflammatory response, and their levels elevate in patients with sepsis, which act as key indicators during the development of severe sepsis. Similarly, the dynamic range for IL-10 was observed to be from 0.1 pg/mL to 1 ng/mL (Fig 5.2d) with an LOD of 1 pg/mL in pooled plasma. IL-10 belongs to the group of immunoregulatory molecules called anti-inflammatory cytokines that prevents the body from the adverse effects of excess inflammatory immune reactions. The key risk factor for sepsis severity and the fatal outcome is the chronic overproduction of IL-10, which indicates patients with sepsis are in a deep immunosuppression state [103]. Data in fig 5.2e shows the dynamic range of TRAIL from 1pg/mL to 1 ng/mL with a detection limit of 1 pg/mL whereas IP-10 displayed a dynamic range of 1 pg/mL to 2 ng/mL (Fig 5.2f) respectively. Additionally, each biomarker demonstrated a statically significant difference between concentrations as determined by one-way ANOVA with 95% confidence intervals (table S2 [117]). The developed DETecT sepsis sensor demonstrated sensitive detection for biomarkers below normal threshold levels as well as the dynamic ranges extended beyond elevated levels predicted in disease states. The surface engineered semi-conducting

nanofilm allows sensitive detection by potentially increasing the surface to volume ratio, allowing plenty of biomolecules to be immobilized onto the electrode surface.

After establishing a sensitive and robust calibration response, the selectivity and specificity of the DETecT Sepsis sensor on EnLiSense's READ platform were evaluated. Every analyte was tested with a series of non-specific markers, starting with the lowest concentration of the cross-reacting molecule, followed by the highest concentration as seen in Fig 5.2 (f-j). Selectivity of the biosensor is extremely important while testing actual clinical samples where the concentrations of the analyte can be much lower than that of the non-specific molecule. Thus, to mimic realistic scenarios, the sensor was additionally tested with a cocktail mixture of low and high non-specific molecules along with the target analyte spiked plasma sample to validate sensor device platform specificity. Non-specific biomarkers (represented as bar's A and B) in fig 5.2 (f-j) showed less than 10 % reactivity compared to the specific response of the target biomarker. Additionally, despite the presence of varying concentrations of cross-reacting molecules (represented as bar C and D in fig 5.2 (f-j) along with the target biomarker, the developed sensor demonstrated similar results (100% reactivity) to that of the specific individual analyte. DETecT sepsis sensor's capability to bind to the functionalized antibody selectively is attributed to the surface-functionalized highly specific monoclonal antibody combined with the effect of blocking buffer. By blocking the active functional groups on the electrode surface, the blocking buffer (superblock) prevents non-specific binding and can help stabilize the biomolecule attached to the electrode surface, thereby increasing the specificity of the biosensor [104]. Specificity is a vital sensor metric to reduce false-positive results and provide accurate detection capability with increased resolution in distinguishing disease state.

Overall, the data confirmed the developed DETEecT sepsis sensor demonstrated high sensitivity coupled with specific and selective response despite the presence of non-specific biomolecules for the multiplexed cytokine biomarker panel in plasma using EIS as the detection technique.

5.5.2 Evaluating DETecT Sepsis sensor performance for repeatability, reproducibility stability, and accuracy in pooled human blood plasma

Repeatability, reproducibility, accuracy, and stability are the main considerations that need to be assessed while evaluating the sensing platform's effectiveness. The coefficient of variation (%CV) was calculated for all the study biomarkers as a measure to assess the dispersion within each reported concentration from n=10 sensors, as shown in Fig 5.3 (a-e). Generally, lower concentration tends to show higher variability and the developed sensor demonstrates the CV range between 3-16%. The results displayed in fig 5.3 (a-e) exhibit a CV < 20% which is clinically accepted as per the guidelines set by the Clinical and Laboratory Standards Institute (CLSI), thereby demonstrating the repeatability of DETecT sepsis sensor within a wide dynamic range [105]. Fig 5.3 (f-j) demonstrates the reproducibility of the electrochemical response for 12 identical sensors with an average concentration indicated by the dotted line for each target analyte. The relative standard deviation (RSD) across all twelve sensors was ~ 10%. The value of RSD indicates good reproducibility and repeatability of the DETecT Sepsis sensor platform.

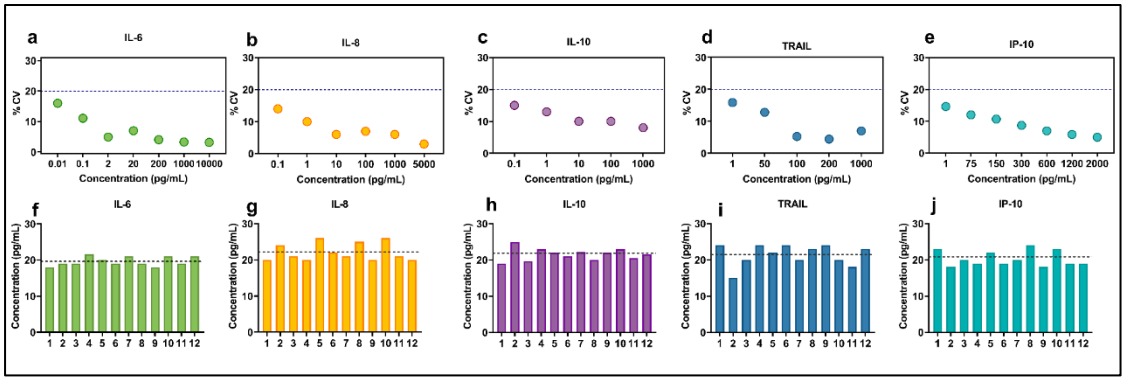

Figure 5.3. (a-e) CV plot examining the precision of DETecT Sepsis sensor for IL-6, IL-8, IL-10, TRAIL and IP-10 in pooled plasma. The dotted line at 20% represents the acceptable limit according to CLSI guidelines (f-j) Repeatability and reproducibility of DETecT sepsis sensor across 12 sensors for IL-6, IL-8, IL-10, TRAIL and IP-10 in pooled plasma respectively. The dotted line represents average concentration across 12 replicates.

Next, DETecT Sepsis sensor performance was tested for its accuracy by the spike and recovery study. Known concentrations (actual) spiked in triplicate correlated with an R^2 value of 0.99 with the measured concentration calculated based on the previously established calibration curve. Fig 5.4 (a-e) demonstrates reliable detection of actual spiked concentration across all five target biomarkers. The recovery percentage was then calculated along with the accuracy of the sensor as represented in fig 5.4 (f-j). As observed from the results, the percent recovery was between ~89-110% for IL-6, IL-8, IL-10 TRAIL, and IP-10, which lies well within the acceptable range for assay validation according to CLSI standards [106]. Once the accuracy was established, the operational stability of DETecT Sepsis sensor was tested for up to five weeks (35 days) with the sensors stored in 4°C. 1 pg/mL concentration for TRAIL and IP-10 was measured thrice (n=3). No significant change in response was observed for TRAIL with only a 3% loss of signal at the end of five weeks, as seen in supplementary Fig S1 [117]. Similarly, a loss of only 5% of the signal response was seen at the end of five weeks specific to IP-10 as seen in supplementary Fig S2 [117]. In summary, both TRAIL and IP-10 retained

95-97% of its original activity post five weeks of storage in 4°C, indicating excellent operational stability. To our knowledge, this is the first demonstration of a pentaplex biomarker sensor that allows simultaneous quantification of pro-and anti-inflammatory biomarkers with a single drop of plasma sample with reliable sensor performance metrics.

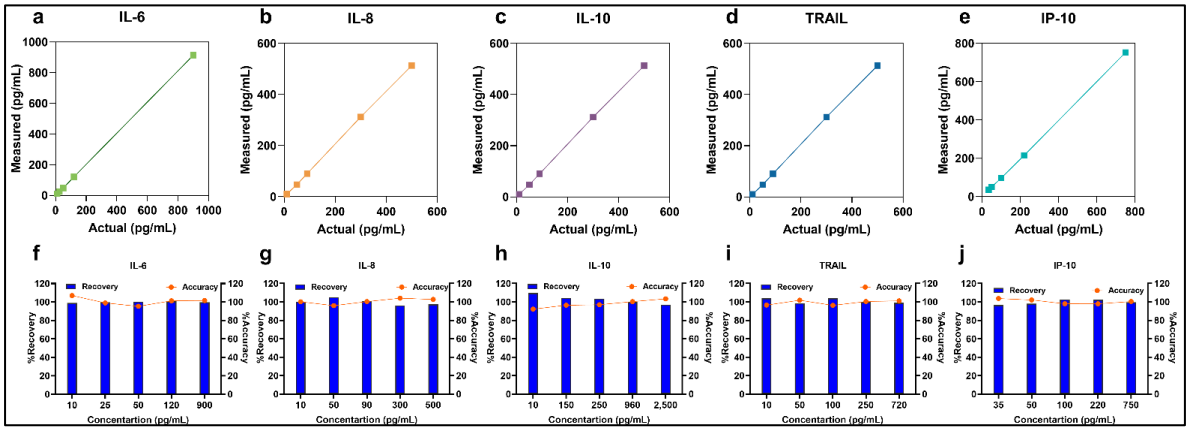

Figure 5.4.(a-e) Actual and measured concentration in pooled plasma represented as correlation plots using the DETecT sepsis sensor. (f-j) Repeatable and reliable sensing capability highlighting the high recovery rate and accuracy of the developed sensing platform.

5.5.3 Validating DETecT Sepsis sensor with clinical patient samples

Clinical translation for the multiplexed POCT technologies requires validation with patient samples. For this study, 20 septic patient plasma samples along with 20 controls (non-septic) healthy plasma samples (Table S3 [117]) were evaluated using the DETecT Sepsis sensor and Luminex as the reference standard. The onset of sepsis was confirmed at 24 hr time point from the hospital. All the 40 samples were tested for IL-6, IL-8, IL-10, TRAIL, and IP-10 using the developed sensor device. Concentrations measured using the sensor correlated well with a Pearson's $r \geq 0.90$ for all the five test biomarkers as seen in Fig 5.5 (a-e). Fig 5.5 (f-j) represents the DETecT Sepsis sensor's capability to distinguish healthy vs. sepsis patient cohorts for IL-6, IL-8 IL-10, TRAIL, and IP-10. We observed that levels of IL-6, IL-8, IL-10, TRAIL, and

IP-10 of the healthy cohort were significantly different from the Septic cohort as confirmed using Mann-Whitney U statistical analysis test. Mean plasma IL-6 levels for the septic cohort were 44.05±74.32 pg/mL as compared to 2.2±0.83 pg/mL of the healthy cohort. IL-8 levels for the healthy cohort were all below 2.44±0.88 pg/mL while mean levels in the septic cohort were around 11.65±16.16 pg/mL. Similarly, for anti-inflammatory IL-10 biomarkers, the mean level established for the healthy cohort was 2.17±0.84 pg/mL and septic patients' mean levels were 15.47±18.18 pg/mL. As seen in Fig 5.5d, TRAIL levels were significantly lower in septic patients with a mean value of 27.62±18.62 pg/mL as compared to the healthy cohort mean levels of 47.69±18.74 pg/mL. Studies have shown to correlate lower levels of TRAIL to poor patient outcomes, thus indicating the overall severity of illness [107], [108]. Mean healthy concentrations for IP-10 were 45.27±34.57 pg/mL whereas septic sample mean levels were measured to be 397.3±572.5 pg/mL. The DETecT Sepsis method was also able to distinguish all the five biomarkers in healthy and septic patient samples with good statistical significance of $p<0.001$ (Table S4 [117]).

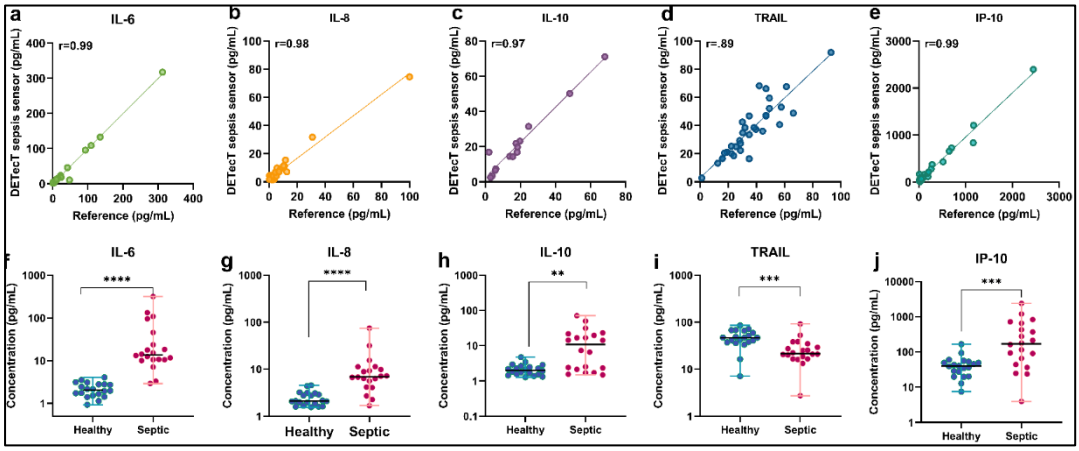

Figure 5.5. (a-e) Correlation between the Reference method (Luminex) and DETecT sepsis sensor platform obtained by analyzing n= 40 patient blood plasma samples with a Pearson's r ≥ 0.90 for IL-6, IL-8, IL-10, TRAIL, and IP-10 biomarkers. (f-j) DETecT Sepsis sensors

capability to distinguish healthy significantly vs. sepsis patient cohorts for IL-6, IL-8 IL-10, TRAIL and IP-10. Note: **p < 0.01, ***P < 0.001, ****P < 0.0001.

5.6 Discussion

Patients with sepsis can be stratified based on evaluating specific immunological response patterns by a promising approach of cytokine profiling [109], [110]. Research has been proposed that a combination of biomarkers may yield better results, as no single biomarker exhibits an accuracy of 100% to predict a reliable outcome. Accordingly, in this work, we developed a unique strategy targeting a combination of five pro and anti-inflammatory cytokine biomarkers to rapidly detect sepsis using the DETecT Sepsis sensor to assess the patient's host response useful in a clinical setting. The empirical research approach adopted for this work was based on the evolving knowledge of host response to infection during sepsis. It is well-identified that sepsis fatality is not specifically induced by infectious microorganisms or pathogens; instead, the subsequent pathological outcome is triggered by dysregulation of the host immune response with a combination of pro and anti-inflammatory processes, contributing to multiple organ failure. DETecT Sepsis sensor provides a descriptive understanding of the host immune response with the pentaplex biomarker strategy enabling patient stratification to predict timely evidence on the arc of sepsis. The sensitive and specific aspect combined with a wide dynamic range of the DETecT sensor device platform allows sepsis stratification to differentiate the patient state enabling appropriate therapeutic interventions.

The combination of pro and anti-inflammatory markers (IL-6, IL-8, and IL-10) reveals host immune response during the early stages of sepsis whereas TRAIL and IP-10 provide information to differentiate between bacterial or viral sources of infection. Each biomarker

provides key information based on the specific pathophysiology. Timing of cytokines release and the symbiosis between pro- and anti-inflammatory agents determines the degree of infection, and their excessive production can be associated with deleterious effects. A clinical investigation detected a high concentration of cytokines in plasma of critically ill patients affected with COVID-19, suggesting that cytokine storm was associated with the severity of the disease as well[111]. Cytokine mediators are elevated in both pediatric and adult patients and are responsible for illicit symptoms including fever, hypotension, and production of acute-phase proteins [112], [113]. They are likely to be prognostic as primary regulators during the early stage of sepsis [114], [115]. Additionally, elevated IL-6 and IL-8 levels are linked with early 48 hours and 28-day mortality in sepsis patients [116]. Moreover, IL-8 is a known mediator of the inflammatory response which plays a major role in neutrophil activation. Our results are in agreement with previous research which illustrated the increase of IL-6 and IL-8 during the first 24 hours of hospital admission as compared to the healthy cohort [116]–[118], thus, demonstrating the role of cytokines biomarkers in identifying sepsis prognosis at an early stage. The role of anti-inflammatory biomarker IL-10 during sepsis is complicated as it depends on the time of intervention of either being protective or destructive to the host. Overproduction of IL-10 in septic patients is an indicator of severity and fatal outcome as the body spirals in a state of immunoparalysis. Therefore, IL-10 in the DETecT pentaplex panel acts as an indicator of immune suppression, and thereby reflects the severity of the patient's condition for sepsis-induced immunosuppression. Since the patient samples tested were collected at a 24-hour time point, the IL-10 levels were not as significant compared to the healthy cohort, thereby indicating an early stage of sepsis. Our results demonstrating the down-

regulated TRAIL profile support the hypothesis that TRAIL participates in sepsis by controlling inflammatory cell apoptosis and promotes inflammation resolution [119]. The presence of TRAIL and IP-10 has been independently used to differentiate viral from bacterial infection[120]–[122]. Moreover, the hypothesis that TRAIL participates in sepsis by controlling inflammatory cell apoptosis and promotes inflammation resolution [119]. Broadly, each selected biomarker demonstrates key elements in activating immune response during sepsis. The approach of multiplexed cytokine profiling would enable rapid sepsis endotyping based on biomarker levels using the DETecT Sepsis sensing platform. Physicians can actively monitor patient status for better prognosis and provide enhanced therapeutic interventions, with multiple measures at patient bedside.

Clinical management of sepsis can be divided into three phases: (i) patient screening; (ii) patient stratification based on evidence-based clinical management and response to treatment therapies; and (iii) prognostic monitoring. As discussed earlier, much effort has been utilized in the first and third phases, while very little progress has been reported with patient stratification methods. Existing methodology lacks the potential to deliver rapid POC results deprived of demanding post-processing to facilitate adequate diagnosis strategies for septic patients. To date, very little work has been done on enabling multiplexed biomarker detection at POC-testing allowing timely treatment. Moreover, transitioning these findings into a clinically feasible test requires a rapid, convenient method that can resolve the lengthy testing process (1-8 hours) while providing accurate results. The developed self-integrated sensing device improvements over existing techniques include (i) direct patient sample measurement without the need for sample preparation or dilution (ii) low sample volume utilization (~40

µL) of blood plasma in a portable hand-held format, that could be used to collect data over multiple time points with (iii) rapid results achieved within ~5 mins (iv) simultaneous multiplexed detection of cytokine panel biomarkers, for classifying patients depending on the levels reflecting severity of illness (v) Sensitive, selective, specific and stable biosensing response enhances the reliability of the detecting mechanism.

Many researchers have leveraged the use of IL-6, IL-8, IL-10, TRAIL, and IP-10 individually, but to our knowledge, this work is the first demonstration of a simultaneous pentaplex biomarker panel for early sepsis diagnosis and monitoring using low sample volume (< 40 µL) achievable rapidly. DETecT Sepsis sensor can be used effectively in the emergency department for early sepsis screening, or it can be used to monitor sepsis prognosis for patients as a bedside monitoring device. Biomarkers linked with sepsis are attributed to the complex immune response pathways, therefore rapid multiplexed detection would enable early therapeutic intervention and improve patient outcomes. Additionally, the sample-to-detection time, measured for all five biomarkers from time of sampling until sensor readout, was ~5 mins, which is >30 times faster than the standard reference method (~5 hours). The repeatable and reproducible results demonstrated by the DETecT Sepsis sensor shows evidence of an accurate and reliable electrochemical biosensing mechanism. When tested against common interferants, the specific sensing capability for the developed pentaplex sensor was not affected. Moreover, the sensor displayed a stable response for over five weeks. To our knowledge, no multiplex point-of-treatment device is available for sepsis detection for near-patient testing without sample dilution with rapid response time. Our data shows the first demonstration of a truly novel multiplexed platform capable of monitoring host response using pentaplex biomarkers

for sepsis detection that would enable patient stratification and sepsis endotypying. This rapid sample-to-result detection capability demonstrated by the DETecT Sepsis sensor establishes it as a value-added POC testing approach in hospitals and emergency departments towards risk stratification of sepsis severity and responses to treatment.

5.7 Conclusion

In summary, DETecT Sepsis device platform provides the first proof of concept for rapid diagnostic screening of sepsis leveraging a host immune response biomarker pane. The developed sensor showed comparable results to the reference standard as shown with Pearson's $r>0.97$ for all the five biomarkers. However, the developed DETecT sepsis sensor achieved quicker response time with lesser completed assay procedure, leveraging a combination of unique surface engineered sensing strategy coupled with an affinity biosensing principle. The results of this research demonstrate a robust, sensitive, specific, and stable performance by the DETecT Sepsis sensor which is highly expected from a POC device. Moreover, it possesses three major advantages over current detection methodology. Firstly, a specific affinity-based transduction mechanism allows the simultaneous detection of IL-6, IL-8, IL-10, TRAIL, and IP-10. Multiplexed detection capability will help provide a precise molecular fingerprint of every patient encouraging initiatives towards precision medicine. Secondly, rapid response time offered by the DETecT sensor enables faster decision-making for physicians to operate within the "golden hour" and initiate required treatment thus, avoiding the dynamic sequence of irreversible organ failure and subsequent death caused due to delayed response time. Finally, small form factor and ease in handling allow flexibility in using the device in a versatile environment (in an emergency department, or for bed-side monitoring) while ultra-low sample

volume (< 40 µL) encourages physicians to collect multiple measurements within a day to monitor patients host immune response and assess the severity of sepsis. The study was limited to a small sample size of septic patients. However, these observations have several implications for research to integrate different host immune response biomarkers with self-integrated POC devices for a better patient outcome. We are currently in the process of expanding our multiplexed capabilities and investigating sepsis pathophysiology via a larger patient cohort. In conclusion, this work has pioneered a potential solution to the current sepsis dilemma, by providing host response strategy to address complexity, shifting the paradigm of the on-going sepsis diagnostic approach.

CHAPTER 6

MULTICOHORT TIMECOURSE ANALYSIS AND CLINICAL INVESTIGATION OF PATIENTS WITH SEPSIS USING DETECT SEPSIS DEVICE 2.0

Prior publication

Ambalika S. Tanak, Dr. Shalini Prasad and Dr. Sriram Muthukumar conceptualized, designed the study and contributed to data. Ambalika S. Tanak performed the experiments, data analysis, data interpretation and wrote the manuscript. Abha Sardesai provided the data on machine learning model. Subramaniam Krishnan, Kevin L.Schully, Danielle V. Clark and Deborah A Striegel provided patient sample resources, reviewed and edited the manuscript. This work is submitted to Cell reports medicine and currently under review.

6.1 Abstract

Disease progression of sepsis has been perceived as a multifaceted phenomenon, considering the temporal host inflammatory response within individuals which requires early diagnosis. Herein, we present a multicohort analysis through temporal inflammatory biomarker profiling using DETecT sepsis device that measures and quantify cytokines (IL-6, IL-8, IL-10), chemokines (TRAIL, IP-10), and well-established inflammatory biomarkers (PCT, CRP) with a sample turnaround time of <5 mins in small volume (<40 uL) patient plasma samples. The DETecT device positively correlated (r>0.97) with the Luminex reference standard during clinical evaluation for a total of 124 patient samples. Low mean bias for all the biomarkers in Bland- Altman analysis indicated good agreement between standard LUMINEX method and the developed DEecT sepsis device. We used the combinatorial power of rapidly measuring a

panel of seven biomarkers, paired with a machine learning model, to effectively predict patient outcome when given two time points in the early stages of sepsis. The device could predict patient mortality and recovery with over 92% accuracy by applying decision tree analysis. We envision this work would facilitate personalized treatment based on biomarker stratification to represent exactly where the patient belongs within the sepsis continuum. Measurable empirical data with a fast turnaround time would facilitate the DETecT sepsis device as a potential enabling technology that can play a crucial role in understanding sepsis prognosis and be leveraged for personalized therapeutics anywhere.

6.2 Introduction

Disease management is crucial for specific diseases to improve patient outcomes [151]. One such disease that needs continuous attention is sepsis. Sepsis is an intricate, heterogeneous condition that is often misdiagnosed with severe health repercussions [141]. Sepsis is characterized by a dysfunctional host immune response comprising inter-woven immune responses, including pro-inflammatory, anti-inflammatory, immunosuppressing, and other complex components that impact all types of immune cells and their compartments. Therefore, mitigation of potential sepsis and research on precise and prompt detection may decrease mortality risk while improving patient outcomes.

Disease management for sepsis has been effectively broken down into six stages (awareness, prediction, diagnosis, prognosis, treatment, and recovery). Much attention and focus are given to the three initial stages of sepsis management [152], [153] (awareness, prediction, and diagnosis [154], [155]. Therefore, it is critical to understand the course of the disease and provide gateways to prevent the disease from progressing into a later stage with a fatal

outcome. Many gold standard techniques include pathogen-driven approaches for disease identification [156]. However, it is believed that sepsis is not solely driven by the pathogen-elicited inflammatory response but by a dysregulated host immune response with a combination of pro-inflammatory and anti-inflammatory processes that correspond to multiple organ failure [94], [118]. Despite this, many current technologies are heavily focused on a time-consuming pathogen-driven approach, and delayed results could prove detrimental to the patient as the patient's state changes by the hour [157].

Furthermore, these current technologies require large sample volumes, making it tedious to measure or account for time-based patient response. Adding to the existing predicament, sepsis management becomes nearly impossible in a resource-limited environment with little or no access to sophisticated clinical analyzers or trained laboratory experts to perform accurate tests [158]. This makes it even more challenging to diagnose the patient's status. Therefore, a one-size-fits-all approach is adopted i.e., administering a broad range of antibiotics for treatment [159]. In bacterial sepsis, it may be advantageous. However, if the patient has a viral source of infection, it can do more harm than good [160]. Moreover, diagnostic ambiguity can delay adapting existing lifesaving treatments, increasing the further abuse and overuse of antimicrobial agents. The patient may even develop antibiotic resistance to the broad-spectrum administered drugs, which is equivalent to opening a pandora's box altogether [161], [162].

Therefore, it is crucial to have the ability to make appropriate decisions at the right time to improve the chances of survival for patients with sepsis. We want to target this area, which is the foundation of the later three stages of sepsis management, i.e., prognosis, treatment, and recovery. This primarily includes patient endotyping and disease stratification. Many

technologies like SeptiFast (Roche Diagnostics) and Iridica Plex ID (Abbot Molecular) focus on detecting sepsis. Further, ImmunoXpert, a blood-based host immune markers-based diagnostic assay, distinguishes bacterial infection from viral infection. This assay integrates the concentrations of three biomarkers: tumor necrosis factor-related apoptosis-inducing ligand (TRAIL), interferon-gamma induced protein-10 (IP-10), and C-reactive protein (CRP). However, little work has been done to examine the host response after the patient has been diagnosed with sepsis, as sepsis pathophysiology is complicated, and the immune response varies from patient to patient. Mapping the immune response prior to physiological initiation of symptoms such as fever throughout the infection and post-infection complications is paramount towards providing appropriate clinical care. Monitoring the patient's host immune response in real-time could provide active feedback on the patient's immune state to alter treatment strategies [163], [164]. Mapping the immune response serves as a tool to ascertain (a) the difference between SIRS and sepsis, (b) severity of sepsis and (c) mortality and survival. Further, identifying sepsis patients who belong to broad immune phenotypes such as hyperactive immune responders or immune-suppressed will assist in biomarker-based patient stratification for precision immunotherapy and appropriate clinical management. Finally, upon initiation of appropriate treatment, these host immune analytes can also potentially serve as response biomarkers monitoring the treatment in real-time. Rapid POC diagnostics in real-time, monitoring host immune analytes leading to evidence-based clinical management is the need of the hour.

Our previous work demonstrates robust sensing performance that can be used as a near-patient POC sensor to detect sepsis [165]. This work focuses on progressing beyond validating the

sensor performance metrics and providing evidence-based clinical biomarker endotyping to help with sepsis prognosis and facilitate personalized treatment strategies. Patient stratification and endotyping will enable improved patient outcomes as it pivots towards precision medicine. During sepsis treatment, biomarker-guided immunotherapy offered at the patient bedside during the appropriate immune phase may empirically be a significant advancement in sepsis management [166]. This work builds on analyzing a cytokine network (by monitoring IL-6, IL-8, and IL-10) [167] to unveil dynamic inflammatory pathogenesis in sepsis and understand the source of pathogen-triggered immune response (bacterial infection presence reflected by levels of TRAIL and of viral infection presence with an increase in IP-10) combined with early and late-stage established biomarkers (PCT and CRP) to provide a complete profile on the patient's immune state at the bedside.

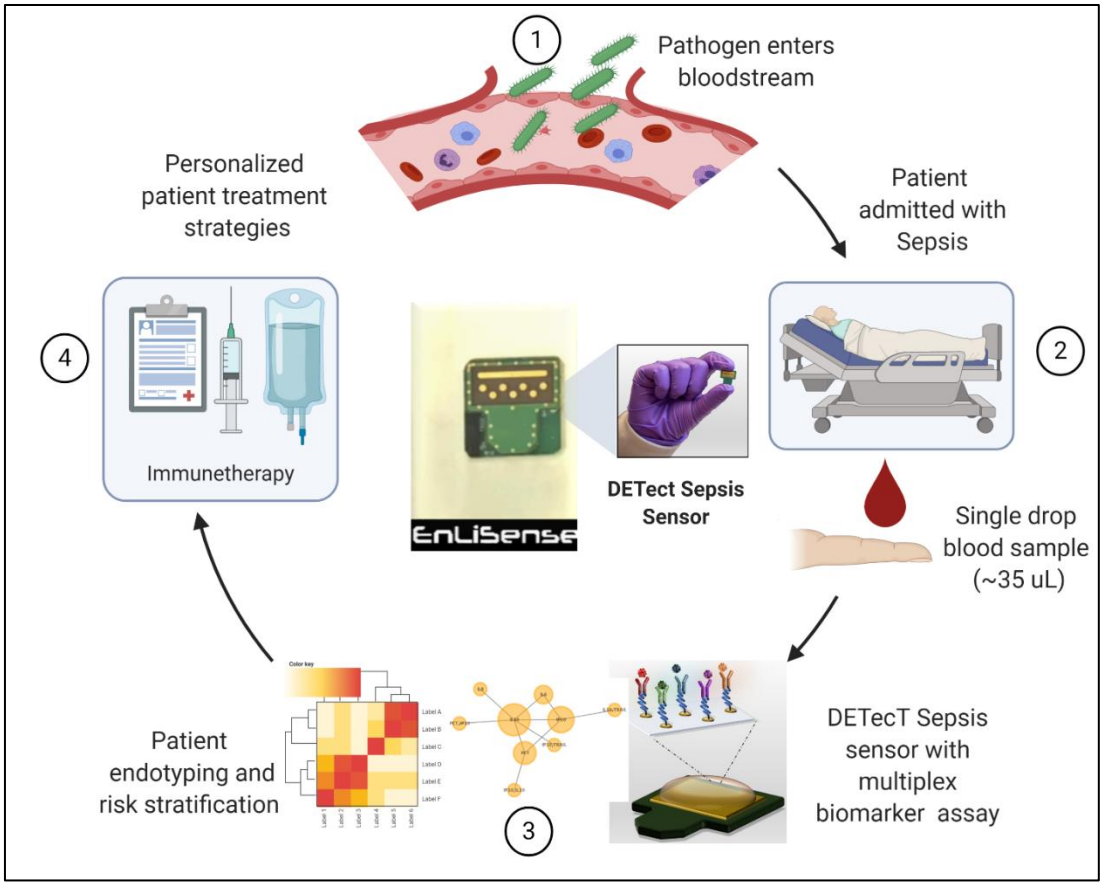

Figure 6.1. Graphical abstract representing the cycle after the infection enters the bloodstream and the scope where DETEcT sepsis device is envisioned to be used at the patient bedside. Image is drawn using Biorender.com.

6.3 Methods

6.3.1 Study design

This study aimed to validate DETecT sepsis device performance metrics and provide evidence-based clinical biomarker endotyping to help with sepsis prognosis. To achieve this, the sensor was explicitly designed to simultaneously detect seven host immune biomarkers as an extension to our recently published work [165] which demonstrated robust sensor performance metrics. This work builds on analyzing cytokine network (by monitoring IL-6, IL-8, and IL-

10) to unveil dynamic inflammatory pathogenesis in sepsis and understand the source of pathogen triggered immune response (bacterial presence reflected by levels of TRAIL and presence of viral infection with an increase in IP-10) combined with early and late-stage clinically established markers (PCT and CRP) to provide a complete profile on the patient's immune state at the bedside. We tested all the (24 hr) sepsis patient samples matched with two time points (at 6hr, n=44) along with 30 healthy controls (total sample size=124) to evaluate clinically valuable markers for sepsis prognosis to capture patient immune status via cytokine profiling. Additionally, we integrated the data with machine learning algorithms to predict the patient outcome for early analysis.

6.3.2 Reagents

Specific IL-6 IL-8, IL-10, TRAIL. IP-10, and CRP antibodies were purchased from Abcam (USA), while PCT antibody was purchased from Fitzgerald (USA). All the stock proteins were preserved for further use at -20°C or according to the storage conditions. To prevent denaturing the proteins, none of the proteins underwent more than 3 freeze-thaw cycles. Antibodies were diluted in PBS to get them to their optimized concentrations before use.

6.3.3 DETecT (Direct Electrochemical Technique Targeting Sepsis) sensor uses EnLiSense's Rapid Electro Analytical Device (READ) preparation

The DETecT sepsis sensor uses EnLiSense's READ platform that comprises of the following: (1) A disposable, single use sensor cartridge with an array of sensing electrodes, individually designed to detect multiple biomarkers simultaneously from a sample in real-time. (2) A handheld, palm-size form factor electronics reader on which the sensor is placed, which

transfers electrochemical output from the sample to other electronic devices via a software interface (configurable to support both wired and wireless communication). Briefly, the detection framework is governed by non-faradaic EIS. An electrochemical impedance response is measured due to subtle changes between antibody-antigen affinity interaction when a small input voltage (10mV) is applied to the sensor over a frequency spectrum by the electronic reader [46], [67], [76]. The sensor requires a small sample volume of <40uL and provides a result within < 5 mins. Assay protocols were similar to our previous work [28], [123]. Sensor characterization and performance were evaluated thoroughly in our recently published work [165].

6.3.4 Patient samples

Patient samples were derived from observational trials of sepsis conducted by the Austere environments Consortium for Enhanced Sepsis Outcomes (ACESO) in Cambodia, Ghana, and the United States (35, 36). The NMRC IRB approved all study protocols in compliance with all applicable Federal regulations governing the protection of human subjects and host country IRBs, and all participants, or their legally authorized representatives, provided written informed consent. Briefly, adult patients presenting to a participating hospital's emergency department with suspected infection (as judged by the attending physician) and met at least two of three SIRS clinical criteria (SEPSIS-2 criteria) were eligible for enrollment. The severity of illness was assessed by calculating the quick Sequential Organ Failure Assessment (qSOFA) score at 6 hours by the participating hospitals (Supplementary fig S24).

The University of Texas authorized this study at Dallas IRB (IRB#19MRO151). Matched patient plasma samples collected six hours (T1) after enrollment (n=44) and 24 hours (T2) after

enrollment (n=50) were provided, stripped of identifying information, by ACESO [128], [168]. Of the total 50 patient samples, 6 patient plasma samples were not collected at six hours, with 44 matched samples. De-identified samples were received at the Biomedical Microdevice and Nanotechnology Laboratory, UT Dallas, processed immediately upon arrival, and stored at a temperature of -20°C until further use. They did not undergo more than two freeze-thaw cycles. An additional 30 plasma samples collected from healthy controls were purchased from Boca Biolistics (Pompano Beach, FL, USA).

6.3.5 Biomarker analysis

Plasma concentrations of pro & anti-inflammatory cytokines (IL-6, IL-8, IL-10), chemokines (TRAIL & IP-10) and inflammatory biomarkers (PCT & CRP) were measured using (1) Luminex as a reference standard (2) DETecT sepsis device as the proposed method of detection in UT Southwestern medical center.

6.3.6 Statistical Analysis

Statistical analysis was performed using GraphPad Prism Software (GraphPad Software Inc., La Jolla, CA). ns: non-significant, *P < 0.05, **P < 0.01, ***P < 0.001, ****P < 0.0001. Data represented as mean ± SEM for n = 3 replicates unless stated otherwise. One-way analysis of variance (ANOVA) was used for the comparison between three or more groups. T-test was used to compare significance for specific signals against non-specific interferons in the cross-reactive study. Differences between healthy and septic cohorts were assessed using non-parametric unpaired Mann-Whitney tests. Biomarkers assessed by two methods were correlated, and the difference between the methods was assessed using Bland-Altman analysis.

Receiver operating characteristics were performed to validate DETecT sepsis sensing device specificity and sensitivity to differentiate healthy from septic patient cohort using Wilson/Brown method with GraphPad Prism. Multidimensional analysis was carried out to determine whether the different conditions of interest could be differentiated based on multiple cytokine profiles. Patients were categorized based on their biomarker concentration levels. Group A was classified for patients whose biomarker concentration decreased from 6 hours to 24 hours and was termed as recovery state. Patients whose biomarker concentrations increased from 6 hours to 24 hours and still survived were termed as late recovery and were placed in group B. Finally, group C contained deceased patients based on the 28- day mortality status.

Principal component analysis (PCA) was used to visually evaluate if a healthy cohort was separable from septic patients along with various other input criteria. In PCA, each point is expressed in a 2- dimensional space by a single point in point so that if 2 patients share similar characteristics, the closer they are to each other. Therefore, the central idea of PCA assessment is to identify if patients with or without a specific outcome may be grouped into two separate categories, or they may not be discernible. The PCA transformation is achieved through various steps. The data is first standardized to have mean values centered at 0 and a variance of 1. This step is essential to mitigate skewing of data due to few large values. Next, all the study biomarker values were transformed before proceeding to the PCA step. The next step was to compute eigen vectors and corresponding eigen values. The eigen decompositions provide the maximum variance and its contribution from the input feature set. The most prominent eigen pairs were sorted in descending order until the original dataset's threshold value of information variance was achieved. The visualization of PCA is done with the help of

the first and second principal components, as they have the maximum variance explained. The variance explained by every component is discussed in the results and discussion section separately. The datapoint represented in the lower dimension were assigned a different color for clarification. PCA was assessed in two different ways. First, we differentiated the data into a healthy and septic cohort. Then, within the septic cohort, we visualized mortality and survival (supplementary fig S2).

Similarly, data was segregated based on T1 &T2 diagnosis and site of infection (supplementary S3-S6). Next, we used a correlation matrix to assess the relation amongst variables. The correlation coefficient was calculated using the Pearson's correlation formula

$$r_{xy} = \frac{n\sum x_i y_i - \sum x_i \sum y_i}{\sqrt{n\sum x_i^2 - (\sum x_i)^2}\sqrt{n\sum y_i^2 - (\sum y_i)^2}}$$

r_{xy} = Pearson r correlation coefficient between x and y

n = number of observations

x_i = value of x (for ith observation)

y_i = value of y (for ith observation)

The formula gives the value r between the two variables x and y where r can range from -1 to 1. Values nearing 1 suggest a strong positive relation; similarly, values nearing -1 represent a robust negative relationship. The value 0 suggests no correlation between the variables. The correlation was visualized using the heatmap. Furthermore, we used agglomerative hierarchical cluster analysis, which allowed identifying patient subgroups sharing similar traits. Patients with similar characteristics were classified within clusters. The percentage difference was calculated between the 6 hr time point and 24 hr time point by the equation {(6

hr – 24 hr)/6 hr}. The process was repeated for all the biomarkers. The Pearson's coefficients were visualized using the correlation matrix and cluster mapping. We used the Apriory algorithm to derive associations within the biomarkers. Apriory algorithm is based on the association between the two components. It is a type of association analysis that yields an association rule. This helps us explore the relationship within the dataset regarding the association between the study biomarkers. The study biomarker has been used as the presence of marker from the given patient's value. This gives us the frequency occurrence of each biomarker. Based on this data, the association has been calculated. The association is presented in terms of support and lift. The support is given by

$$supp\ (X) = \frac{|\{X \subset T\}|}{|T|}$$

Confidence is defined as

$$conf(X \rightarrow Y) = \frac{supp(X\ \cup\ Y)}{supp\ (X)}$$

Lift is defined as

$$lift\ (X \rightarrow Y) = \frac{supp\ (X \cup Y)}{supp\ (X) \times supp\ (Y)}$$

Based on the above values, we chose support more than 50% and confidence to be more than 80%. In other words, this means we chose the combination in which it occurs in 50% of the dataset, and within that, we see more than 80% occurrence.

The data was categorized based on the difference between T1 (6 hr) and T2 (24 hr). The derived association rules were tested to have minimum 0.2 support and 0.14 within the survival group, and their confidence was evaluated. We used network visualization to envision the

results from this algorithm, where each node represents the biomarker in association with the edge represented as the association rule. Finally, a machine learning model was built to predict patient mortality [169]. The input parameters for the machine learning model were taken as the difference between the matched patient time-points T1 (6 hr) and T2 (24 hr) along with age, gender, and qSOFA. The training dataset comprised 70% data, while 30% data was used for testing. We have used the decision tree for the classification algorithm as it has shown to be one of the best performing algorithms with high accuracy (supplementary S12). The decision tree is kept shallow to improve the accuracy of the model. If the decision tree is deep, it may include an outlier and try to overfit the data. Hence to avoid overfitting, the decisions tree is as shallow as possible. Here we tried various parameters. The depth of the decision tree should be comparable to the classes present in the dataset. Without tuning for the depth, the model gives a tree with depth 5, but a tree of depth 2 can achieve the same results. Therefore, we have kept the maximum depth as 2 (supplementary fig s13).

6.4 Results

6.4.1 Patient characteristics for sepsis evaluation

50 patients were included from three locations (Cambodia, Ghana & the United States) for this work. Following adjudication, 3 (6%) patients were excluded for patient demographic representation as they were missing metadata. However, all the patient samples were tested, biomarker levels were quantified on the reference Luminex standard and DETect device and data analysis was included as biomarker levels were agnostic to the patient demographic information. Septic patients were measured across two-time points T1 and T2 (6 hr and 24 hr post-hospitalization) and 30 samples were collected from a healthy control totaling to 124

samples. The adjudicated diagnosis (fig 6.2A) and adjudicated location (fig 6.2B) indicate that 29% of the patients with sepsis had respiratory tract infection, followed by 20% of patients with bacteremia as the primary adjudicated diagnosis. Visual representation of the patients enrolled in this study is included in supplementary fig S1 & table S1. Of the patients with sepsis, 26 were male and 21 were female, as shown in sup fig S1B. The average age was 47 (18-85). Median quick sequential organ failure analysis (qSOFA) was 2 (0-3). 72% of patients survived, 20% died, and no data was collected for the remaining 8% of the study population at the end of 28 days. There was no significant difference in age (Supplementary fig S16-S22) and gender between the patients with sepsis and the healthy controls.

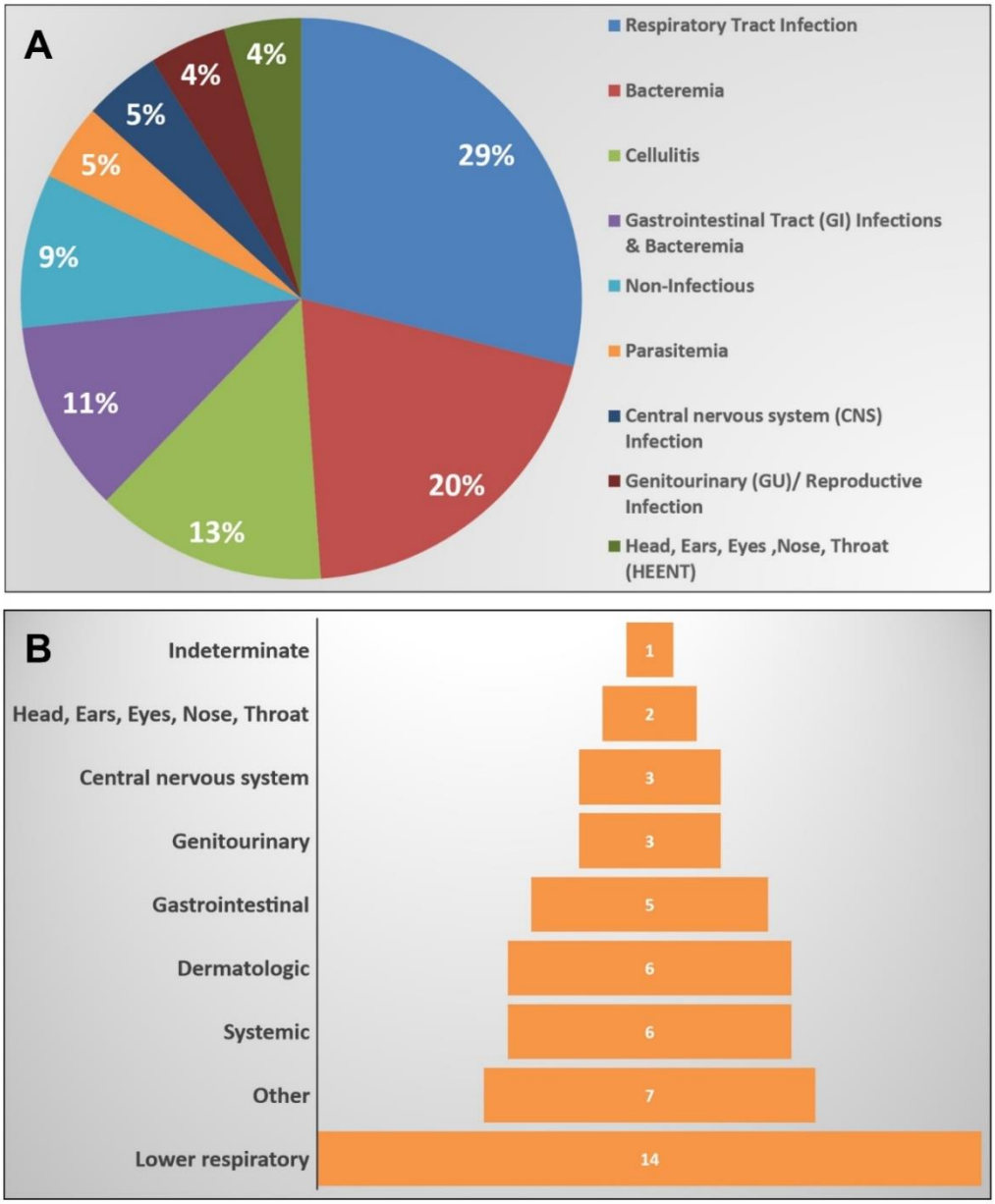

Figure 6.2.A) Adjudicated diagnosis for the 47 sepsis patient samples represented as a pie chart E) Adjudicated location at the time of patient enrollment with patient classification.

6.4.2 Quantification of host immune response biomarkers using patient samples

Our approach was to choose specific biomarkers that could reflect the everchanging state within the host immune response to gauge the nature of sepsis progression. Fig 6.3A shows

the pathway of an activated host immune response post local infection and how DETecT sepsis device can be of importance to quantify the uncontrolled cytokine release in plasma. A combination of pro-inflammatory and anti-inflammatory biomarkers of IL-6, IL-8 and IL-10 were chosen to indicate the hyperimmune and immune suppression state of the patient host immune response. IL-6 and IL-8 have been positively correlated with the early 24 hours after sepsis initiation. In comparison, IL-10 levels have been shown to reflect the immune suppression state to suppress the hyperimmune response. The second combination of biomarkers consisted of pathogen-related biomarkers. Previous studies have indicated that significant differences in TRAIL levels from control samples have been correlated to the bacterial presence.

In contrast, increased levels of IP-10 have positively correlated to the presence of viral infection. Therefore, the combination of TRAIL and IP-10 will indicate relevant pathogen information which can assist physicians in initiating pathogen-specific treatment response. The last combination includes well-established biomarkers of CRP and PCT, which have been widely accepted to indicate the presence of sepsis as an early and late-stage biomarker.

To provide dynamic information regarding patient immune response, a panel of seven biomarkers was quantified using DETecT sepsis device for a total of 80 patient samples as seen in fig 6.3(B-H) and patient characteristics have been tabulated in Supplementary (table S1). There was a significant difference between the healthy control samples and the septic patient cohort for all seven biomarkers. All biomarkers except TRAIL showed a significant increase for patients with sepsis. TRIAL showed an inverse trend where septic-patient sample concentrations were significantly lower than the healthy control cohort. The significant

differences observed between healthy and septic samples indicate the chosen biomarkers' importance (supplementary table S2).

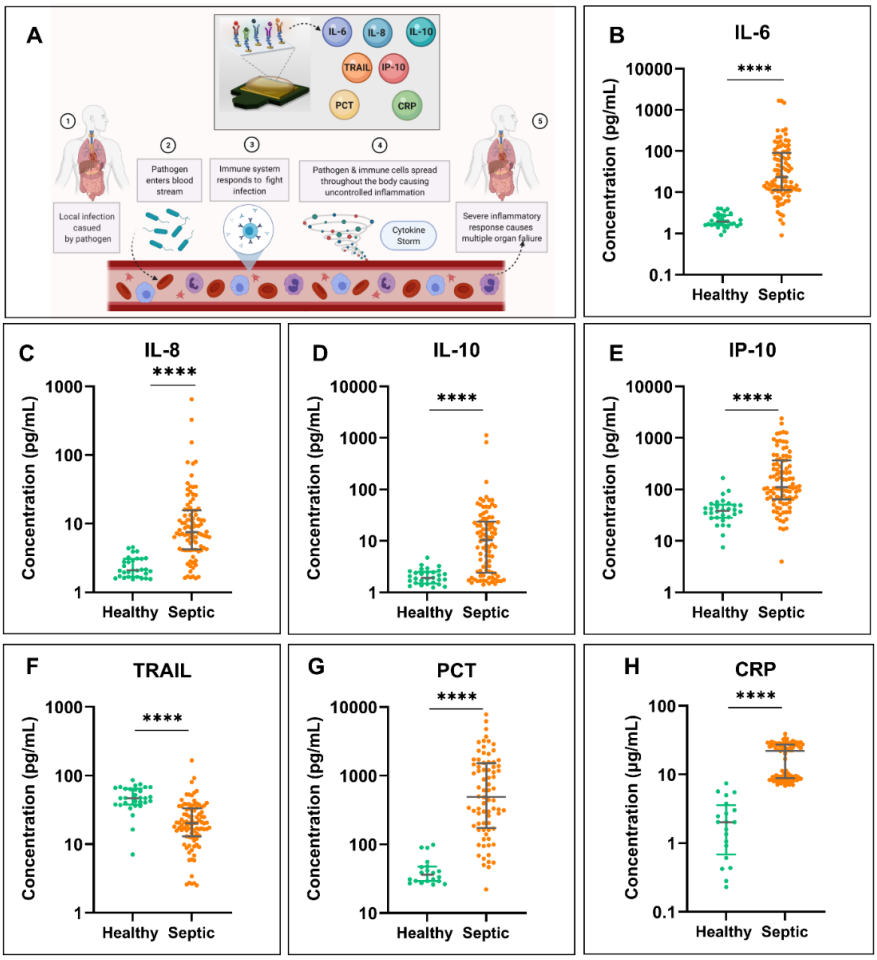

Figure 6.3. A) Projected Inflammatory host immune response post-infection and effectiveness of DETecT sepsis device quantifying the presence of the cytokines expressed in plasma. (B-G) Quantification of host immune biomarkers using DETecT sepsis device classifying healthy (n=30) vs septic patient cohort (n=124) with samples collected from healthy samples and two time points from septic patient cohort. Significance between the groups was calculated using Mann- Whitney U statistical test. Note: **p < 0.01, ***P < 0.001, ****P < 0.0001.

6.4.3 Patient sample validation comparing DETecT sepsis device with reference standard LUMINEX technique for pre-clinical utility

It is vital for the developed sensor to exhibit strong agreement with the current standard reference technique to be used in clinical use-case. Thus, DETecT sepsis device performance

was validated with clinical reference LUMINEX as a standard technique to evaluate the quantification of the seven biomarkers in patient plasma samples as represented in schematic fig 6.4A. All patient samples (including healthy controls) were tested using both methods. Concentrations measured by DETecT sepsis device correlated well with the LUMINEX standard for all seven biomarkers (Pearson's $r > 0.94$), as seen in fig 6.4 (B-H). In addition, the concentrations were tested over a wide dynamic range for the healthy and septic patient cohorts to capture the diseased state and recovery state according to the physiologically relevant ranges.

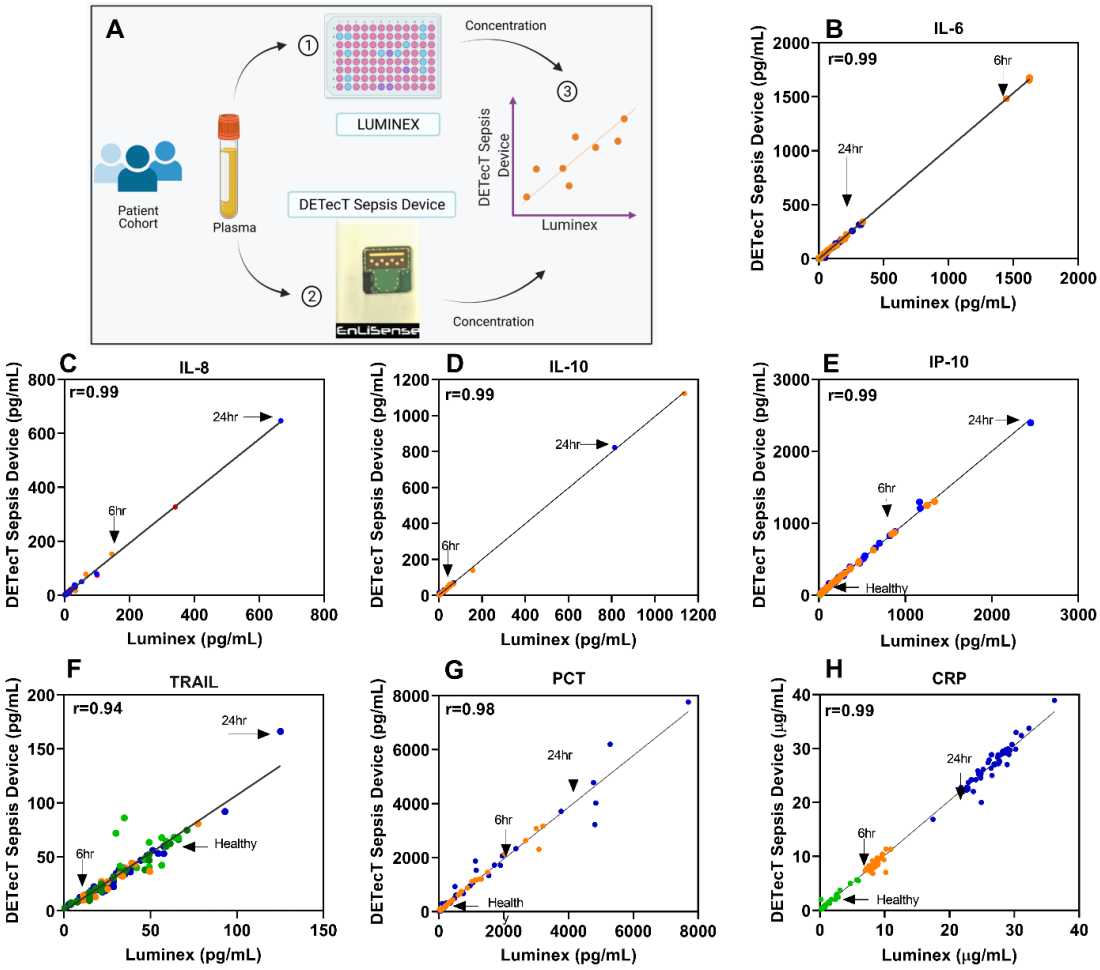

Figure 6.4.A.Schematic of patient plasma samples for correlation of DETecT sepsis device with LUMINEX reference standard. (B-H) Patient sample validation using reference LUMINEX method for IL-6, IL-8, IL-10, TRAIL, IP-10, CRP and PCT correlated with DETecT sepsis device.

The difference between the two methods was assessed using Bland-Altman analysis, as seen in Fig 6.5. Low mean bias and low variance of the mean bias for all seven biomarkers show the degree of closeness in measuring patient samples by both methods (fig 6.5B-H). Therefore, the developed sensor showed comparable results when validated against the clinical reference LUMINEX standard. These results provide confidence in the DETecT sepsis device. Additionally, to comprehend the overall device accuracy to differentiate between healthy state

and septic state for each test biomarker, Receiver operating Curve (ROC) analysis was used. Patients with confirmed sepsis were compared with healthy control subjects, and values were obtained using the cutoff that reflected the best discrimination as determined by the ROC (supplementary table S3 for cutoff values). Area under the curve (AUC) for all the seven biomarkers was above 0.83 (supplementary fig S25), which signifies that the chosen biomarkers distinguished healthy and septic cohorts with good sensitivity and specificity using DETecT sepsis device. CRP showed the best ability to discriminate healthy from the septic cohort with an AUC of 0.99. The next good analytes following CRP were PCT and IL-6 with an AUC of 0.97 followed by IL-8. This indicated that CRP, PCT, IL-6 and IL-8 would provide 97-99% sensitivity & specificity for discriminating healthy and septic cohorts. Therefore, the clinically established biomarkers (CRP & PCT) combined with the pro-inflammatory (IL-6 and IL-8) markers provide robust accuracy using the DETecT sepsis device. Lastly, the anti-inflammatory biomarker IL-10 showed the least AUC of 0.83. LUMINEX did not report many concentrations in healthy subjects for IL-10, which resulted in a very low AUC of 0.56. On the contrary, the DETecT sepsis device showed quantification for all healthy subjects for IL-10 due to its ultra-sensitive detection capability. This is an advantage with DETecT sepsis device as the recovery state of the patient can also be captured by tracking low concentrations in plasma.

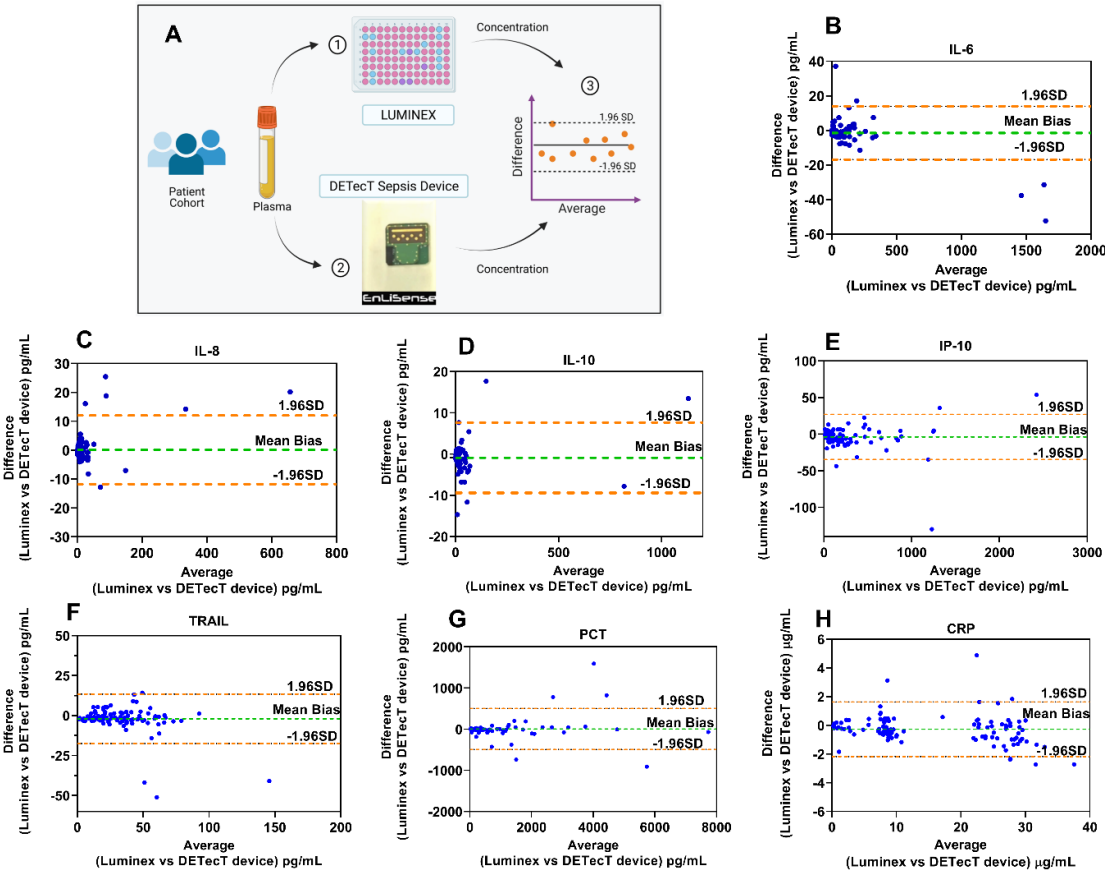

Figure 6.5. Schematic of patient plasma samples for method comparison between DETecT sepsis device and LUMINEX reference standard. (B-H) Bland Altman analysis measures the degree of closeness across the developed DETecT sepsis device and reference standard LUMINEX method using patient plasma samples.

6.4.4 Patient categorization based on the signature combination of biomarkers

We classified the patients into three groups according to the difference between the biomarker concentrations. Group A (n=26) consisted of patients who recovered from sepsis and survived by observing a decrease in biomarker concentration between 6 hour and 24-hour time points. Group B (n=8) was classified with patients who recovered late and survived sepsis (despite biomarker concentration increase from 6 hour to 24 hour). Group C (n=10) were patients who died during the study based on 28-day mortality status (Supplementary fig S23). The samples

were grouped into non-overlapping categories. More information about categorizing can be found in the methods section. A distinct trend between the temporal response and the patient outcome was observed. Fig 6.6A shows the concentration of specific biomarkers between T1 (6hr) and T2 (24hr) time points classified in groups A, B, and C. The concentration decreases significantly from T1 to T2 for IL-6, IL-8, IL-10, and PCT, indicating early recovery for patients in group A. This signifies IL-6, IL-8, andL-10 (Marchant et al., 199), and PCT can be used as early-stage biomarkers for identifying sepsis prognosis.

Despite a significant increase in IL-10, IP-10, PCT and CRP concentration, patients clustered in group B survived the initial 28 days post-admission and were classified as late recovered patients. High levels of IL-10 concentration (mean 123±283 pg/mL) within the first 24 hours is known to inhibit and eventually stop inflammatory response, making it an anti-inflammatory cytokine [170]. This behavior is seen in patients categorized in group B who survived 28 days post-admission. Biomarker concentrations did not change significantly for patients who died within 28 days except for IL-10 and CRP. This shows that initial two-time points (6 hr and 24 hrs) may not be sufficient to predict the 28 days survival status based on the current grouping system for this study as many factors may affect the biomarker concentrations like patient history, antibiotic, treatments, etc.

The difference between T1 and T2 for each group for a given biomarker is shown in fig 6.6B. IL-6 showed significant differences between early recovered patients (group A) compared to late recovered patient groups (group B), followed by significance between early recovery (group A) and non-survivors (group C) which demonstrates that dynamic time-based response can be observed to help understand changes in the host immune state. IL-10 showed significant

between-group differences indicating that IL-10 can respond dynamically, reflecting possible changes in the patient's immune state. TRAIL, IP-10, and PCT distinguished patients classified under group B from group C significantly, indicating the use of these biomarkers can identify recovered patients from non-survivors within the first 24 hours. IP-10 showed significance from group A to group B and group B to group C when compared individually. This highlights that IP-10 concentrations may change at the 24 hr time point indicated as a later stage biomarker. Thus, the hypothesis that PCT is an early-stage marker for the clinically established markers and CRP is a late-stage marker is verified. The PCT levels for group A significantly decreased, whereas the CRP levels for group B show significance. Both biomarkers show significance in patients who had a poor outcome, which signifies the importance of the early and stage biomarkers during disease prognosis.

Patient history with information on underlying conditions affects the biomarker concentrations. Thus, categorizing the patients based on comorbid conditions may provide better patient-centric treatment strategies. Connecting the patient history with the biomarker levels could provide valuable insights into why patients are stratified into specific groups. Group A contained 25% of patients with respiratory tract infection and had a history of chronic lung disease. The adjudicated location classified as other (including bacteremia, cellulitis, or non-infectious) accounted for 21% of patients. Genitourinary (GU), head, eyes, ears, nose, and throat (HEENT), and dermatology accounted for 21% of patients in each category. 18% of patients from group A suffered from a gastrointestinal infection. The remaining 14% of patients were categorized under systemic infection. For the 8 patients classified under group B, 3 patients died with 1 year (within 34,44 and 150 days after initial admission). Lower

respiratory tract infection and dermatologic diagnosis each accounted for 38% of the patients. In contrast, systemic and GU each contributed to 13% of the total patients classified in group B. Similarly, in group C, out of all the patients who died within 28-days, 50 % had diabetes, and 40% suffered from hypertension.

Biomarker levels were correlated with lab results for the septic patient group across both time points to determine any coherent relationship. The highest correlation of 0.98 between biomarkers was found between PCT (24hr) and IL-8 (24hr), CRP (6hr) and IL-8 (24hr), and IL-10 (6hr) with PCT (6hr). Il-6 and IL-8 correlated well with a coefficient of 0.91, while TRAIL and IP-10 showed a 0.85 correlation coefficient. When the biomarker levels were compared with lab results, TRAIL (6hr) and Chloride, PCT (24hr) and blood urea nitrogen (bun), TRAIL (6hr) and alanine transaminase (alt) and TRAIL (6hr) with eosinophils showed a correlation of 0.9. TRAIL has been implicated in the pathogenesis of metabolic disorders, including diabetes and hypercholesterolemia in experimental studies [171]. Additionally, a low number of eosinophils in blood tests can indicate blood infection (sepsis). Studies have shown after an episode of hypotension or shock, aspartate aminotransferase (AST) and alanine aminotransferase (ALT) are rapidly and significantly elevated, with AST predominating over ALT [172].

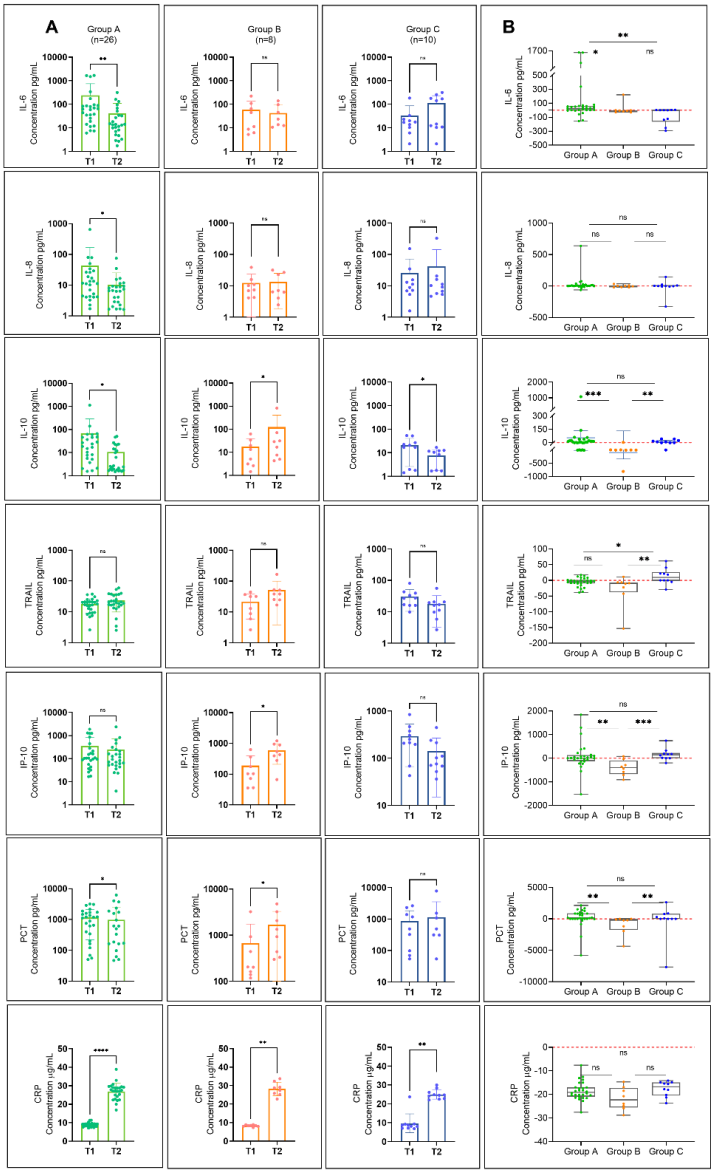

Figure 6.6.A. Patient categorization based on the signature combination of biomarkers. Patient plasma samples were measured using the DETecT sepsis device at 6 hr and 24 hr with 124 samples in total. Patients were classified into three groups; group A: recovered (n=26), group B: late recovery (n=8), and group C: died (n=10) B. Temporal changes were seen in septic patients across three groups is represented as the difference between the two time points. Each box indicates the lower and upper quartile values, and the line in between represents the median, and the whiskers are represented as 1.5 times the value. The line at 0 indicates no difference between T1 (6 hr) and T2 (24 hr). Significance between the groups was calculated using the Two-sided Man Whitney U statistical test.

6.4.5 Exploratory sepsis analysis shows biomarker associations across patient cohorts

We used PCA to visualize the 80-patient cohort using each biomarker's T1 and T2 values (fig 6.7A). PCA analysis shows healthy control samples could be separated from the septic patient cohort with minimal overlap. The separation boundary between healthy and septic cohorts is seen in the plot, with separation occurring at x = -1. The septic subjects have more spread for the y-axis than the healthy subjects. The PC1 component is dominated by CRP (T2) with a 47% contribution, followed by TRAIL (T1), CRP (T1), PCT (T1), TRAIL (T2). The PC2 component is dominated by IL-10 (T2) with 60% weightage, followed by TRAIL (T2), IP-10 (T2), IL-8 (T2), and PCT (T2). Noticeably, the predominant features of PC2 are all from T2. The respective weightage of PC1 and PC2 components is represented in supplementary table S4.

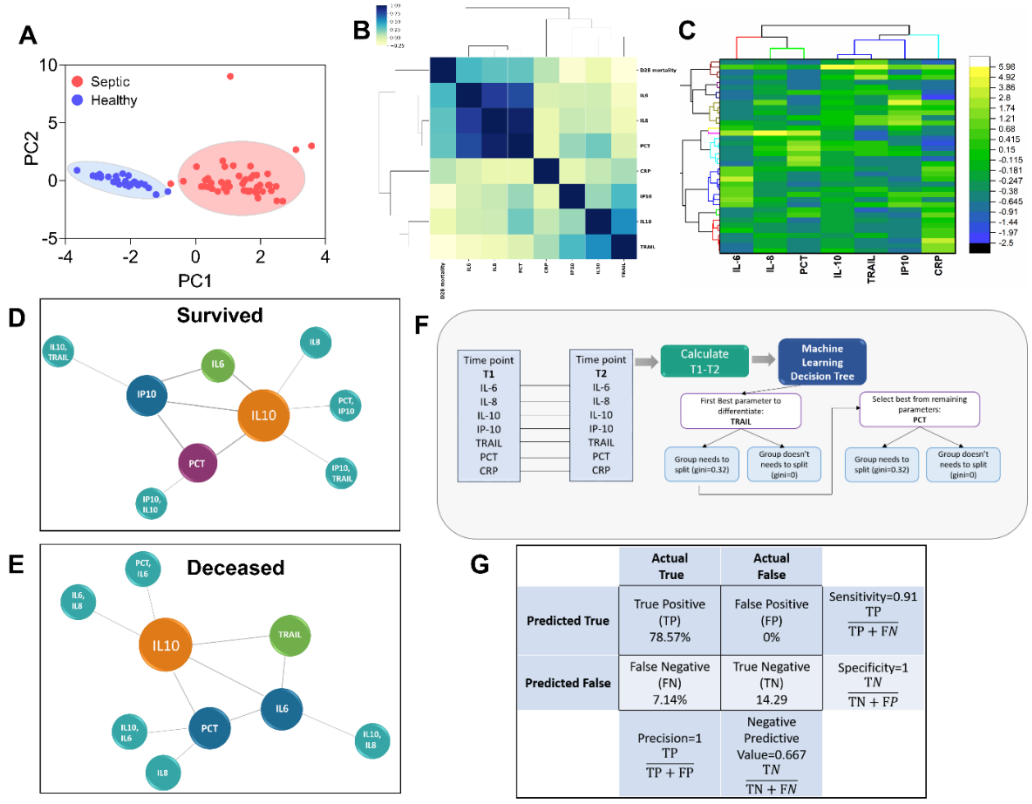

Figure 6.7. Exploratory analysis of patient samples with sepsis. A) Principal component analysis representing the clear differentiation of the healthy cohort from the septic patient cohort. B) Correlation and cluster analysis of matched patients considering percentage change of each biomarker level across T1(6 hr) and T2(24 hr) with respect to T1(6 hr) considered as baseline. C) Cluster analysis heat map of all patients with seven biomarkers. Each column represents the biomarker level, and each row represents every patient sample. D) The network visualizes biomarkers associated with patient survival considering a change in biomarker levels from T1 (6 hr) to T2 (24 hr) using an Apriori algorithm. E) Network visualized for biomarkers associated with deceased patient state considering a change in biomarker levels from T1(6 hr) to T2(24 hr) using Apriory algorithm. The size of each node represents the number of associations with other biomarkers. The most significant size has a maximum of 6 associations, whereas the smallest node size is associated with only one other biomarker. F) Machine learning-based survival prediction using a decision tree where matched patient sample time-points for all seven biomarkers and age, gender, and qSOFA are considered input parameters. The first subgroup split is based on TRAIL, while the second level is based on PCT with threshold values of 17.931 pg/mL and 2390 pg/mL, respectively. Gini impurity is tending towards 0, indicating the purity of the node and model's success in classifying survived patients from deceased with an accuracy of 92.85 %. G) Confusion matrix classifies survived from the deceased patient cohort with a false-positive error of 7.14 % due to the small data set. False-negative error is absent, reducing chances of type 1 error.

Next, we performed survival analysis to predict the survival ratio in the patient cohort (supplementary fig S7). From admission, the chances of survival drop to 65% at the end of 350 days, whereas the survival ratio is 90% until 30 days. This elucidates the 28- day mortality is higher for septic patient cohorts. Further, we analyzed hierarchical clustering of Pearson's correlation with the two matched time-points for all seven biomarkers for all patients, as seen in fig 6.7B. The figure is the combination of the cluster mapping and correlation heat map. The cluster mapping shows the two dominant clusters. Correlation and cluster analysis of matched patient samples were considered as a percentage change of each biomarker level across T1 (6 hr) and T2 (24 hr) with respect to T1 (6 hr) biomarker level as the baseline. From the correlation matrix, the highest Pearson coefficient of 0.95 was between IL-8 and PCT followed by IL-6 and IL-8 (0.81) and PCT and IL-6 (0.71). These pairs of biomarkers show a similar trend, followed by IL-10 and TRAIL, which show a correlation of 0.54. Refer to supplementary fig S8-S11 for individual correlation and cluster analysis of matched patients for two-time points.

Similarly, fig 6.7C is a cluster heat map with patient ID as rows and biomarkers represented as columns. The first cluster was formed between IL-8 and PCT, followed by IL-10 and TRAIL. These subgroups intern correlated with IL-6 and IP-10, respectively. The second subgroup formed a cluster with CRP and finally joined the first subgroup of IL-6.

The network of biomarkers associated with the survived state (fig 6D) and deceased state (fig 6.7E), using the change in biomarker levels from 6 hr to 24 hr (as seen in fig 5B) were created using the Apriory algorithm (supplementary fig S14 & S15 for network analysis based on threshold analysis). The size of each node represents the number of associations with other biomarkers. The most significant node size has a maximum of six associations. In contrast, the

smallest node size is associated with only one other biomarker. As seen in fig 6.7D, IL-10 associates with six biomarkers for the survived patient cohort, followed by IP-10 with four and PCT with three. IL-10 showed dominance with five associations in the deceased state, followed by IL-6 and PCT with four each. The different levels of associations within 6 to 24 hours of admission in varying conditions can be helpful in patient endotyping and risk stratification through rapid screening using the DETecT sepsis device for improved patient outcomes. In addition, these biomarker associations can help direct the clinician on the type of medication to improve patient survival by understanding immune response at a particular time within sepsis pathophysiology.

Additionally, a machine learning-based decision tree algorithm was utilized to classify healthy and septic patient cohorts accurately, where matched patient sample time-points for all seven biomarkers and age, gender, and qSOFA were considered input parameters. We integrated the patient sample data using a machine learning algorithm and selected a decision tree as the best fit for other algorithms (supplementary fig S3). The difference between the two time points for all the biomarkers was given as input. Based on the time difference, the decision tree algorithm classifies TRAIL as the first sub-group with a 17.931 pg/mL threshold followed by PCT with a 2390 pg/mL threshold. Gini impurity was seen to be tending towards 0, indicating the purity of the node and model's success in classifying survived patients from deceased with an accuracy of 92.85 %.

Furthermore, fig 6.7G illustrates the confusion matrix, which classifies patients who survived from the deceased patient cohort with a false positive error of 7.14 % due to a small data set. A false-negative error was absent, reducing the chances of type 1 error. With this study, we

leveraged the combinatorial power of rapidly measuring a panel of seven biomarkers and combined it with machine learning model to accurately predict the patient outcome when presented with two-time points in the earlier stages of sepsis. This elucidates the capability of DETecT sepsis platform to be used as a holistic enabling technology useful for patient endotyping and risk stratification, providing valuable insights for physicians while treating patients with sepsis.

6.5 Discussion

Herein, we present the validation of the developed DETecT sepsis device as an enabling technology to visualize patient sepsis outcomes. We stratified patient samples at 2 matched time points and 30 healthy donor samples by measuring a panel of 7 host immune response biomarkers on a single platform. Our approach aimed to efficiently characterize patient samples as in an analytical, empirical longitudinal system for clinicians. The DETecT sepsis device was able to quantify 7 biomarkers simultaneously using as little as 40 µL of the patient sample, which provided results in less than 5 mins. The developed DETecT sepsis device can be imagined as an enabling technology capable of stratifying patients based on the temporal immune response.

Furthermore, the device may provide a means to quantify the biomarker levels and gauge if the patient is recovering based on active feedback at the patient's bedside. This could facilitate quicker response time for clinicians to administer specific drugs during a state of infection. The developed sensor outperforms the comparable clinical analyzers that require many additional steps for assay preparations and has a longer turnaround time for results to be reported. In conclusion, we demonstrated the value of combining cytokines, chemokines, and

protein host immune response biomarkers using small sample volume (<40 uL) and rapid response time (~5 mins) at the patient bedside to enable technology to monitor sepsis. Analytical understanding and a machine learning approach help provide meaningful information on configuring treatment strategies for personalized medicine for patients diagnosed with sepsis.

6.5.1 Limitation of the study

At first, although we have assessed seven biomarkers in various combinations, prospective validation would be further required. Second, a comparatively limited number of patients were involved in this study. Therefore, additional research is required to explain the role of the cytokine network in sepsis pathogenesis. Furthermore, since the septic patient samples were collected from three different locations, there could be a difference in how the samples were collected based on varying timelines. Furthermore, control samples were collected from healthy individuals from one location. Additional work will be required to determine how these values compare to patients hospitalized for reasons other than sepsis.

Future work will include building on this framework presented here using the DETecT sepsis device technology and validating with expanded sample sets representing a geographically, ethnically, and etiologically diverse set of host responses to infections. Failure to develop effective therapeutics and limitations of diagnostic tests in sepsis is often attributed to the heterogeneity inherent to the disease [173]. Therefore, we see the value of the DETecT sepsis platform in enabling personalized, rapid, and precise on-demand patient assessment. We hope that our research will serve as a basis for future studies on patient endotypying relying on the classification of selected biomarkers, including larger patient cohorts across multiple locations.

Although blood culture remains the gold standard for initial sepsis identification, rapid bedside POC testing will allow physicians to administer personalized patient treatment relying on individual host immune responses. DETecT sensor is an enabling technology that provides two diagnostic advantages over the current lab methods (i) it quantifies a panel of 7 pro and anti-inflammatory biomarkers that provide information on activation or downregulation of host immune response indicating the phase of sepsis (ii) Active patient immune feedback on status can help alter treatment strategies where immunomodulators or suppressants can be administered towards personalized medicine. Sepsis management would become more effective by monitoring patients' dynamic host immune response with multiple time-course analyses due to the proposed device's low sample volume (<40 uL). Utilizing the DETecT sepsis device with minimal sample handling also facilitates its usability in a low resource-challenging environment with reliable results. This enabling technology promises to be paradigm-shifting in achieving sepsis endotyoing by leveraging the plethora of biomarker information in easily accessible patient body fluid samples.

within the “golden hour” and initiate required treatment thus, avoiding the dynamic sequence of irreversible organ failure and subsequent death caused due to delayed response time. Finally, small form factor and ease in handling allow flexibility in using the device in a versatile environment (in an emergency department, or for bed-side monitoring) while ultra-low sample volume (< 40 µL) encourages physicians to collect multiple measurements within a day to monitor patients host immune response and assess the severity of sepsis. The study was limited to a small sample size of septic patients. However, these observations have several implications for research to integrate different host immune response biomarkers with self-integrated POC

devices for a better patient outcome. We are currently in the process of expanding our multiplexed capabilities and investigating sepsis pathophysiology via a larger patient cohort. In conclusion, this work has pioneered a potential solution to the current sepsis dilemma, by providing host response strategy to address complexity, shifting the paradigm of the on-going sepsis diagnostic approach.

CHAPTER 7

VALIDATION OF DETECT SEPSIS 2.0 DEVICE IN DIRECT WHOLE BLOOD PATIENT SAMPLES

7.1 Prior publication

AmbalikaS.Tanak performed the experiments, designed the experimental protocol, analyzed the data, and wrote the manuscript. Ambalika S. Tanak, Dr. Shalini Prasad and Dr. Sriram Muthukumar provided feedback on data interpretation. Abha Sardesai provided data on machine learning models.

This manuscript will be submitted to Bioengineering and Translational medicine journal in November 2021. The paper discusses the simultaneous detection of eight sepsis biomarkers directly in patient whole blood and identify relationship between multiple biomarkers groups.

7.2 Abstract

Sepsis is a silent killer, caused by syndromic reaction of the body's immune system to an infection that is typically the ultimate pathway to mortality due to numerous infectious diseases, including COVID-19 across the world. In United states alone, sepsis claims 220,000 lives, with a dangerously high fatality rate between 25-50%. Early detection and treatment can avert 80% sepsis mortality which is currently unavailable in most healthcare institutions. The novelty in this work is the ability to simultaneously detect eight (IL-6, IL-8, IL-10, IP-10, TRAIL, d-dimer, CRP, and G-CSF) heterogeneous immune response biomarkers directly in WB without the need for dilution or sample processing. The DETecT Sepsis (Direct Electrochemical Technique Targeting Sepsis) 2.0 sensor device leverages EIS as a technique

to detect subtle binding interactions at the metal/semi-conductor sensor interface and reports results within 5 minutes using only two drops (~100 uL) of blood. The device positively (r>0.87) correlated with lab reference standard LUMINEX for clinical translation using 40 patient samples. The developed device showed diagnostic accuracy greater than 80% (AUC> 0.8) establishing excellent specific and sensitive response. Portable handheld user friendly feature coupled with precise quantification of immune biomarkers makes the device amenable in a versatile setting providing insights on patient's immune response. This work highlights an innovative solution of enhancing sepsis care and management in the absence of a decision support device in the continuum of sepsis care.

7.3 Introduction

Sepsis and sepsis-related complications like multi-organ failure is indeed a substantial challenge on the healthcare systems and a major research concern for scientist around the world. Sepsis pathogenesis still remains unclear, despite significant fundamental research and clinical trials [174]. Sepsis is increasingly being recognized as incredibly diverse disease resulting from abnormalities within the inflammatory pathways. In the intensive care unit (ICU), sepsis is one of the most prevalent causes of mortality and in the United States alone, sepsis is responsible for up to half of all in-hospital fatalities. The global incidence of hospital-related sepsis in adults is estimated to be over 270 per 100,000, with an astonishing 26% overall death rate. There are 19.4 million cases and 5.3 million fatalities worldwide each year, excluding sepsis incidence amongst children and that which occur outside the hospital [175]. In the presence of an infection through pathogen, sepsis is developed as a systemic complication of the host immune system [176]. The pathogenic invader is the catalyst, while

the overzealous immune response of the host is to blame for the extensive organ damage that is a hallmark of the disease. The identification of several key biomarkers enable improved risk stratification and treatment decision making has stemmed from better understanding of the inflammatory events that contribute to host tissue damage in sepsis. There is substantial evidence that monitoring key biomarkers in the hyperinflammatory cytokine storm and acute phase response provide valuable diagnostic and prognostic indication of disease progression4. Interestingly, critically ill COVID-19 patients are known to have sepsis, often accompanied by infection and organ failure with elevated concentrations of cytokines ultimately leading to tissue damage, need for mechanical ventilator, and eventually death [177] . Cytokines are substances released by innate and adaptive immune system components that serve as signaling pathways or activators of the inflammatory response, which play a pivotal role in the development of sepsis [178].

Comprehensive mapping of the biomolecular milieu at a particular time point, is required for the development of viable treatment approaches. Previous research has identified a connection between blood levels of various cytokines, the severity of inflammatory response, and sepsis prognosis [141], [179]–[181]. The present workflow in a clinical setting follows a systemic process depending on the technology and manpower available to diagnose patients with sepsis. If a patient remotely exhibits early indications of sepsis (i.e SIRS criteria) antibiotics are immediately administered to target a variety of infectious sources before a disease is diagnosed [182]–[184]. Although this may enhance patient survival, such antibiotic regimens are futile and lead to antibiotic resistance [185], [186]. Parallelly, large volume of blood samples is collected in order to identify the causative pathogens and fine-tune the antibiotic prescription

for the patient. A bacterial culture, gram staining, and drug resistance test are amongst the few clinical tests used to verify whether the particular treatment successfully limits pathogen proliferation. The major disadvantage with these methods is that results arrive days after the patient is hospitalized, which may lead to missing out on a valuable timeframe for accurate medical diagnosis and planning effective interventions. The remaining techniques for quantifying sepsis-related biomarkers, such as flow cytometry and lactate tests, have a tendency of providing inadequate diagnosis in most scenarios because they often require large sample volume, have constrained detection ranges, are difficult to discern results, which only delays prognosis from trained clinicians, limiting their usage in resource-constrained environments across the world um[187]–[190]. Although some of the commercial POC sepsis technologies have managed to improve their reliability and efficiency in clinical tests, none of them have multiplexing capabilities any further than their focused primary biomarkers class, limiting their ability to obtain an extensive sepsis immunological patient profile.

A solution to this everlasting problem is the development of POC biosensing device with a capability to overcome all the underlying issues with the existing testing methodologies. To this direction, we have developed a multiplexed panel of simultaneously detecting eight crucial biomarkers by using merely two drops (~100 uL) of undiluted WB to rapid assess the patient immune response and project the possibility of patient undergoing sepsis, rapidly with a sample to result turnaround time of 5 minutes. The effort to bring results closer to patient bedside is propelled by designing miniaturized portable hardware coupled with sensitive EIS technique to assist clinicians to monitor disease progression and provide guided treatment. Our vision is to develop a sensing device that can appease the ASSURED (Affordable, Sensitive, Specific,

user-friendly, Rapid and Robust, Equipment free and Deliverable to end users) criteria set out by the World health Organization which could also be useful anywhere [191], [192]. The developed device is specially designed to be effective in resource-replete conditions where the objective is to attain quick test results, with minimal sample handling, along with a projection of disease severity with the help of machine learning model to aid in planning of an emergency intervention.

7.4 Methods

7.4.1 Experimental design of the study

This work is designed to validate the performance of the developed DeTecT sepsis 2.0 device for simultaneous detection of valuable sepsis biomarkers directly in WB. For this, the sensor was designed to perform multiplexed detection with good sensitivity and specificity. To validate the efficacy of the sensor against WB samples, 30 WB patient samples were procured from Discovery life science (Atlanta), that were declared positive for sepsis using reference laboratory standard technique. Parallelly, 10 healthy WB samples were procured from Carter blood bank (Texas) as positive control samples. Multiplexed biomarkers used for this work was IL-6, IL-8, IL-10, IP-10, TRAIL, Granulocyte-colony stimulating factor (G-csf), D-dimer, CRP. All the antigens and antibodies were purchased from Abcam. All the stock proteins were aliquoted and stored in -20°C until further use. To prevent denaturing the proteins, none of the proteins underwent more than 3 freeze-thaw cycles. Antibodies were diluted in PBS to get them to their optimized concentrations before use.

7.4.2 DETecT (Direct Electrochemical Technique Targeting Sepsis) 2.0 sensor uses EnLiSense's Rapid Electro Analytical Device (READ) preparation

The DeTecT sepsis 2.0 device consists of a uniquely designed sensor with sixteen independent electrodes on a single PCB platform. The gold deposited electrodes are equally spaced on the PCB surface to provide uniform fluid flow. All the sixteen working electrodes is deposited with a thin layer of zinc oxide (ZnO) uniformly to attain high sensitivity. The deposited sensor is then mounted on a handheld reader device which encompasses the portable electronics with EIS module for the signal detection. The reader is compatible to support both wired and wireless communication. The detection mechanism is based on EIS framework where subtle changes that occur at the electrode solution interface can be detected on applying a small input voltage over a frequency spectrum. The sensor requires sample of approximately 100 uL which is equivalent to two drops of blood. The detection occurs immediately, and results can be read within 5 minutes. Shorter measurement times ensures the blood does not clot and measurement is taken promptly. Assay development, sensor characterization and validation were performed using similar protocols followed in our previous work[117]. Machine learning algorithms were implemented to visualize and predict the healthy and septic patient groups using supervised and unsupervised algorithms.

7.4.3 Statistical analysis

Graphpad software was used to perform statistical analysis (GraphPad Software Inc., La Jolla, CA). *P 0.05, **P 0.01, ***P 0.001, ****P 0.0001. ns: non-significant, *P 0.05, **P 0.01, ***P 0.001, ****P 0.0001. Unless otherwise noted, data is provided as mean SEM for n = 3

replicates. For comparisons between three or more groups, one-way analysis of variance (ANOVA) was performed. In the cross-reactive investigation, the T-test was utilized to examine the importance of particular signals vs non-specific interferons. Non-parametric unpaired Mann-Whitney tests were used to compare the healthy and septic cohorts. Biomarkers were compared using two methodologies, and the difference between them was determined using Bland-Altman analysis. Wilson/Brown method using GraphPad Prism was used to assess DETecT sepsis 2.0 device specificity and sensitivity to identify healthy from septic patient group using receiver operating parameters. Along with many additional input criteria, principal component analysis (PCA) was utilized to visually evaluate if a healthy cohort could be distinguished from septic patients.

7.5 Results

7.5.1 Spike and recovery

The blood panel with eight biomarkers each have individual standard curves containing wide dynamic range to cover healthy and sick individuals with varying dose concentrations. Efficacy of the DETecT Sepsis 2.0 device was done by spiking a known concentration to the blood matrix and measuring the concentration using the calibrated curve for each biomarker (figure 7.1, A-H). The recovery of the spiked sample was determined by comparing it to calibrated dose response curve for individual biomarkers. Mean recovery concentration for the blood panel biomarkers was 105±6 % which lies within the accepted assay range according to the CLSI standards [78]. When compared individually, the coefficient of determination, $R2 > 0.97$ implies the assay for the sensor device is linear with negligible matrix effect.

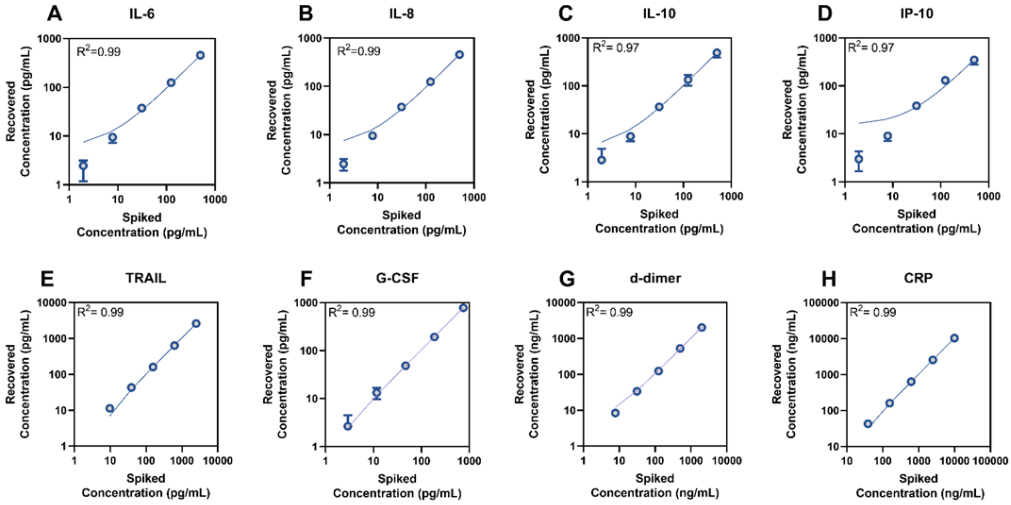

Figure 7.1. (A-H) Spike and recovery in WB sample using n=3 sensors to demonstrate assay linearity using DETecT Sepsis 2.0 device for IL-6, IL-8, IL-10, IP-10, TRAIL, G-CSF, d-dimer and CRP with R2>0.97.

7.5.2 Specificity

Analytical specificity and selectivity of the DETecT Sepsis 2.0 device was evaluated by cross reactivity study using bovine serum albumin (BSA) in WB buffer matrix. Every analyte was tested with low concentration of BSA followed by high concertation of BSA depending on the target analyte's dynamic range. This was followed by adding low concertation of target specific analyte and signal response was measured. Percent reactivity was calculated depending on the signal response for individual target analytes. As seen in figure 7.2 (A-H), DETecT Sepsis 2.0 device was able to distinguish the specific target signal with ~100% reactivity and non-specific signal accounted less than ~10% reactivity. When evaluating actual clinical samples, where the concentration of the actual analyte might be significantly lower than those of the non-specific molecule, the biosensor's selectivity is essential. Overall reactivity less than 10% for the non-specific BSA molecule indicates that DETecT Sepsis 2.0

device selectively binds to the target analyte with minimal interference from the non-specific molecules present in WB samples.

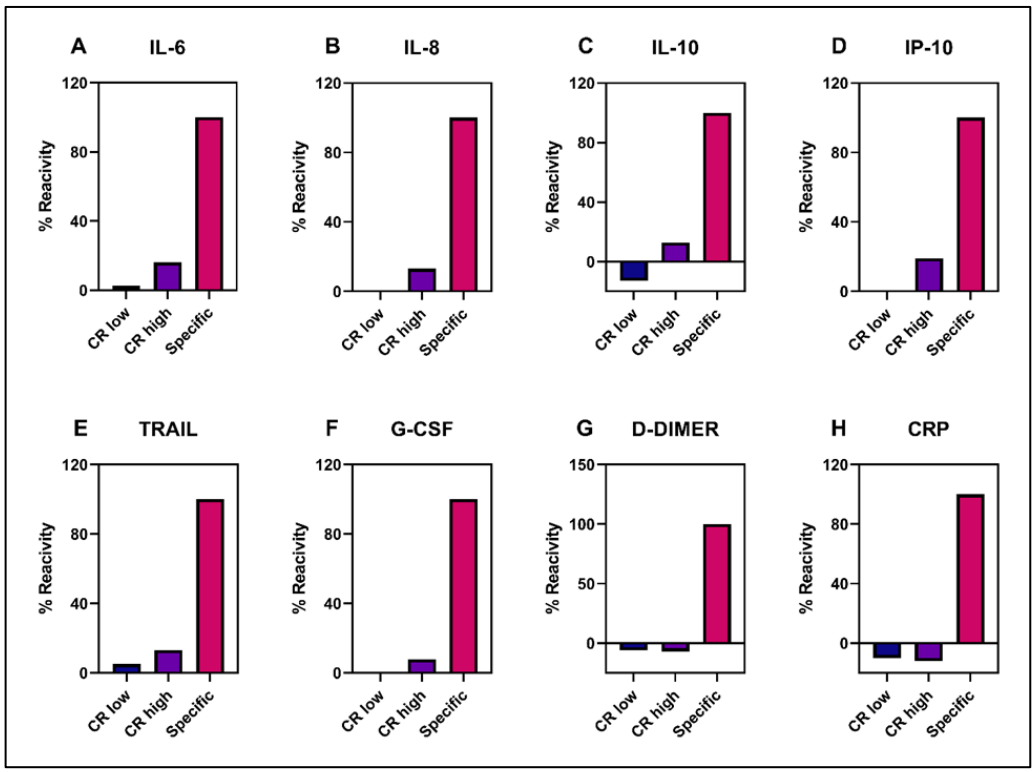

Figure 7.2.(A-H) The specificity of DETecT Sepsis 2.0 device for each of the target biomarker was evaluated using cross reactivity study.CR high: high concentration of BSA. CR Low: low concentration of BSA. All the analytes are spiked in WB buffer matrix.

7.5.3 Clinical validation of DETecT Sepsis 2.0 device with reference standard LUMINEX using whole blood patient samples

It is crucial to understand and validate the performance of the developed sensor platform with an existing reference method and measure the accuracy of the sensor. For clinical validation, 40 patient blood samples were measured using the DETecT Sepsis 2.0 device and reference LUMINEX standard method (Figure 7.3 A-H).

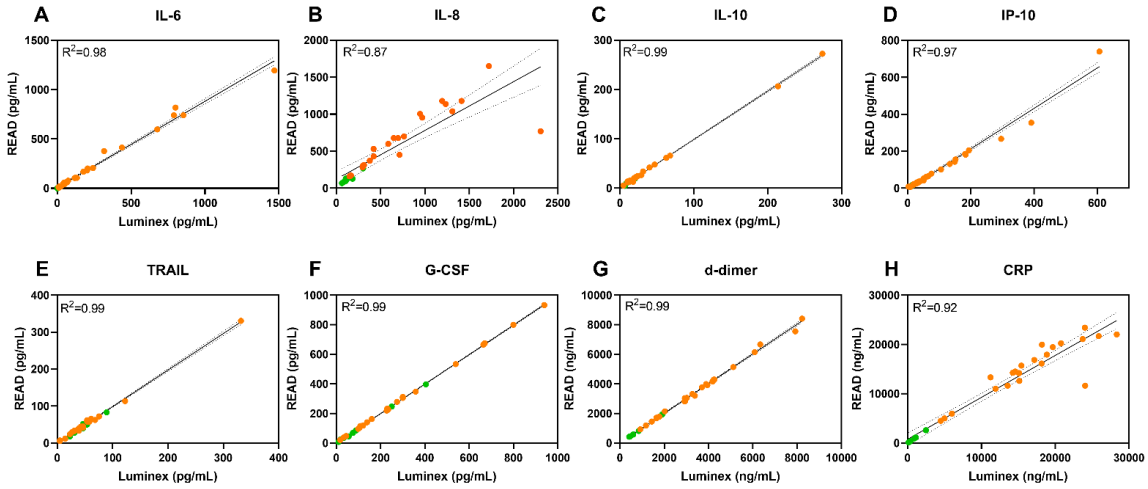

Figure 7.3.(A-H) Clinical validation of blood panel using DETecT Sepsis 2.0 device. The DETecT Sepsis 2.0 device was validated using standard LUMINEX as a reference method against n=40 patient samples in whole blood matrix. All biomarkers showed positive correlation with coefficient of determination (R2>0.87).

The concentrations measured by both methods correlated positively with coefficient of determination (R2>0.97) for IL-6, IL-10, IP-10, TRAIL, G-CSF, and d-dimer. Whereas IL-8 and CRP correlated well with an R2> 0.87. Additionally, the wide dynamic range ensure to capture both healthy and the diseased state of the patient which can be useful as a monitoring device. To evaluate the pre-clinical utility of the developed sensor platform, it is essential for the sensors performance to be in agreement with current lab standards. Hence, we compared the performance of DETecT Sepsis 2.0 device with LUMINEX using Bland-Altman analysis as seen in figure 7.4 (A-H). The difference between each pair is plotted on the y axis while the average of each pair of measurement is plotted on the x axis. Low mean bias between the two methods shows good degree of agreement between Luminex reference standard and DETecT Sepsis 2.0 device. Individual mean bias values can be found in supplementary information. Since all the points except few lies well within the limit of agreement (±1.96 SD), the two methods are in agreement. The dispersion of the points is minimally observed, and the points

are reasonably near the mean bias line. Mean bias and the limit of agreement provide information on the usability of the new measuring method as a quantifiable measure. The data measured across the blood panel biomarkers show equal distribution across the mean bias in both positive and negative direction. This indicates not one method overpredicts or underpredicts the concentration values.

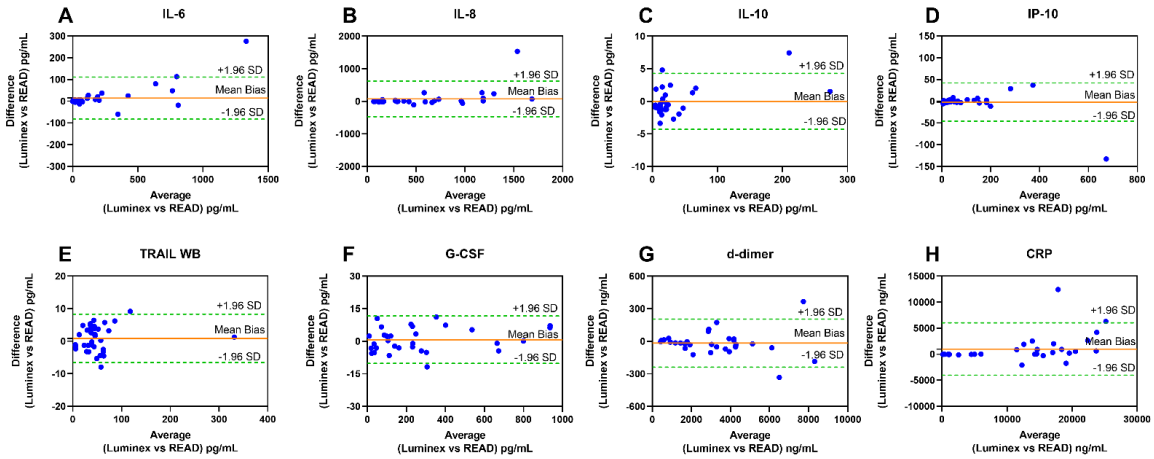

Figure 7.4.(A-H) Bland Altman analysis comparing the developed device and reference Luminex standard using n=40 patient blood samples.

Sepsis being a complicated disease with dysregulated immune response, measuring it with a single biomarker may not be informative. To know how sepsis affects the patient's immune response, it is necessary to look at different group of biomarkers that can provide valuable insights. Therefore, we focused on cytokines, chemokines, and infectious biomarkers simultaneously to gauge the active patient state. Quantification of IL-6, IL-8, IL-10, IP-10, TRAIL, G-CSF, d-dimer, and CRP was done using DETecT Sepsis 2.0 device with 10 healthy WB control samples and 30 septic WB patient samples (Figure 7.5 A-H). 100 uL of patient WB samples was directly added to the DETecT Sepsis 2.0 device without dilution or additional sample preparation. Mean blood concentration for IL-6 was 0.7 ±0.37 pg/mL and that of septic

cohort was 214±297 pg/mL. IL-8 showed mean concentration of 135±55 pg/mL for healthy and 706±401 pg/mL for septic patients. Healthy WB concentration for IL-10 and IP-10 were 9±5.37 pg/mL and 15±5.8 pg/mL, whereas septic IL-10 and IP-10 blood concentration were 34±54 pg/mL 102±144 pg/mL respectively. Similarly, G-CSF mean healthy concentration was 97±125 pg/mL and patients with sepsis had blood concentration of 320±264 pg/mL. D-dimer and CRP significantly classified healthy from septic cohort with mean healthy blood concentration of 551±556 pg/mL and 818±758 pg/mL while septic blood concentration from 3636±1818ng/mL 15481±6122 ng/mL respectively, with no overlapping interquartile ranges. The multiplexed panel of eight biomarkers showed statistical significance between healthy controls against septic patient cohort, with TRAIL as an exception. TRAIL has a negative trend where healthy cohort shows higher mean concentration of 42 pg/mL and the septic cohort shows slightly lower mean concentration of 37 pg/mL. TRAIL is a potent inducer of cell death. Lower levels of TRAIL have been associated with increased possibility of organ dysfunction, septic shock and higher rate of in-hospital mortality [135], [193]. Although plasma levels of TRAIL septic samples showed the capability to distinguish healthy from the diseased patient group [194], there are many factors associated with poor significance in WB samples.

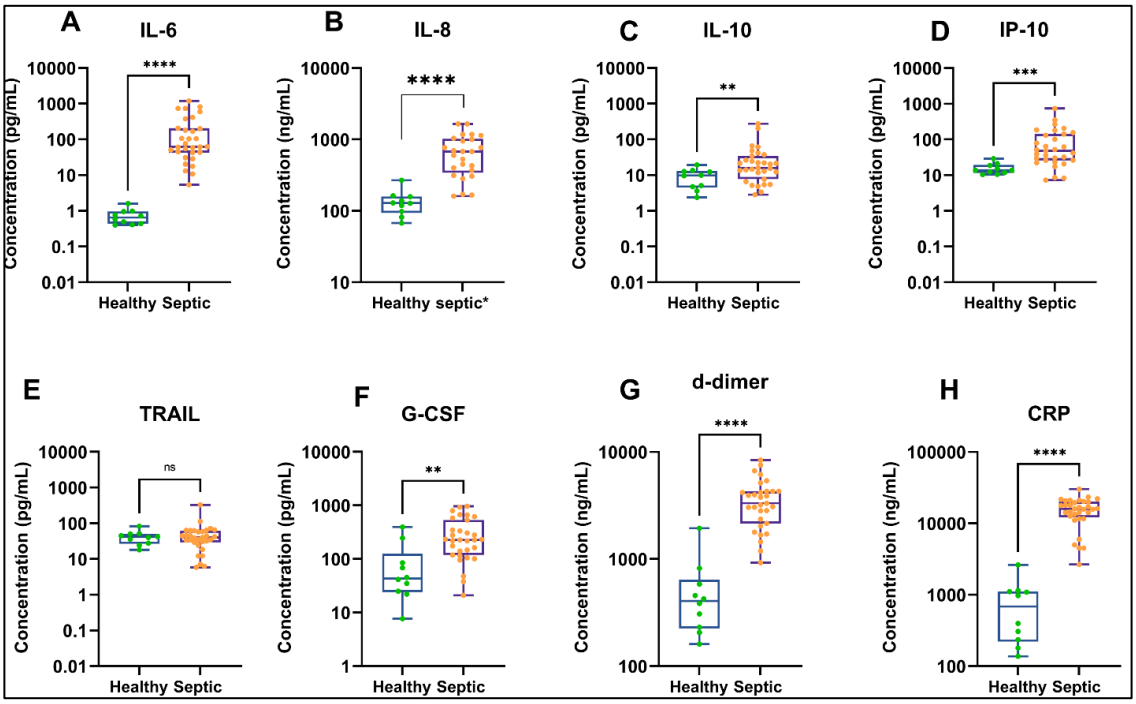

Figure 7.5.(A-H) Classification of infectious cytokine panel using n=40 patient blood samples into healthy and septic patient cohort for IL-6, IL-8, IL-10, IP-10, TRAIL, G-CSF, d-dimer, and CRP. Statistical analysis was performed using Mann-Whitney U test to determine the significance between healthy and septic patient cohort. Note: ns: no significance, **p < 0.01, ***P < 0.001, ****P < 0.0001.

7.5.4 Diagnostic Accuracy of DETecT Sepsis 2.0 device

The utility of DETecT Sepsis 2.0 device in a clinical setting was tested using receiver operating curve. It is essential for the device to identify specificity and sensitivity of the device to minimize false positive results. Area under the curve (AUC) helps to evaluate the diagnostic performance of the test device. The ability of the device to identify patients with sepsis positively is termed as device sensitivity. On the contrary, in AUC, specificity is defined as the device capability to identify non-septic patients as negative. As seen in figure 7.6, IL-6 and CRP had the highest discriminative value with an AUC of 1 (95% Confidence interval of 1 to 1) followed by IL- 8 and d-dimer with an AUC of 0.98 (CI 0.93 to 1). IL-6 had a sensitivity of

100%, and a specificity of 80% with a cut off 0.97 pg/mL was used to differentiate healthy from the septic patient cohort. CRP at a cut off value of 1882 ng/mL had a sensitivity of 100% and specificity of 90%. For IL-8 had sensitivity of 96% at a cut off value set as 161.6 pg/mL and specificity of 80% to distinguish healthy from septic cohort. With a cut off at 872 ng/mL, d-dimer showed a 96% sensitivity and 90% specificity. IP-10 and G-CSF showed moderate discriminative value with an AUC of 0.87 (CI: 0.76 to 0.98) and 0.82 (CI:0.65 to 0.99) respectively. IP-10 had 90% sensitivity and 70% specificity at a cut off at 16.26 pg/mL followed by 93% sensitivity and 60% specificity at cut off value of 46.43 pg/mL for G-CSF. Overall, the AUC for the blood panel biomarkers was above 0.90 for IL-6, IL-8, d-dimer and CRP which can be used as reliable biomarkers o differentiate healthy from the septic patient cohort.

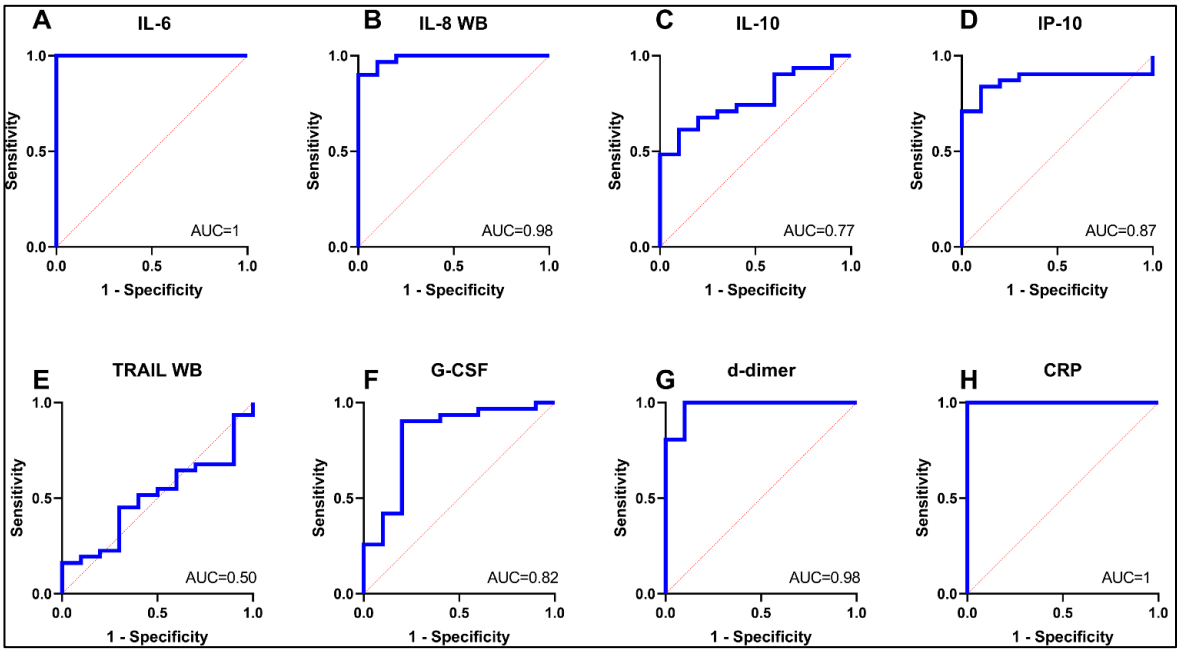

Figure 7.6.(A-H) Receiver operating characteristic curve for blood panel biomarkers using DETecT Sepsis 2.0 device. Areas under the curve for individual biomarker is labelled at the bottom right of each graph.

Understanding how the effect of combined biomarkers have on the ability to distinguish healthy from the septic patient group, principal component analysis was performed. All eight biomarkers were added as input to simply the results and narrow down he results. The summary plot selected 3 major components PCA1, PCA2 and PCA3 accounting for 29.23, 22.26 and 16.99% of the sample variability respectively. The biomarkers that are responsible to distinguish healthy from septic cohort comprise of PCA1, PCA2, PCA3, PCA4, PCA5 and PCA6 with the cumulative proportion of variance of 94% according of the scree plot (supplementary). Thus, the scree plot suggests, 6 components out of the 8 are sufficient to provide meaningful insight on the patient status. The loading plot for this data seen in supplementary shows that IL-6, IL-10, and CRP are positively correlated as they are clustered together. Whereas G-CSF, IL-8 and d-dimer form another cluster and are well correlated with

each other. Third cluster formed is between TRAIL and IP-10 showing a correlation of 0.8. As seen in figure 7.7A, for the blood cytokine biomarkers, were able to distinguish healthy control subjects from the septic patient cohort. Heat map analysis shows that healthy and septic profile is separated with top one-fourth section with very low values represented in blue with values towards lower end of the colored scale bar. All the patients with sepsis showed very high CRP levels followed by d-dimer, G-csf and IL-8. Heat map correlation between patients was analyzed to visualize patterns within the different biomarkers as seen in figure 8B. Data suggests that patients with high IP-10 levels also had high TRAIL blood concentration. Next, we evaluated the degree to which certain pair of biomarkers correlated using pearson's correlation matrix, seen in figure 7.7C. TRAIL and IP-10 showed the highest correlation of 0.81 followed by d-dimer and IL-8 with a coefficient of 0.5. D-dimer levels have been known to be associated with the activation of pro-inflammatory cytokine cascade. The paucity of correlation of d-dimer with anti-inflammatory cytokine IL-10 implies that existence of d-dimer may represent an imbalance between pro-inflammatory and anti-inflammatory cytokines [195].

On acquiring results from the multiplexed cytokines panel from healthy and septic patients using DeTecT sepsis 2.0 device, we implemented the use of machine learning model to predict the outcomes. Confusion matrix represented in figure 7.7D represents the actual and predicted state using logistic regression algorithm. The machine learning algorithm used here is the supervised version. We have used basic logistic regression algorithm to stratify the patient from healthy and septic state. The logistic regression is common classification algorithm for two-class stratification. Since the objective here is to provide decision support for clinicians in

determine the probability of patient being healthy or septic it provides valuable input. We observed the accuracy of logistic regression to be 0.923% sufficient to be confidant about the implementation of the algorithm while allowing room for generalization. The true positive here are of 69.23% and true negative are of about 23.08%. Total false positive which is type I error is found to be 7.69% and none false negative are observed on test dataset. This builds the confidence on the algorithm that no positive case would be unnoticed. Furthermore, supplementary table S1 shows another metrics about the classification algorithm. In case of class imbalance, it would be more robust. The f-1 score gives the overall weighted score for the algorithm and in this case, it is same as accuracy 0.92. The precision for healthy group was found to be 0.75 and 1.00 for septic. The individual f-1 score for healthy group is 0.86 and 0.95 for the septic one. This shows algorithm is able to classify the data correctly.

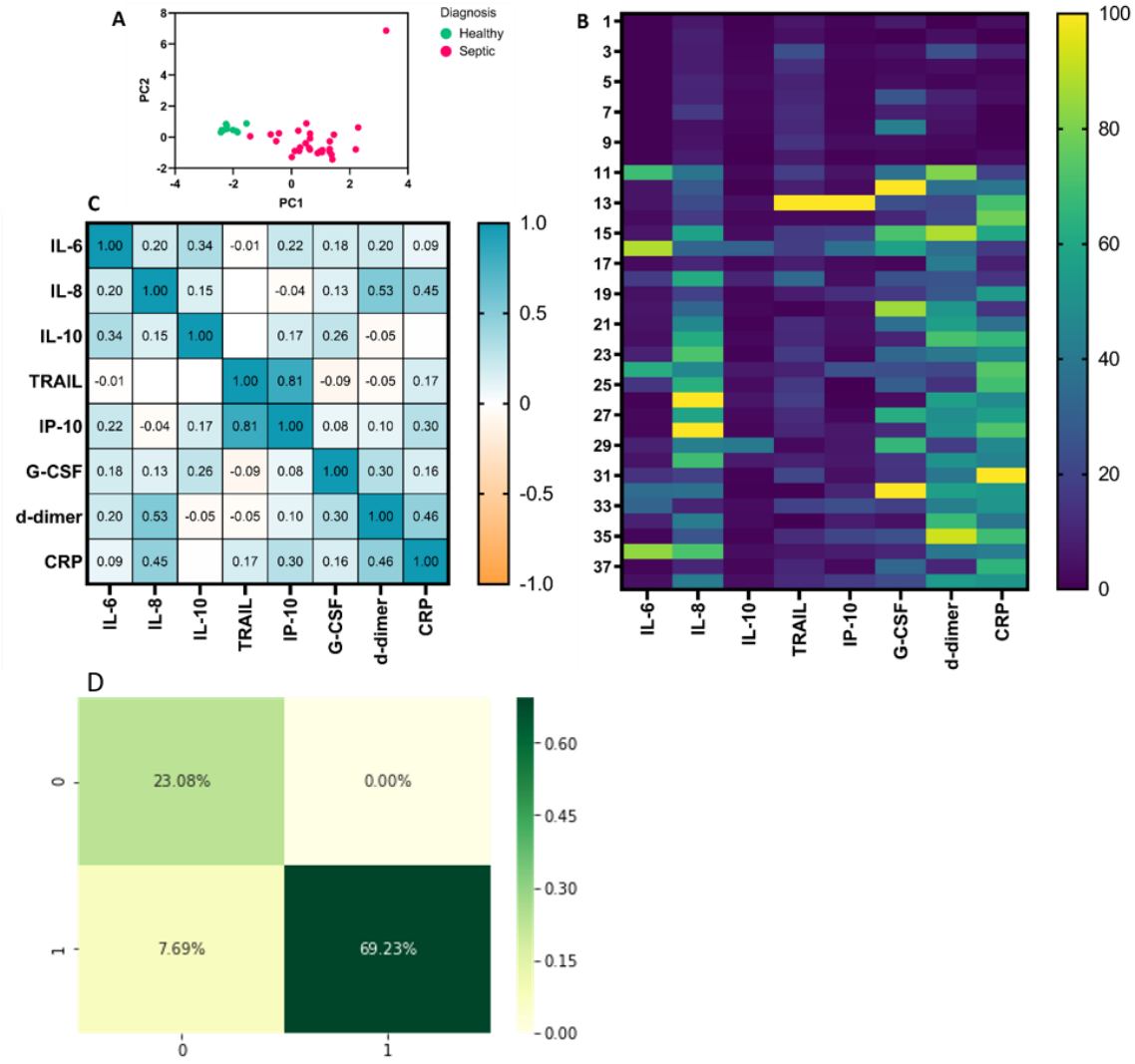

Figure 7.7. A) Principal component analysis representing the healthy and septic classification by adding IL-6, IL-8, IL-10, IP-10, TRAIL, G-CSF, d-dimer, and CRP as input variables. B) Heat map plotted to evaluate the correlation between patient data across multiplexed blood biomarker panel. C) Correlation analysis between blood panel biomarkers. D) Confusion matrix showing accuracy of logistic regression machine learning model.

7.6 Discussion

Sepsis is a complicated disease to tackle. With such complicated pathophysiology, differing from individuals based on their immune response, it can be burdensome to track the disease progression. From previous research on the vast availability of biomarkers, certain biomarkers

provide good understanding of how the patients' immune response is changing. Unfortunately relying on single biomarker for such a complex disease can be of very little use. Therefore, in this study we combined key biomarkers that provide a snapshot of patient's immune response. Timing of cytokine release is attributed to disease severity. Proinflammatory immune biomarkers such as IL-6, IL-8 and IL-10 highlight the patient status at the beginning of sepsis. The importance of proinflammatory and anti-inflammatory cytokine biomarkers has been developed and used for sepsis diagnosis as the paradigm of sepsis pathogenesis has evolved through time with many medical treatments. In patients with severe sepsis, cytokine profiling could be a useful strategy for recognizing various immune response patterns, expressing the diversity of patient groups with identical biological deregulation. This works reflects a multiplexed cytokine analysis in WB samples using DeTecT 2.0 device to be able to identify patients with sepsis and the utility of biomarker associations with disease severity. The results in our work confirm that IL-6, IL-8, d-dimer and CRP are primarily the best indicators of identifying patients with sepsis.

The vast heterogeneity in the immune response of septic patients has made the development of efficient immunotherapies and prediction of infection outcomes that leads to organ failure or death maybe the major cause of lack of progress. Therefore, detection of multiplexed biomarkers has the potential to improve diagnostic efficacy. Furthermore, one of the biggest technological gaps is the availability of rapid detection of these biomarkers at patient bedside. When a patient suspected with sepsis arrives in the hospital, time is of essences to treat the patient with the right approach. A study reveals early goal-oriented therapy reduced in-hospital mortality as compared to conventional care (30 to 46 %) [196]. Additionally, in septic shock,

starting antibiotics within one hour improves survival, where every hour antibiotics are delayed reduces survival by 8%. Choosing the right set of biomarkers may provide valuable insight on understanding the pathophysiology of sepsis in each patient. Cytokines are known to be the first biomarkers to respond to inflammation. [197]. This is also reflected by the results where IL-6 and IL-8 have shown significant difference between healthy and septic patient cohort, seen in figure 7.5.

It is observed that 20-25% patients with sepsis have disseminated intravascular coagulation (DIC) which may lead to organ failure, thereby significantly increasing the risk of mortality [198]. The activation of a coagulation deluge is a typical and early occurrence in septic patients with infection, and several molecules involved in this process are also key inflammatory response amplifies. Fibrinolysis is activated by d-dimer which causes coagulation. Role of d-dimer is significant in identifying the severity of immune response, as d-dimer signifies the level of blood coagulation which in turn can reflect severity in host immune response, leading to organ failure [199]. This work showed results in line to the results shown with the previous study of d-dimer in sepsis. A higher mortality rate and hospitalization was found to be correlated with patients with higher d-dimer levels8. Level of D-dimer in our septic patient cohort was nearly 10 times higher than of healthy patient group [181], [182] and correlated moderately with CRP, thus becoming a potential biomarker for identifying infected individuals with high risk of mortality in a simple and quick manner. The levels of CRP have known to be markers of sepsis. CRP levels increase within the first 6 hours of the infection. Although it is a generic biomarker for inflammation, the incidence in that of sepsis is much higher [200]. CRP is also used as a standard for measuring sepsis as part of clinical standard, or blood

culture. CRP is also a marker used to test for adverse outcomes with COVID-19 [183]. The concertation difference between healthy and septic patient cohort is almost 200 times, which indicates characteristic response to the infection. Several studies have shown that increased CRP concentration especially in patients in ICU have increased risk of organ failure and higher chances of mortality[184], [185]. IL-6 is an essential cytokine which is a key activator for acute phase response, particularly, triggering the production of CRP, a well-known proinflammatory marker for atherothrombotic vascular disease14. Tracking IL-6 in connection with CRP have shown to have prognostic value for early detection of sepsis [201]. The threshold value of IL-6 and CRP was 1.6 pg/mL and 2619 ng/mL which was in line with previous studies [123], [202]. IL-6 is also a known to be one of the first mediators to provocate the cytokine storm in patients with sepsis and COVID-19 [203]. Therefore, monitoring the levels of IL-6 along with other proinflammatory markers provides evidence of the how the patient's immune response is reacting during the infection. Diagnostic accuracy of a single marker in a complex disease like sepsis is difficult to predict the dynamic state of the patient [204]. There is a novel combination of biomarker that showcase various immune response phases within the patient provides valuable information to the clinicians to make crucial decisions on therapeutics. For instance, if the presenting patient shows higher proinflammatory levels of biomarkers, the clinician can provide immunosuppressants to dial down the immune response, and avoid the catastrophic event of a cytokine storm, which could lead to uncontrollable side effects like multiple organ failure, or even death. Herein IL-10 plays a crucial role to determine the state of immune response. IL-10 is known to act as a double-edged sword during infection as it acts based on the body's feedback. For instance, if the patient is in the state of hyper immune state,

IL-10 is triggered as an anti-inflammatory signal to lower the over responsive effects of the inflammatory response. Whereas, if the body is in the state of immunosuppression, IL-10 triggers the necessary biomarkers to activate the pro-inflammatory response, to curb the infection in the body during infection. The right role of IL-10 is unknow during sepsis, but as it has a dual nature, the diagnostic accuracy can be affected. Therefore, it is necessary to club IL-10 along with other proinflammatory markers to completely understand the nature of the individual biomarker. Overproduction of IL-10 have been associated with severe outcome and mortality [187]. IL-10 suppresses the activity of proinflammatory cytokines and chemokines including IL-6, IL-8, IP-10 and G-csf [188]. Its major role is to limit damage to the host. But in doing so, it also grants free pass to the pathogen to multiple or sustain within the host, thereby harming the host eventually. Therefore, if IL-10 is expressed at an inopportune time, such as too early during virulent infection, or too late during avirulent infection, it can cause overwhelming infection or severe tissue damage [189]. This work is in line with the research done previously where 75% IL-10 production is at 34 pg/mL all the way upto 272 pg/mL in septic patient cohort [190]. Progression of TRAIL and IP-10 has been researched over different patient groups and have said to be distinguishing factors for bacterial and viral sepsis. Especially, lower levels of TRAIL show more severe outcomes.

Detection of biomarkers in WB is a completely different arena compared to regular standard diagnostics. There are a few advantages of exploring blood as a biofluid for ease in detection. This work focuses on the potential of using a POC device capable of measuring eight biomarkers simultaneously in a small sample of WB within 5 minutes.

In a clinically relevant environment, effective detection and prediction of patient at risk of developing sepsis is key for successful management. Integrating machine learning model with the multiplexed cytokine results in blood, enables a unique way to predict the possibility of a patient with sepsis with high accuracy (AUC >0.92). The application of machine learning based predictive technology might aid medical decision-making by adding new components to assist proper and early diagnosis of patients with sepsis.

Our work has a few limitations, even though a combination of cytokines shows high accuracy for predicting patients with sepsis. The limited sample size restricts the extent to which our findings can be extended to other patient cohorts. Furthermore, only a single time point cytokine measurement was considered, and although blood measurement is crucial for early prognosis, it may not elucidate the depth of the influence of cytokines in disease etiology as compared to those offered by sequential measurements. However, specific cytokine accuracy was high for predicting the patient state and disease severity. Although it is tempting to presume that variations in cytokine concentrations are linked to pathophysiology of organ failure, we believe, no single cytokine can be credited for the entire severity of the disease. Cytokine concentrations in blood could also be elevated merely as indicators of tissue injury, without necessarily playing a direct role.

The multiplexing capability of DeTect 2.0 device directly in WB at patient bedside provides opportunities to create a panel of sepsis biomarkers that includes well studied cytokine biomarkers with good prognostic value along with other biomarkers to accommodate for similar disease like COVID-19 to expand the potential application of the device. To gain comprehensive understanding of complex interactions that occurs during disease progression,

we acknowledge that newer techniques can benefit, rather than studying individual effect of the chosen biomarkers.

Apart from the current limitations, DeTect Sepsis device 2.0 has several advantages over existing analytical techniques. Firstly, high detection sensitivity of DeTecT sepsis 2.0 device coupled with wide dynamic range and good specificity provides rapid and accurate results to improve sepsis stratification. Next, the miniaturized portable device can be used anywhere, from patient bedside to emergency department or even in an ambulance. Secondly, low sample requirement equivalent of two drops of blood (~100 uL) provides rapid information on a panel of eight useful biomarkers which can provide valuable insights on the patients host immune response at that instant. Lastly, integrating machine learning algorithm with the multiplexed cytokine panel offers the user (for instance, a clinicians) valuable insights and can be valuable asset as a clinical decision support system for improved patient outcomes.

Till date, there is no POC device that can rapidly assess the biomarker concentrations without sample dilution in WB with low sample volume (~100 uL). This translational research work would support and benefit the clinical community in rapidly assessing the state of the patient's immune response at the time of intervention, thus providing real-time valuable information. In conclusion, simultaneous detection of eight cytokine biomarkers combined with machine learning model can reveal complicated cytokine patterns reflecting systemic response linked to severe sepsis, organ failure and death. Based on the cytokine profiles provided by the DeTecT sepsis 2.0 device, clinicians can assess disease severity and forecast distinct clinical presentations and outcomes.

CHAPTER 8

CONCLUSION AND FUTURE WORK

This dissertation has successfully demonstrated a prototype of a multiplexed, highly sensitive, near-patient bedside POC biosensing device with a rapid response time applicable in a diverse scope across healthcare industry. The miniaturized diagnostic biosensor can be used to measure PTH as a single biomarker as a guide to clinicians during a parathyroidectomy surgery as well as for early detection of complex infectious disease such as sepsis by leveraging a combination of host immune response biomarkers. This research has contributed towards the 1) assessing the unique semiconducting ZnO interactions to provide controlled binding efficacy for target biomarkers to increase sensitivity across a single analyte 2) evaluating the developed biosensing assay performance for clinical utility 3) strategies to expand the biosensing capability to assess performance of multiplexed biomarkers on a single platform with rapid response time 4) in-depth clinical validation by testing the performance of the biosensing device against stand laboratory reference method using patient samples from three geographical locations 5) innovative solutions for translating the performance metrics to test patient samples directly in WB toward in-field testing application. This dissertation has established the framework for a versatile electrochemical POC biosensing device that can measure up to eight biomarkers simultaneously with a rapid response time, high sensitivity while using approximately two drops (~100 uL) of WB without sample dilution.

Every biosensing device developed in this work has demonstrated sensitive, selective, and precise detection of single and multiplexed biomarkers in complex body fluids such as serum,

plasma and WB. Early detection of sepsis included measuring cytokines such as IL-6, IL-8, IL-10, chemokines such as TRAIL, IP-10 and infectious biomarkers including d-dimer, G-CSF, CRP and PCT simultaneously without compromising on sensitivity or specificity. This is attributed to the selective functionalization of highly specific capture probes integrated with the sensitive detection capability of EIS. Multiplexed detection will facilitate the creation of a precise molecular fingerprint for every patient, enhancing precision medicine endeavors. The DETecT Sepsis device's quick response time promotes faster clinical decision making for healthcare professionals, allowing them to operate for early intervention. Additionally, this research is developed to address ASSURED (Affordable, Sensitive, Specific, User Friendly, Rapid and Robust, Equipment free and Deliverable to end users) that can be used toward in-field testing application especially in resource limited areas. Thus, the next version of DeTecT Sepsis 2.0 device demonstrated the potential of using direct WB without the need for dilution (thereby making it user friendly which can be operated by minimally trained individuals), with smaller sample volumes (to avoid patient discomfort and contaminations) while measuring eight host immune response biomarkers simultaneously.

In conclusion, the developed versatile portable biosensing device prototype with the ability for rapid detection of multiplexed biomarkers in WB can be used to detect other infectious diseases like COVID-19, for better patient outcomes. We have also explored the combinatorial effects of using DeTecT Sepsis device paired with machine learning algorithm to provide calculated prediction to guide clinicians with better outcomes. Clinical utility of machine learning models is currently limited; thus, it is critically needed across a wide range of patient population to establish clinical impact, verify predictive validity, and close the gap between medical data

and patient bedside treatment. The implementation of machine learning- based predictive technologies may assist medical decision-making by introducing new aspects to assist the correct and early identification of complex diseases such as sepsis. The developed sensor technology would enable medical practitioners to facilitate targeted patient interventions for complex diseases as a rapid prognostic approach that could avert mortality as an imperative clinical resource.

REFERENCES

[1] "Biosensors Market Size Share and Trends forecast to 2026 | MarketsandMarkets™." https://www.marketsandmarkets.com/Market-Reports/biosensors-market-798.html (accessed Oct. 19, 2021).

[2] Varnakavi. Naresh and N. Lee, "A Review on Biosensors and Recent Development of Nanostructured Materials-Enabled Biosensors," *Sensors (Basel, Switzerland)*, vol. 21, no. 4, pp. 1–35, Feb. 2021, doi: 10.3390/S21041109.

[3] B. Srinivasan and S. Tung, "Development and Applications of Portable Biosensors:," *https://doi.org/10.1177/2211068215581349*, vol. 20, no. 4, pp. 365–389, Apr. 2015, doi: 10.1177/2211068215581349.

[4] T. W. R. E. A. for C.-19 T. (REACT) W. Group *et al.*, "Association Between Administration of Systemic Corticosteroids and Mortality Among Critically Ill Patients With COVID-19: A Meta-analysis," *JAMA*, vol. 324, no. 13, pp. 1330–1341, Oct. 2020, doi: 10.1001/JAMA.2020.17023.

[5] N. P. Pai, C. Vadnais, C. Denkinger, N. Engel, and M. Pai, "POC Testing for Infectious Diseases: Diversity, Complexity, and Barriers in Low- And Middle-Income Countries," *PLOS Medicine*, vol. 9, no. 9, p. e1001306, Sep. 2012, doi: 10.1371/JOURNAL.PMED.1001306.

[6] P. Yager, G. J. Domingo, and J. Gerdes, "POC Diagnostics for Global Health," *http://dx.doi.org/10.1146/annurev.bioeng.10.061807.160524*, vol. 10, pp. 107–144, Jul. 2008, doi: 10.1146/ANNUREV.BIOENG.10.061807.160524.

[7] C. ME *et al.*, "Electrochemical magnetic microbeads-based biosensor for POC serodiagnosis of infectious diseases," *Biosensors & bioelectronics*, vol. 80, pp. 24–33, Jun. 2016, doi: 10.1016/J.BIOS.2016.01.021.

[8] G. D, M. R, V. J, and R. E, "Electrochemical Biosensors - Sensor Principles and Architectures," *Sensors (Basel, Switzerland)*, vol. 8, no. 3, pp. 1400–1458, Mar. 2008, doi: 10.3390/S80314000.

[9] V. Kamakoti, N. R. Shanmugam, A. S. Tanak, B. Jagannath, and S. Prasad, "Investigation of molybdenum-crosslinker interfaces for affinity based electrochemical biosensing applications," *Applied Surface Science*, vol. 436, pp. 441–450, Apr. 2018, doi: 10.1016/j.apsusc.2017.12.026.

[10] W. Boumya *et al.*, “Electrochemical impedance spectroscopy measurements for determination of derivatized aldehydes in several matrices,” *Heliyon*, vol. 3, no. 10, p. e00392, 2017.

[11] D. HH, P. TJ, S. S, C. X, and P. ZK, “A Novel Combination of Biomarkers to Herald the Onset of Sepsis Prior to the Manifestation of Symptoms,” *Shock (Augusta, Ga.)*, vol. 49, no. 4, pp. 364–370, Apr. 2018, doi: 10.1097/SHK.0000000000001010.

[12] S. NR, M. S, T. AS, and P. S, “Multiplexed electrochemical detection of three cardiac biomarkers cTnI, cTnT and BNP using nanostructured ZnO-sensing platform,” *Future cardiology*, vol. 14, no. 2, pp. 131–141, Mar. 2018, doi: 10.2217/FCA-2017-0074.

[13] N. R. Shanmugam, S. Muthukumar, and S. Prasad, “A review on ZnO-based electrical biosensors for cardiac biomarker detection,” *Future Science OA*, vol. 3, no. 4, 2017, doi: 10.4155/FSOA-2017-0006.

[14] R. Yakimova, L. Selegård, V. Khranovskyy, R. Pearce, A. Lloyd Spetz, and K. Uvdal, “ZnO materials and surface tailoring for biosensing,” *Frontiers in bioscience (Elite edition)*, vol. 4, no. 1, pp. 254–278, 2012.

[15] D. B. Endres, R. Villanueva, C. F. Sharp, and F. R. Singer, “Measurement of parathyroid hormone.,” *Endocrinology and metabolism clinics of North America*, vol. 18, no. 3, pp. 611–29, Sep. 1989, Accessed: Mar. 02, 2020. [Online]. Available: http://www.ncbi.nlm.nih.gov/pubmed/2673765

[16] S. Ş. Ç, N. S. K. M, and S. MK, “A new immobilization procedure for development of an electrochemical immunosensor for parathyroid hormone detection based on gold electrodes modified with 6-mercaptohexanol and silane,” *Talanta*, vol. 144, pp. 210–218, Jun. 2015, doi: 10.1016/J.TALANTA.2015.06.010.

[17] H. M. Özcan *et al.*, “Ultrasensitive Impedimetric Biosensor Fabricated by a New Immobilisation Technique for Parathyroid Hormone,” *Applied Biochemistry and Biotechnology 2015 176:5*, vol. 176, no. 5, pp. 1251–1262, May 2015, doi: 10.1007/S12010-015-1643-X.

[18] C.-G. A, de la E.-M. A, E.-C. M, R.-H. CJ, de T. C, and M. A, “Detection of parathyroid hormone-like hormone in cancer cell cultures by gold nanoparticle-based lateral flow immunoassays,” *Nanomedicine : nanotechnology, biology, and medicine*, vol. 12, no. 1, pp. 53–61, Jan. 2016, doi: 10.1016/J.NANO.2015.09.012.

[19] B. JP, B. L, K. A, and C. NE, “Hyperparathyroidism,” *Lancet (London, England)*, vol. 391, no. 10116, pp. 168–178, Jan. 2018, doi: 10.1016/S0140-6736(17)31430-7.

[20] S. R. Nussbaum, A. R. Thompson, K. A. Hulcheson, R. D. Gaz, and C. Wang, “Intraoperative measurement of parathyroid hormone in the surgical management of hyperparathyroidism,” *Surgery*, vol. 104, no. 6, pp. 1121–1127, 1988.

[21] I. GL and D. GT, “A new, practical intraoperative parathyroid hormone assay,” *American journal of surgery*, vol. 168, no. 5, pp. 466–468, 1994, doi: 10.1016/S0002-9610(05)80101-1.

[22] K. T, I. M, and F. M, “Critical Governance Issue of Parathyroid Hormone Assays and its Selection in the Management of Chronic Kidney Disease Mineral and Bone Disorders,” *Therapeutic apheresis and dialysis : official peer-reviewed journal of the International Society for Apheresis, the Japanese Society for Apheresis, the Japanese Society for Dialysis Therapy*, vol. 22, no. 3, pp. 220–228, Jun. 2018, doi: 10.1111/1744-9987.12690.

[23] B. A and A. H. A, “Parathyroid hormone: what are we measuring and does it matter?,” *Annals of clinical biochemistry*, vol. 39, no. Pt 3, pp. 169–172, 2002, doi: 10.1258/0004563021901928.

[24] D. P, B. JH, R. A, R. L, A. C, and C. T, “Evidence that the amino-terminal composition of non-(1-84) parathyroid hormone fragments starts before position 19,” *Clinical chemistry*, vol. 51, no. 1, pp. 169–176, 2005, doi: 10.1373/CLINCHEM.2004.040485.

[25] H. GL and C. AB, “Intraoperative parathyroid hormone testing: survey of testing program characteristics,” *Archives of pathology & laboratory medicine*, vol. 126, no. 9, pp. 1045–1049, Sep. 2002, doi: 10.5858/2002-126-1045-IPHT.

[26] A. A, R. JV, H. NA, and M. PA, “Biosensors for whole-cell bacterial detection,” *Clinical microbiology reviews*, vol. 27, no. 3, pp. 631–646, 2014, doi: 10.1128/CMR.00120-13.

[27] F. PE, D. M, C. P, R. JM, L. S. B, and R. D, “Modern clinical microbiology: new challenges and solutions,” *Nature reviews. Microbiology*, vol. 11, no. 8, pp. 574–585, Aug. 2013, doi: 10.1038/NRMICRO3068.

[28] V. Kamakoti, N. R. Shanmugam, A. S. Tanak, B. Jagannath, and S. Prasad, “Investigation of molybdenum-crosslinker interfaces for affinity based electrochemical biosensing applications,” *Applied Surface Science*, vol. 436, pp. 441–450, Apr. 2018, doi: 10.1016/J.APSUSC.2017.12.026.

[29] S. NR, M. S, and P. S, “Ultrasensitive and low-volume POC diagnostics on flexible strips - a study with cardiac troponin biomarkers,” *Scientific reports*, vol. 6, Sep. 2016, doi: 10.1038/SREP33423.

[30] B. TW, R. S. N, S. AP, K. SC, and P. S, “Novel Nanomonitor ultra-sensitive detection of troponin T,” *Clinica chimica acta; international journal of clinical chemistry*, vol. 442, pp. 96–101, Mar. 2015, doi: 10.1016/J.CCA.2015.01.013.

[31] T. S and N. HB, “Simulation of a Love wave device with ZnO nanorods for high mass sensitivity,” *Ultrasonics*, vol. 84, pp. 150–161, Mar. 2018, doi: 10.1016/J.ULTRAS.2017.10.004.

[32] T. N and K. DH, “Metal oxide modified ZnO nanomaterials for biosensor applications,” *Nano convergence*, vol. 5, no. 1, Dec. 2018, doi: 10.1186/S40580-018-0159-9.

[33] W. Raza and K. Ahmad, “A highly selective Fe@ZnO modified disposable screen printed electrode based non-enzymatic glucose sensor (SPE/Fe@ZnO),” *Materials Letters*, vol. 212, pp. 231–234, Feb. 2018, doi: 10.1016/J.MATLET.2017.10.100.

[34] J. Zhang, B. Zhao, Z. Pan, M. Gu, and A. Punnoose, “Synthesis of ZnO Nanoparticles with Controlled Shapes, Sizes, Aggregations, and Surface Complex Compounds for Tuning or Switching the Photoluminescence,” *Crystal Growth and Design*, vol. 15, no. 7, pp. 3144–3149, Jul. 2015, doi: 10.1021/CG5017017.

[35] M. Tak, V. Gupta, and M. Tomar, “Flower-like ZnO nanostructure based electrochemical DNA biosensor for bacterial meningitis detection,” *Biosensors and Bioelectronics*, vol. 59, pp. 200–207, 2014.

[36] K. L. Foo, U. Hashim, K. Muhammad, and C. H. Voon, “Sol–gel synthesized zinc oxide nanorods and their structural and optical investigation for optoelectronic application,” *Nanoscale Research Letters 2014 9:1*, vol. 9, no. 1, pp. 1–10, Aug. 2014, doi: 10.1186/1556-276X-9-429.

[37] J. Geng, G.-H. Song, X.-D. Jia, F.-F. Cheng, and J.-J. Zhu, “Fast One-Step Synthesis of Biocompatible ZnO/Au Nanocomposites with Hollow Doughnut-Like and Other Controlled Morphologies,” *Journal of Physical Chemistry C*, vol. 116, no. 7, pp. 4517–4525, Feb. 2012, doi: 10.1021/JP212092H.

[38] S. NR, M. S, S. AP, and P. S, “Electrochemical nanostructured ZnO biosensor for ultrasensitive detection of cardiac troponin-T,” *Nanomedicine (London, England)*, vol. 11, no. 11, pp. 1345–1358, Jun. 2016, doi: 10.2217/NNM-2016-0048.

[39] P. O, B. T, K. J, S. D, and L. F, “Impedance spectroscopy and biosensing,” *Advances in biochemical engineering/biotechnology*, vol. 109, pp. 195–237, Nov. 2008, doi: 10.1007/10_2007_081.

[40] P. Chakraborty, T. Majumder, S. Dhar, and S. P. Mondal, “Non-enzymatic glucose sensing using hydrothermally grown ZnO nanorods: sensitivity augmentation by carbon doping and carbon functionalization,” *Materials Research Express*, vol. 5, no. 9, p. 095011, Aug. 2018, doi: 10.1088/2053-1591/AAD5BE.

[41] P. E. S. and and L. J. Whitman, “Detection Limits for Nanoscale Biosensors,” *Nano Letters*, vol. 5, no. 4, pp. 803–807, Apr. 2005, doi: 10.1021/NL050298X.

[42] C. Y. Lim *et al.*, “Succinimidyl Ester Surface Chemistry: Implications of the Competition between Aminolysis and Hydrolysis on Covalent Protein Immobilization,” *Langmuir*, vol. 30, no. 43, pp. 12868–12878, Nov. 2014, doi: 10.1021/LA503439G.

[43] B. L. F. and and R. M. Corn*, “Covalent Attachment and Derivatization of Poly(l-lysine) Monolayers on Gold Surfaces As Characterized by Polarization−Modulation FT-IR Spectroscopy,” *Analytical Chemistry*, vol. 68, no. 18, pp. 3187–3193, Sep. 1996, doi: 10.1021/AC9605861.

[44] “Photoelectrochemistry,” *Modern Electrochemistry 2B*, pp. 1539–1597, Jan. 2006, doi: 10.1007/0-306-48036-0_1.

[45] B. M, V. V, R. RK, B. T, C. J, and P. S, “Nanomonitors: electrical immunoassays for protein biomarker profiling,” *Nanomedicine (London, England)*, vol. 3, no. 4, pp. 423–436, Aug. 2008, doi: 10.2217/17435889.3.4.423.

[46] A. S. Tanak, S. Muthukumar, I. A. Hashim, and S. Prasad, “Rapid electrochemical device for single-drop point-of-use screening of parathyroid hormone,” *https://doi.org/10.2217/bem-2019-0011*, vol. 2, no. 1, pp. 13–27, Jun. 2019, doi: 10.2217/BEM-2019-0011.

[47] A. Panneer Selvam, S. Muthukumar, V. Kamakoti, and S. Prasad, “A wearable biochemical sensor for monitoring alcohol consumption lifestyle through Ethyl glucuronide (EtG) detection in human sweat,” *Scientific Reports 2016 6:1*, vol. 6, no. 1, pp. 1–11, Mar. 2016, doi: 10.1038/srep23111.

[48] R. NJ, H. HB, and H. WR, “Electrochemical biosensors,” *Chemical Society reviews*, vol. 39, no. 5, pp. 1747–1763, Apr. 2010, doi: 10.1039/B714449K.

[49] E. Katz and I. Willner, “Probing Biomolecular Interactions at Conductive and Semiconductive Surfaces by Impedance Spectroscopy: Routes to Impedimetric Immunosensors, DNA-Sensors, and Enzyme Biosensors,” *Electroanalysis*, vol. 15, no. 11, pp. 913–947, Jul. 2003, doi: 10.1002/ELAN.200390114.

[50] E. P. Randviir and C. E. Banks, “Electrochemical impedance spectroscopy: an overview of bioanalytical applications,” *Analytical Methods*, vol. 5, no. 5, pp. 1098–1115, Feb. 2013, doi: 10.1039/C3AY26476A.

[51] B.-Y. Chang and S.-M. Park, “Electrochemical Impedance Spectroscopy,” *http://dx.doi.org/10.1146/annurev.anchem.012809.102211*, vol. 3, no. 1, pp. 207–229, Jun. 2010, doi: 10.1146/ANNUREV.ANCHEM.012809.102211.

[52] D. JS and P. N, “Label-Free Impedance Biosensors: Opportunities and Challenges,” *Electroanalysis*, vol. 19, no. 12, pp. 1239–1257, Jun. 2007, doi: 10.1002/ELAN.200603855.

[53] R. J. McEnroe, M. F. Burritt, D. M. Powers, D. W. Rheinheimer, and B. H. Wallace, *Interference testing in clinical chemistry; approved guideline*. CLSI, 2005.

[54] S. LJ, W. FH, and R. AT, “Rapid intraoperative immunoassay of parathyroid hormone and other hormones: a new paradigm for POC testing,” *Clinical chemistry*, vol. 50, no. 7, pp. 1126–1135, Jul. 2004, doi: 10.1373/CLINCHEM.2003.030817.

[55] H. A, H. M, Z. H, E. G. M, M. F, and R. J, “Development and validation of a novel cell-based assay for potency determination of human parathyroid hormone (PTH),” *Journal of pharmaceutical and biomedical analysis*, vol. 98, pp. 345–350, 2014, doi: 10.1016/J.JPBA.2014.06.004.

[56] J. P. Bilezikian, L. Bandeira, A. Khan, and N. E. Cusano, “Hyperparathyroidism,” *The Lancet*, vol. 391, no. 10116. Lancet Publishing Group, pp. 168–178, Jan. 13, 2018. doi: 10.1016/S0140-6736(17)31430-7.

[57] I. M. Cordellat, “Hiperparatiroidismo: ¿primario o secundario?,” *Reumatologia Clinica*, vol. 8, no. 5, pp. 287–291, Sep. 2012, doi: 10.1016/j.reuma.2011.06.001.

[58] S. M. Wilhelm *et al.*, “The American Association of Endocrine Surgeons guidelines for definitive management of primary hyperparathyroidism,” *JAMA surgery*, vol. 151, no. 10, pp. 959–968, 2016.

[59] C. M. Nelson and N. S. Victor, “Rapid Intraoperative Parathyroid Hormone Assay in the Surgical Management of Hyperparathyroidism,” *The Permanente Journal*, vol. 11, no. 1, p. 3, 2007, doi: 10.7812/TPP/04-082.

[60] A. Mohebati and A. R. Shaha, “Imaging techniques in parathyroid surgery for primary hyperparathyroidism,” *American Journal of Otolaryngology - Head and Neck Medicine and Surgery*, vol. 33, no. 4, pp. 457–468, 2012, doi: 10.1016/j.amjoto.2011.10.010.

[61] V. Fedirko *et al.*, “Prediagnostic circulating parathyroid hormone concentration and colorectal cancer in the European prospective investigation into cancer and nutrition cohort,” *Cancer Epidemiology Biomarkers and Prevention*, vol. 20, no. 5, pp. 767–778, 2011, doi: 10.1158/1055-9965.EPI-10-1212.

[62] J. L. Shaker and L. Deftos, “Calcium and Phosphate Homeostasis,” in *Endocrine and Reproductive Physiology*, Elsevier, 2013, pp. 77-e1. doi: 10.1016/b978-0-323-08704-9.00004-x.

[63] T. M. Murray, L. G. Rao, P. Divieti, and F. R. Bringhurst, “Parathyroid hormone secretion and action: Evidence for discrete receptors for the carboxyl-terminal region and related biological actions of carboxyl-terminal ligands,” *Endocrine Reviews*, vol. 26, no. 1. Oxford Academic, pp. 78–113, Feb. 01, 2005. doi: 10.1210/er.2003-0024.

[64] A. J. Leiker *et al.*, “Factors that influence parathyroid hormone half-life: Determining if new intraoperative criteria are needed,” *JAMA Surgery*, vol. 148, no. 7, pp. 602–606, Jul. 2013, doi: 10.1001/jamasurg.2013.104.

[65] “Intraoperative Parathyroid Hormone Testing, Endocrine Surgery | UW Health | Madison, WI.” https://www.uwhealth.org/endocrine-surgery/intraoperative-parathyroid-hormone-testing-/25445 (accessed Mar. 16, 2020).

[66] A. S. Tanak, S. Muthukumar, I. A. Hashim, and S. Prasad, “Rapid electrochemical device for single-drop point-of-use screening of parathyroid hormone,” *Bioelectronics in Medicine*, vol. 2, no. 1, pp. 13–27, Mar. 2019, doi: 10.2217/bem-2019-0011.

[67] A. S. Tanak, B. Jagannath, Y. Tamrakar, S. Muthukumar, and S. Prasad, “Non-faradaic electrochemical impedimetric profiling of procalcitonin and C-reactive protein as a dual marker biosensor for early sepsis detection,” *Analytica Chimica Acta: X*, vol. 3, p. 100029, Nov. 2019, doi: 10.1016/j.acax.2019.100029.

[68] R. Sharma *et al.*, “Label-free electrochemical impedance biosensor to detect human interleukin-8 in serum with sub-pg/ml sensitivity,” *Biosensors and Bioelectronics*, vol. 80, pp. 607–613, Jun. 2016, doi: 10.1016/j.bios.2016.02.028.

[69] B. L. Garrote, A. Santos, and P. R. Bueno, “Perspectives on and Precautions for the Uses of Electric Spectroscopic Methods in Label-free Biosensing Applications,” *ACS Sensors*, vol. 4, no. 9. American Chemical Society, pp. 2216–2227, Sep. 27, 2019. doi: 10.1021/acssensors.9b01177.

[70] M. A. Sawhney and R. S. Conlan, “POISED-5, a portable on-board electrochemical impedance spectroscopy biomarker analysis device,” *Biomedical Microdevices*, vol. 21, no. 3, pp. 1–14, Sep. 2019, doi: 10.1007/s10544-019-0406-9.

[71] E. Ghafar-Zadeh *et al.*, “Handheld impedance biosensor system using engineered proteinaceous receptors,” *Biomedical Microdevices*, vol. 12, no. 6, pp. 967–975, Jul. 2010, doi: 10.1007/s10544-010-9451-0.

[72] A. Adler and A. Boyle, “Electrical impedance tomography: Tissue properties to image measures,” *IEEE Transactions on Biomedical Engineering*, vol. 64, no. 11, pp. 2494–2504, Nov. 2017, doi: 10.1109/TBME.2017.2728323.

[73] B. Sanchez and S. B. Rutkove, “Electrical Impedance Myography and Its Applications in Neuromuscular Disorders,” *Neurotherapeutics*, vol. 14, no. 1. Springer New York LLC, pp. 107–118, Jan. 01, 2017. doi: 10.1007/s13311-016-0491-x.

[74] D. Sankhala, S. Muthukumar, and S. Prasad, “A Four-Channel Electrical Impedance Spectroscopy Module for Cortisol Biosensing in Sweat-Based Wearable Applications,” *SLAS Technology*, vol. 23, no. 6, pp. 529–539, Dec. 2018, doi: 10.1177/2472630318759257.

[75] R. Neill Carey *et al.*, “User Verification of Precision and Estimation of Bias; Approved Guideline-Third Edition,” vol. 34, p. 12, 2014, Accessed: Oct. 19, 2021. [Online]. Available: www.clsi.org.

[76] A. S. Tanak, S. Muthukumar, I. A. Hashim, and S. Prasad, “Establish pre-clinical diagnostic efficacy for parathyroid hormone as a point-of-surgery-testing-device (POST),” *Scientific Reports 2020 10:1*, vol. 10, no. 1, pp. 1–9, Nov. 2020, doi: 10.1038/s41598-020-75856-2.

[77] R. Carey, F. Anderson, H. George, A. Hartmann, and A. Kallner, “User verification of performance for precision and trueness; approved guideline—second edition,” in *Clinical and Laboratory Standards Institute Document EP 15-A2 2005*, vol. 25, 2005, pp. 1–64.

[78] D. W. Tholen, A. Kallner, J. W. Kennedy, J. S. Krouwer, and K. Meier, “Evaluation of precision performance of quantitative measurement methods; approved guideline—second edition,” *Evaluation*, vol. 24, no. 25, 2004.

[79] J. F. Pierson-Perry *et al.*, “Evaluation of Detection Capability for Clinical Laboratory Measurement Procedures; Approved Guidance-Second Edition. EP17-A2,” 2012.

[80] V. Jarrige, J. H. Nieuwenhuis, J. P. H. F. van Son, M. F. W. C. Martens, and J. L. M. Vissers, “A fast intraoperative PTH POC assay on the Philips handheld magnotech system,” *Langenbeck’s Archives of Surgery*, vol. 396, no. 3, pp. 337–343, Mar. 2011, doi: 10.1007/s00423-010-0733-z.

[81] A. Blumsohn and A. al Hadari, “Parathyroid hormone: what are we measuring and does it matter?,” *Annals of clinical biochemistry*, vol. 39, no. Pt 3, pp. 169–72, May 2002, doi: 10.1258/0004563021901928.

[82] S. M. S. and W. M. Catharine M. Sturgeon, “Variation in parathyroid hormone immunoassay results—a critical governance issue in the management of chronic kidney disease,” *Nephrol Dial Transplant.*, vol. 26, no. 11, pp. 3440–3445, Nov. 2011, Accessed: Mar. 02, 2020. [Online]. Available: https://www.ncbi.nlm.nih.gov/pmc/articles/PMC3203632/

[83] E. Cavalier, P. Delanaye, L. Nyssen, and J. C. Souberbielle, “Problems with the PTH assays,” *Annales d’Endocrinologie*, vol. 76, no. 2, pp. 128–133, May 2015, doi: 10.1016/j.ando.2015.03.018.

[84] S. Melmed, K. S. Polonsky, P. R. Larsen, and H. Kronenberg, *Williams textbook of endocrinology*, 13th ed. 2015.

[85] J. H. Eckfeldt, *Tietz Textbook of Clinical Chemistry*, Third., vol. 39, no. 7. Wiley-Blackwell, 1999. doi: 10.1046/j.1537-2995.1999.39070794.x.

[86] J. H. Brossard, M. Cloutier, L. Roy, R. Lepage, M. Gascon-Barré, and P. D'Amour, "Accumulation of a non-(1-84) molecular form of parathyroid hormone (PTH) detected by intact PTH assay in renal failure: importance in the interpretation of PTH values.," *The Journal of Clinical Endocrinology & Metabolism*, vol. 81, no. 11, pp. 3923–3929, Nov. 1996, doi: 10.1210/jcem.81.11.8923839.

[87] D. GOLTZMAN, H. GOMOLIN, A. DELEAN, M. WEXLER, and J. L. MEAKINS, "Discordant Disappearance of Bioactive and Immunoreactive Parathyroid Hormone after Parathyroidectomy*," *The Journal of Clinical Endocrinology & Metabolism*, vol. 58, no. 1, pp. 70–75, Jan. 1984, doi: 10.1210/jcem-58-1-70.

[88] C. Nedeva, J. Menassa, and H. Puthalakath, "Sepsis: Inflammation Is a Necessary Evil," *Frontiers in Cell and Developmental Biology*, vol. 0, no. JUN, p. 108, 2019, doi: 10.3389/FCELL.2019.00108.

[89] G. D. de La Rosa *et al.*, "Toward an operative diagnosis in sepsis: a latent class approach," *BMC Infectious Diseases 2008 8:1*, vol. 8, no. 1, pp. 1–9, Feb. 2008, doi: 10.1186/1471-2334-8-18.

[90] S. L. Gellatly and R. E. W. Hancock, "Pseudomonas aeruginosa : new insights into pathogenesis and host defenses," *Pathogens and Disease*, vol. 67, no. 3, pp. 159–173, Apr. 2013, doi: 10.1111/2049-632X.12033.

[91] R. K. Chakraborty and B. Burns, "Systemic Inflammatory Response Syndrome," *StatPearls*, Jul. 2021, Accessed: Oct. 20, 2021. [Online]. Available: https://www.ncbi.nlm.nih.gov/books/NBK547669/

[92] F. Gül, M. K. Arslantaş, İ. Cinel, and A. Kumar, "Changing Definitions of Sepsis," *Turkish Journal of Anaesthesiology and Reanimation*, vol. 45, no. 3, p. 129, 2017, doi: 10.5152/TJAR.2017.93753.

[93] L. J. Schlapbach *et al.*, "World Sepsis Day: a global agenda to target a leading cause of morbidity and mortality," *https://doi.org/10.1152/ajplung.00369.2020*, vol. 319, no. 3, pp. L518–L522, Sep. 2020, doi: 10.1152/AJPLUNG.00369.2020.

[94] R. S. Hotchkiss, L. L. Moldawer, S. M. Opal, K. Reinhart, I. R. Turnbull, and J. L. Vincent, "Sepsis and septic shock," *Nature Reviews Disease Primers*, vol. 2, no. 1. Nature Publishing Group, pp. 1–21, Jun. 30, 2016. doi: 10.1038/nrdp.2016.45.

[95] C. Rhee and M. Klompas, “Sepsis trends: increasing incidence and decreasing mortality, or changing denominator?,” *Journal of Thoracic Disease*, vol. 12, no. Suppl 1, p. S89, Feb. 2020, doi: 10.21037/JTD.2019.12.51.

[96] A. Lever and I. Mackenzie, “Sepsis: definition, epidemiology, and diagnosis,” *BMJ : British Medical Journal*, vol. 335, no. 7625, p. 879, Oct. 2007, doi: 10.1136/BMJ.39346.495880.AE.

[97] R. Gauer, “Early Recognition and Management of Sepsis in Adults: The First Six Hours,” *American Family Physician*, vol. 88, no. 1, pp. 44–53, Jul. 2013, Accessed: Oct. 19, 2021. [Online]. Available: www.aafp.org/afp.

[98] C. Caraballo, J. Ascuntar, C. Hincapié, C. Restrepo, E. Bernal, and F. Jaimes, “Association between site of infection and in-hospital mortality in patients with sepsis admitted to emergency departments of tertiary hospitals in Medellin, Colombia,” *Revista Brasileira de Terapia Intensiva*, vol. 31, no. 1, p. 47, 2019, doi: 10.5935/0103-507X.20190011.

[99] G. S. Martin, “Sepsis, severe sepsis and septic shock: changes in incidence, pathogens and outcomes,” *Expert review of anti-infective therapy*, vol. 10, no. 6, p. 701, Jun. 2012, doi: 10.1586/ERI.12.50.

[100] C. J. Hauser and L. E. Otterbein, “Danger signals from mitochondrial DAMPS in trauma and post-injury sepsis,” *European Journal of Trauma and Emergency Surgery 2018 44:3*, vol. 44, no. 3, pp. 317–324, May 2018, doi: 10.1007/S00068-018-0963-2.

[101] T. H. Mogensen, “Pathogen recognition and inflammatory signaling in innate immune defenses,” *Clinical Microbiology Reviews*, vol. 22, no. 2, pp. 240–273, Apr. 2009, doi: 10.1128/CMR.00046-08.

[102] Y. Wang, Y. Ouyang, B. Liu, X. Ma, and R. Ding, “Platelet activation and antiplatelet therapy in sepsis: A narrative review,” *Thrombosis Research*, vol. 166, pp. 28–36, Jun. 2018, doi: 10.1016/J.THROMRES.2018.04.007.

[103] S. Dhooria, I. S. Sehgal, and R. Agarwal, “The quest for the optimal blood pressure in septic shock,” *Journal of Thoracic Disease*, vol. 8, no. 9, p. E1019, 2016, doi: 10.21037/JTD.2016.08.27.

[104] A. Kumar *et al.*, “Duration of hypotension before initiation of effective antimicrobial therapy is the critical determinant of survival in human septic shock,” *Critical Care Medicine*, vol. 34, no. 6, pp. 1589–1596, Jun. 2006, doi: 10.1097/01.CCM.0000217961.75225.E9.

[105] H. il Kim and S. Park, “Sepsis: Early Recognition and Optimized Treatment,” *Tuberculosis and Respiratory Diseases*, vol. 82, no. 1, p. 6, Jan. 2019, doi: 10.4046/TRD.2018.0041.

[106] A. Deveau *et al.*, “Bacterial–fungal interactions: ecology, mechanisms and challenges,” *FEMS Microbiology Reviews*, vol. 42, no. 3, pp. 335–352, May 2018, doi: 10.1093/FEMSRE/FUY008.

[107] J. L. Vincent, “The Clinical Challenge of Sepsis Identification and Monitoring,” *PLoS Medicine*, vol. 13, no. 5, May 2016, doi: 10.1371/journal.pmed.1002022.

[108] C. A. Akdis, “Therapies for allergic inflammation: Refining strategies to induce tolerance,” *Nature Medicine*, vol. 18, no. 5. Nature Publishing Group, pp. 736–749, May 04, 2012. doi: 10.1038/nm.2754.

[109] H. B. Burke, “Predicting Clinical Outcomes Using Molecular Biomarkers,” *Biomarkers in Cancer*, vol. 8, no. 8, p. BIC.S33380, Jan. 2016, doi: 10.4137/bic.s33380.

[110] K. E. Rudd *et al.*, “Global, regional, and national sepsis incidence and mortality, 1990–2017: analysis for the Global Burden of Disease Study,” *The Lancet*, vol. 395, no. 10219, pp. 200–211, Jan. 2020, doi: 10.1016/S0140-6736(19)32989-7.

[111] M. Singer *et al.*, “The Third International Consensus Definitions for Sepsis and Septic Shock (Sepsis-3),” *JAMA*, vol. 315, no. 8, pp. 801–810, Feb. 2016, doi: 10.1001/JAMA.2016.0287.

[112] M. Schouten, W. J. Wiersinga, M. Levi, and T. van der Poll, “Inflammation, endothelium, and coagulation in sepsis,” *Journal of Leukocyte Biology*, vol. 83, no. 3, pp. 536–545, Mar. 2008, doi: 10.1189/jlb.0607373.

[113] W. Alhazzani *et al.*, “Surviving Sepsis Campaign: guidelines on the management of critically ill adults with Coronavirus Disease 2019 (COVID-19),” *Intensive Care Medicine*, vol. 46, no. 5, pp. 854–887, May 2020, doi: 10.1007/s00134-020-06022-5.

[114] M. Arentz *et al.*, “Characteristics and Outcomes of 21 Critically Ill Patients with COVID-19 in Washington State,” *JAMA - Journal of the American Medical Association*, vol. 323, no. 16. American Medical Association, pp. 1612–1614, Apr. 28, 2020. doi: 10.1001/jama.2020.4326.

[115] P. K. Bhatraju *et al.*, “Covid-19 in Critically Ill Patients in the Seattle Region — Case Series,” *New England Journal of Medicine*, vol. 382, no. 21, pp. 2012–2022, May 2020, doi: 10.1056/NEJMoa2004500.

[116] J. Phua *et al.*, “Intensive care management of coronavirus disease 2019 (COVID-19): challenges and recommendations,” *The Lancet Respiratory Medicine*, vol. 8, no. 5. Lancet Publishing Group, pp. 506–517, May 01, 2020. doi: 10.1016/S2213-2600(20)30161-2.

[117] A. S. Tanak, S. Muthukumar, S. Krishnan, K. L. Schully, D. v. Clark, and S. Prasad, “Multiplexed cytokine detection using electrochemical POC sensing device towards rapid sepsis endotyping,” *Biosensors and Bioelectronics*, vol. 171, p. 112726, Jan. 2021, doi: 10.1016/J.BIOS.2020.112726.

[118] R. S. Hotchkiss, G. Monneret, and D. Payen, “Immunosuppression in sepsis: A novel understanding of the disorder and a new therapeutic approach,” *The Lancet Infectious Diseases*. 2013. doi: 10.1016/S1473-3099(13)70001-X.

[119] A. M. Dupuy *et al.*, “Role of biomarkers in the management of antibiotic therapy: An expert panel review: I - currently available biomarkers for clinical use in acute infections,” *Annals of Intensive Care*, vol. 3, no. 1. Springer Verlag, pp. 1–8, Jul. 09, 2013. doi: 10.1186/2110-5820-3-22.

[120] C. Albert-Vega, D. M. Tawfik, S. Trouillet-Assant, L. Vachot, F. Mallet, and J. Textoris, “Immune functional assays, from custom to standardized tests for precision medicine,” *Frontiers in Immunology*, vol. 9, no. OCT. Frontiers Media S.A., Oct. 16, 2018. doi: 10.3389/fimmu.2018.02367.

[121] I. L. Gunsolus, T. E. Sweeney, O. Liesenfeld, and N. A. Ledeboer, “Diagnosing and managing sepsis by probing the host response to infection: Advances, opportunities, and challenges,” *Journal of Clinical Microbiology*, vol. 57, no. 7, Jul. 2019, doi: 10.1128/JCM.00425-19.

[122] B. Jagannath, S. Muthukumar, and S. Prasad, “Electrical double layer modulation of hybrid room temperature ionic liquid/aqueous buffer interface for enhanced sweat based biosensing,” *Analytica Chimica Acta*, vol. 1016, pp. 29–39, Aug. 2018, doi: 10.1016/j.aca.2018.02.013.

[123] A. S. Tanak, B. Jagannath, Y. Tamrakar, S. Muthukumar, and S. Prasad, "Non-faradaic electrochemical impedimetric profiling of procalcitonin and C-reactive protein as a dual marker biosensor for early sepsis detection," *Analytica Chimica Acta: X*, vol. 3, p. 100029, Nov. 2019, doi: 10.1016/j.acax.2019.100029.

[124] Y. Cho, T. A. Le, and H. Lee, "Understanding surface modulation to improve the photo/electrocatalysts for water oxidation/reduction," *Molecules*, vol. 25, no. 8. MDPI AG, Apr. 01, 2020. doi: 10.3390/molecules25081965.

[125] D. K. Kim *et al.*, "Solution-based stoichiometric control over charge transport in nanocrystalline CdSe devices," *ACS Nano*, vol. 7, no. 10, pp. 8760–8770, Oct. 2013, doi: 10.1021/nn403132x.

[126] N. R. Shanmugam, S. Muthukumar, and S. Prasad, "Ultrasensitive and low-volume POC diagnostics on flexible strips-a study with cardiac troponin biomarkers," *Scientific Reports*, vol. 6, no. 1, pp. 1–10, Sep. 2016, doi: 10.1038/srep33423.

[127] K. L. Schully *et al.*, "Melioidosis in lower provincial Cambodia: A case series from a prospective study of sepsis in Takeo Province," *PLoS Neglected Tropical Diseases*, vol. 11, no. 9, Sep. 2017, doi: 10.1371/journal.pntd.0005923.

[128] K. L. Schully and D. v. Clark, "Aspiring to precision medicine for infectious diseases in resource limited settings," in *Genomic and Precision Medicine: Infectious and Inflammatory Disease*, Elsevier, 2019, pp. 105–115. doi: 10.1016/B978-0-12-801496-7.00008-3.

[129] H. Chaudhry *et al.*, "Role of cytokines as a double-edged sword in sepsis," *In Vivo*, vol. 27, no. 6. NIH Public Access, pp. 669–684, Nov. 2013.

[130] A. S. Tanak, S. Muthukumar, I. A. Hashim, and S. Prasad, "Rapid electrochemical device for single-drop point-of-use screening of parathyroid hormone," *Bioelectronics in Medicine*, vol. 2, no. 1, pp. 13–27, Mar. 2019, doi: 10.2217/bem-2019-0011.

[131] C. A. Gogos, E. Drosou, H. P. Bassaris, and A. Skoutelis, "Pro- versus anti-inflammatory cytokine profile in patients with severe sepsis: A marker for prognosis and future therapeutic options," *Journal of Infectious Diseases*, vol. 181, no. 1, pp. 176–180, 2000, doi: 10.1086/315214.

[132] Y. Xiao and S. N. Isaacs, “Enzyme-linked immunosorbent assay (ELISA) and blocking with bovine serum albumin (BSA)-not all BSAs are alike,” *Journal of Immunological Methods*, vol. 384, no. 1–2, pp. 148–151, Oct. 2012, doi: 10.1016/j.jim.2012.06.009.

[133] CLSI, *Evaluation of precision of quantitative measurement procedures ; approved guideline—third edition*. 2014.

[134] U. Andreasson *et al.*, “A practical guide to immunoassay method validation,” *Frontiers in Neurology*, vol. 6, no. Aug, 2015, doi: 10.3389/fneur.2015.00179.

[135] E. J. Schenck *et al.*, “Circulating cell death biomarker TRAIL is associated with increased organ dysfunction in sepsis,” *JCI Insight*, vol. 4, no. 9, 2019, doi: 10.1172/jci.insight.127143.

[136] Y. Tian *et al.*, “Soluble Tumor Necrosis Factor Related Apoptosis Inducing Ligand Level as a Predictor of Severity of Sepsis and the Risk of Mortality in Septic Patients,” *PLoS ONE*, vol. 8, no. 12, p. e82204, Dec. 2013, doi: 10.1371/journal.pone.0082204.

[137] J. C. Marshall, “Biomarkers of sepsis,” *Current Infectious Disease Reports*, vol. 8, no. 5. Springer, pp. 351–357, Sep. 2006. doi: 10.1007/s11908-006-0045-1.

[138] L. Ulloa, K. T.-T. in molecular medicine, and undefined 2005, “The ‘cytokine profile’: a code for sepsis,” *Elsevier*, Accessed: May 14, 2020. [Online]. Available: https://www.sciencedirect.com/science/article/pii/S1471491404003168

[139] C. Huang *et al.*, “Clinical features of patients infected with 2019 novel coronavirus in Wuhan, China,” *The Lancet*, vol. 395, no. 10223, pp. 497–506, Feb. 2020, doi: 10.1016/S0140-6736(20)30183-5.

[140] J. L. Banyer, N. H. R. Hamilton, I. A. Ramshaw, and A. J. Ramsay, “Cytokines in innate and adaptive immunity,” *Reviews in Immunogenetics*, vol. 2, no. 3. pp. 359–373, Jan. 01, 2000.

[141] C. Nedeva, J. Menassa, and H. Puthalakath, “Sepsis: Inflammation Is a Necessary Evil,” *Frontiers in Cell and Developmental Biology*, vol. 0, no. JUN, p. 108, 2019, doi: 10.3389/FCELL.2019.00108.

[142] P. Damas *et al.*, “Cytokine serum level during severe sepsis in human IL-6 as a marker of severity,” *Annals of Surgery*, vol. 215, no. 4, pp. 356–362, 1992, doi: 10.1097/00000658-199204000-00009.

[143] A. Viallon *et al.*, “Serum and ascitic procalcitonin levels in cirrhotic patients with spontaneous bacterial peritonitis: Diagnostic value and relationship to pro-inflammatory cytokines,” *Intensive Care Medicine*, vol. 26, no. 8, pp. 1082–1088, 2000, doi: 10.1007/s001340051321.

[144] F. A. Bozza *et al.*, “Cytokine profiles as markers of disease severity in sepsis: A multiplex analysis,” *Critical Care*, vol. 11, no. 2, p. R49, Apr. 2007, doi: 10.1186/cc5783.

[145] T. Hou, D. Huang, R. Zeng, Z. Ye, and Y. Zhang, “Accuracy of serum interleukin (IL)-6 in sepsis diagnosis: A systematic review and meta-analysis,” *International Journal of Clinical and Experimental Medicine*, vol. 8, no. 9, pp. 15238–15245, Sep. 2015.

[146] P. T. N. Thao, T. T. Tra, N. T. Son, and K. Wada, “Reduction in the IL-6 level at 24 h after admission to the intensive care unit is a survival predictor for Vietnamese patients with sepsis and septic shock: A prospective study 11 Medical and Health Sciences 1103 Clinical Sciences,” *BMC Emergency Medicine*, vol. 18, no. 1, Nov. 2018, doi: 10.1186/s12873-018-0191-4.

[147] S. A. Renshaw *et al.*, “Acceleration of Human Neutrophil Apoptosis by TRAIL,” *The Journal of Immunology*, vol. 170, no. 2, pp. 1027–1033, Jan. 2003, doi: 10.4049/jimmunol.170.2.1027.

[148] K. Oved *et al.*, “A novel host-proteome signature for distinguishing between acute bacterial and viral infections,” *PLoS ONE*, vol. 10, no. 3, Mar. 2015, doi: 10.1371/journal.pone.0120012.

[149] Y. van der Does, A. Tjikhoeri, C. Ramakers, P. P. M. Rood, E. C. M. van Gorp, and M. Limper, “TRAIL and IP-10 as biomarkers of viral infections in the emergency department,” *Journal of Infection*, vol. 72, no. 6. W.B. Saunders Ltd, pp. 761–763, Jun. 01, 2016. doi: 10.1016/j.jinf.2016.03.004.

[150] C. B. van Houten *et al.*, “A host-protein based assay to differentiate between bacterial and viral infections in preschool children (OPPORTUNITY): a double-blind, multicentre, validation study,” *The Lancet Infectious Diseases*, vol. 17, no. 4, pp. 431–440, Apr. 2017, doi: 10.1016/S1473-3099(16)30519-9.

[151] J. M. Cramm and A. P. Nieboer, “Disease Management: The Need for a Focus on Broader Self-Management Abilities and Quality of Life,” *Population Health Management*, 2015, doi: 10.1089/pop.2014.0120.

[152] T. Evans, “Diagnosis and management of sepsis,” *Clinical Medicine, Journal of the Royal College of Physicians of London*, vol. 18, no. 2. Royal College of Physicians, pp. 146–149, Apr. 01, 2018. doi: 10.7861/clinmedicine.18-2-146.

[153] R. L. Gauer, “Early Recognition and Management of Sepsis in Adults: The First Six Hours,” Jul. 2013. Accessed: Dec. 14, 2020. [Online]. Available: www.aafp.org/afp.

[154] N. Nesaragi and S. Patidar, “Early Prediction of Sepsis From Clinical Data Using Ratio and Power-Based Features,” *Critical Care Medicine*, vol. 48, no. 12, pp. e1343–e1349, Dec. 2020, doi: 10.1097/ccm.0000000000004691.

[155] M. A. Reyna *et al.*, “Early Prediction of Sepsis From Clinical Data,” *Critical Care Medicine*, vol. 48, no. 2, pp. 210–217, Feb. 2020, doi: 10.1097/CCM.0000000000004145.

[156] N. T. Trung, N. S. Thau, M. H. Bang, and L. H. Song, “PCR-based Sepsis@Quick test is superior in comparison with blood culture for identification of sepsis-causative pathogens,” *Scientific Reports*, 2019, doi: 10.1038/s41598-019-50150-y.

[157] B. K. Lopansri *et al.*, “Physician agreement on the diagnosis of sepsis in the intensive care unit: Estimation of concordance and analysis of underlying factors in a multicenter cohort,” *Journal of Intensive Care*, vol. 7, no. 1, p. 13, Feb. 2019, doi: 10.1186/s40560-019-0368-2.

[158] K. E. Rudd *et al.*, “The global burden of sepsis: Barriers and potential solutions,” *Critical Care*, vol. 22, no. 1. BioMed Central Ltd., p. 123305059, Sep. 23, 2018. doi: 10.1186/s13054-018-2157-z.

[159] M. L. Martínez, E. P. Plata-Menchaca, J. C. Ruiz-Rodríguez, and R. Ferrer, “An approach to antibiotic treatment in patients with sepsis,” *Journal of Thoracic Disease*, vol. 12, no. 3. AME Publishing Company, pp. 1007–1021, Mar. 01, 2020. doi: 10.21037/jtd.2020.01.47.

[160] N. Alam *et al.*, “Prehospital antibiotics in the ambulance for sepsis: a multicentre, open label, randomised trial,” *The Lancet Respiratory Medicine*, vol. 6, no. 1, pp. 40–50, Jan. 2018, doi: 10.1016/S2213-2600(17)30469-1.

[161] J. J. Patel and P. A. Bergl, “COUNTERPOINT: Should Broad-Spectrum Antibiotics Be Routinely Administered to All Patients With Sepsis as Soon as Possible? No,” *Chest*, vol. 156, no. 4. Elsevier Inc, pp. 647–649, Oct. 01, 2019. doi: 10.1016/j.chest.2019.05.031.

[162] C. Rhee *et al.*, “Prevalence of Antibiotic-Resistant Pathogens in Culture-Proven Sepsis and Outcomes Associated With Inadequate and Broad-Spectrum Empiric Antibiotic Use,” *JAMA network open*, vol. 3, no. 4, p. e202899, Apr. 2020, doi: 10.1001/jamanetworkopen.2020.2899.

[163] B. Jagannath, K. C. Lin, M. Pali, D. Sankhala, S. Muthukumar, and S. Prasad, “A Sweat-based wearable enabling technology for realtime monitoring of il-1β and crp as potential markers for nflammatory bowel disease,” *Inflammatory Bowel Diseases*, vol. 26, no. 10, pp. 1533–1542, Oct. 2020, doi: 10.1093/ibd/izaa191.

[164] A. Lazăr, A. M. Georgescu, A. Vitin, and L. Azamfirei, “Precision Medicine and its Role in the Treatment of Sepsis: A Personalised View,” *The Journal of Critical Care Medicine*, vol. 5, no. 3, pp. 90–96, Aug. 2019, doi: 10.2478/jccm-2019-0017.

[165] A. S. Tanak, S. Muthukumar, S. Krishnan, K. L. Schully, D. v. Clark, and S. Prasad, “Multiplexed cytokine detection using electrochemical POC sensing device towards rapid sepsis endotyping,” *Biosensors and Bioelectronics*, vol. 171. Elsevier Ltd, p. 112726, Jan. 01, 2021. doi: 10.1016/j.bios.2020.112726.

[166] B. Reddy *et al.*, “POC sensors for the management of sepsis,” *Nature Biomedical Engineering*. 2018. doi: 10.1038/s41551-018-0288-9.

[167] B. Jagannath, K. Lin, M. Pali, D. Sankhala, S. Muthukumar, and S. Prasad, “Temporal profiling of cytokines in passively expressed sweat for detection of infection using wearable device,” *Bioengineering & Translational Medicine*, p. e10220, Apr. 2021, doi: 10.1002/btm2.10220.

[168] M. Rozo *et al.*, “An observational study of sepsis in takeo province cambodia: An in-depth examination of pathogens causing severe infections,” *PLoS Neglected Tropical Diseases*, vol. 14, no. 8, pp. 1–23, Aug. 2020, doi: 10.1371/journal.pntd.0008381.

[169] A. U. Sardesai *et al.*, “An approach to rapidly assess sepsis through multi-biomarker host response using machine learning algorithm,” *Scientific Reports 2021 11:1*, vol. 11, no. 1, pp. 1–10, Aug. 2021, doi: 10.1038/s41598-021-96081-5.

[170] K. W. Moore, R. de Waal Malefyt, R. L. Coffman, and A. O’Garra, “Interleukin-10 and the interleukin-10 receptor,” *Annual Review of Immunology*, vol. 19. Annual Reviews 4139 El Camino Way, P.O. Box 10139, Palo Alto, CA 94303-0139, USA , pp. 683–765, Nov. 28, 2001. doi: 10.1146/annurev.immunol.19.1.683.

[171] W. Cheng *et al.*, "Soluble TRAIL Concentration in Serum Is Elevated in People with Hypercholesterolemia," *PLOS ONE*, vol. 10, no. 12, p. e0144015, Dec. 2015, doi: 10.1371/journal.pone.0144015.

[172] Y. Yao, D. Wang, and Y. Yin, "Advances in sepsis-associated liver dysfunction," *Burns & Trauma*, vol. 2, no. 3, p. 97, 2014, doi: 10.4103/2321-3868.132689.

[173] J. Carlet, J. Cohen, T. Calandra, S. M. Opal, and H. Masur, "Sepsis: Time to reconsider the concept," *Critical Care Medicine*, vol. 36, no. 3, pp. 964–966, Mar. 2008, doi: 10.1097/CCM.0B013E318165B886.

[174] J. A. Gilbert, "Sepsis care bundles: a work in progress," *The Lancet Respiratory Medicine*, vol. 6, no. 11, pp. 821–823, Nov. 2018, doi: 10.1016/S2213-2600(18)30362-X.

[175] C. Fleischmann *et al.*, "Assessment of global incidence and mortality of hospital-treated sepsis current estimates and limitations," *American Journal of Respiratory and Critical Care Medicine*, vol. 193, no. 3, pp. 259–272, Feb. 2016, doi: 10.1164/rccm.201504-0781OC.

[176] M. Singer *et al.*, "The third international consensus definitions for sepsis and septic shock (sepsis-3)," *JAMA - Journal of the American Medical Association*, vol. 315, no. 8. American Medical Association, pp. 801–810, Feb. 23, 2016. doi: 10.1001/jama.2016.0287.

[177] D. M. del Valle *et al.*, "An inflammatory cytokine signature predicts COVID-19 severity and survival," *Nature Medicine 2020 26:10*, vol. 26, no. 10, pp. 1636–1643, Aug. 2020, doi: 10.1038/s41591-020-1051-9.

[178] S. Kany, J. T. Vollrath, and B. Relja, "Cytokines in Inflammatory Disease," *International Journal of Molecular Sciences*, vol. 20, no. 23, Dec. 2019, doi: 10.3390/IJMS20236008.

[179] A. K. G. Melo *et al.*, "Biomarkers of cytokine storm as red flags for severe and fatal COVID-19 cases: A living systematic review and meta-analysis," *PLOS ONE*, vol. 16, no. 6, p. e0253894, Jun. 2021, doi: 10.1371/JOURNAL.PONE.0253894.

[180] S. Caserta, M. Mengozzi, F. Kern, S. F. Newbury, P. Ghezzi, and M. J. Llewelyn, "Severity of Systemic Inflammatory Response Syndrome Affects the Blood Levels of Circulating Inflammatory-Relevant MicroRNAs," *Frontiers in Immunology*, vol. 0, p. 1977, Feb. 2018, doi: 10.3389/FIMMU.2017.01977.

[181] S. MERA *et al.*, “Multiplex cytokine profiling in patients with sepsis,” *APMIS*, vol. 119, no. 2, pp. 155–163, Feb. 2011, doi: 10.1111/J.1600-0463.2010.02705.X.

[182] B. K. Ashley and U. Hassan, “Point-of-critical-care diagnostics for sepsis enabled by multiplexed micro and nanosensing technologies,” *Wiley Interdisciplinary Reviews: Nanomedicine and Nanobiotechnology*, vol. 13, no. 5, p. e1701, Sep. 2021, doi: 10.1002/WNAN.1701.

[183] S. Sharma and P. Srivastava, “Resistance of Antimicrobial in Pseudomonas aeruginosa,” *International Journal of Current Microbiology and Applied Sciences*, vol. 5, no. 3, pp. 121–128, Mar. 2016, doi: 10.20546/IJCMAS.2016.503.017.

[184] B. Reddy *et al.*, “POC sensors for the management of sepsis,” *Nature Biomedical Engineering 2018 2:9*, vol. 2, no. 9, pp. 640–648, Sep. 2018, doi: 10.1038/s41551-018-0288-9.

[185] Z. A. Khan, M. F. Siddiqui, and S. Park, “Current and Emerging Methods of Antibiotic Susceptibility Testing,” *Diagnostics 2019, Vol. 9, Page 49*, vol. 9, no. 2, p. 49, May 2019, doi: 10.3390/DIAGNOSTICS9020049.

[186] Pradipta *et al.*, “Antibiotic resistance in sepsis patients: Evaluation and recommendation of antibiotic use,” *North American Journal of Medical Sciences*, vol. 5, no. 6, p. 344, 2013, doi: 10.4103/1947-2714.114165.

[187] V. N. Umlauf, S. Dreschers, and T. W. Orlikowsky, “Flow Cytometry in the Detection of Neonatal Sepsis,” *International Journal of Pediatrics*, vol. 2013, pp. 1–6, 2013, doi: 10.1155/2013/763191.

[188] F. Venet, A. Lepape, and G. Monneret, “Clinical review: flow cytometry perspectives in the ICU - from diagnosis of infection to monitoring of injury-induced immune dysfunctions,” *Critical Care 2011 15:5*, vol. 15, no. 5, pp. 1–9, Oct. 2011, doi: 10.1186/CC10333.

[189] S. Mukhopadhyay *et al.*, “Variation in Sepsis Evaluation Across a National Network of Nurseries,” *Pediatrics*, vol. 139, no. 3, Mar. 2017, doi: 10.1542/PEDS.2016-2845.

[190] L. Hein-Kristensen, L. Wiese, J. A. L. Kurtzhals, and T. Staalsoe, “In-depth validation of acridine orange staining for flow cytometric parasite and reticulocyte enumeration in an experimental model using Plasmodium berghei,” *Experimental Parasitology*, vol. 123, no. 2, pp. 152–157, Oct. 2009, doi: 10.1016/J.EXPPARA.2009.06.010.

[191] K. J. Land, D. I. Boeras, X.-S. Chen, A. R. Ramsay, and R. W. Peeling, "REASSURED diagnostics to inform disease control strategies, strengthen health systems and improve patient outcomes," *Nature Microbiology 2018 4:1*, vol. 4, no. 1, pp. 46–54, Dec. 2018, doi: 10.1038/s41564-018-0295-3.

[192] S. Smith, J. G. Korvink, D. Mager, and K. Land, "The potential of paper-based diagnostics to meet the ASSURED criteria," *RSC Advances*, vol. 8, no. 59, pp. 34012–34034, Sep. 2018, doi: 10.1039/C8RA06132G.

[193] T. Nicholson *et al.*, "LATE-BREAKING ABSTRACT: Plasma level of TRAIL is associated with severity of sepsis and predicts survival after critical illness," *European Respiratory Journal*, vol. 48, no. suppl 60, p. OA3021, Sep. 2016, doi: 10.1183/13993003.CONGRESS-2016.OA3021.

[194] A. S. Tanak, S. Muthukumar, S. Krishnan, K. L. Schully, D. v. Clark, and S. Prasad, "Multiplexed cytokine detection using electrochemical POC sensing device towards rapid sepsis endotyping," *Biosensors and Bioelectronics*, vol. 171, p. 112726, Jan. 2021, doi: 10.1016/J.BIOS.2020.112726.

[195] A. F. Shorr, S. J. Thomas, S. A. Alkins, T. M. Fitzpatrick, and G. S. Ling, "D-dimer Correlates With Proinflammatory Cytokine Levels and Outcomes in Critically Ill Patients," *Chest*, vol. 121, no. 4, pp. 1262–1268, Apr. 2002, doi: 10.1378/CHEST.121.4.1262.

[196] R. E *et al.*, "Early goal-directed therapy in the treatment of severe sepsis and septic shock," *The New England journal of medicine*, vol. 345, no. 19, pp. 1368–1377, Nov. 2001, doi: 10.1056/NEJMOA010307.

[197] M. D. Turner, B. Nedjai, T. Hurst, and D. J. Pennington, "Cytokines and chemokines: At the crossroads of cell signalling and inflammatory disease," *Biochimica et Biophysica Acta (BBA) - Molecular Cell Research*, vol. 1843, no. 11, pp. 2563–2582, Nov. 2014, doi: 10.1016/J.BBAMCR.2014.05.014.

[198] Z. S, H. CE, and W. WA, "Disseminated intravascular coagulation in sepsis," *Chest*, vol. 128, no. 4, pp. 2864–2875, 2005, doi: 10.1378/CHEST.128.4.2864.

[199] N. Tang, Y. Pan, C. Xu, and D. Li, "Characteristics of emergency patients with markedly elevated D-dimer levels," *Scientific Reports 2020 10:1*, vol. 10, no. 1, pp. 1–5, May 2020, doi: 10.1038/s41598-020-64853-0.

[200] N. Cui, H. Zhang, Z. Chen, and Z. Yu, “Prognostic significance of PCT and CRP evaluation for adult ICU patients with sepsis and septic shock: retrospective analysis of 59 cases:,” *https://doi.org/10.1177/0300060518822404*, vol. 47, no. 4, pp. 1573–1579, Jan. 2019, doi: 10.1177/0300060518822404.

[201] F. Liu *et al.*, “Prognostic value of interleukin-6, C-reactive protein, and procalcitonin in patients with COVID-19,” *Journal of Clinical Virology*, vol. 127, p. 104370, Jun. 2020, doi: 10.1016/J.JCV.2020.104370.

[202] D. Molano Franco, I. Arevalo-Rodriguez, M. Roqué i Figuls, N. G. Montero Oleas, X. Nuvials, and J. Zamora, “Plasma interleukin-6 concentration for the diagnosis of sepsis in critically ill adults,” *Cochrane Database of Systematic Reviews*, vol. 2019, no. 4, Apr. 2019, doi: 10.1002/14651858.CD011811.PUB2.

[203] D. Ragab, H. Salah Eldin, M. Taeimah, R. Khattab, and R. Salem, “The COVID-19 Cytokine Storm; What We Know So Far,” *Frontiers in Immunology*, vol. 0, p. 1446, Jun. 2020, doi: 10.3389/FIMMU.2020.01446.

[204] A. Teggert, H. Datta, and Z. Ali, “Biomarkers for POC Diagnosis of Sepsis,” *Micromachines 2020, Vol. 11, Page 286*, vol. 11, no. 3, p. 286, Mar. 2020, doi: 10.3390/MI11030286.

BIOGRAPHICAL SKETCH

Ambalika Sanjeev Tanak completed her preliminary and middle school education from the Indian High School, Dubai, UAE. She completed her high school education in Saraswathi Education Society, Thane, MAHARASHTRA. She received her Bachelor of Biomedical Engineering degree from Mumbai University in 2013. She started her master's program at The University of Texas at Dallas in the fall of 2014. She joined Biomedical Microdevices and Nanotechnology Laboratory (BMNL) as a graduate researcher in summer of 2015 and completed her Master of Science degree in Biomedical engineering in July 2016 with thesis submission under the guidance of Dr. Shalini Prasad. She continued to pursue her PhD under Dr. Shalini Prasad's supervision in Fall of 2016 where she gained significant expertise in designing and developing POC biosensors for diverse application from concept to execution. She is proficient in cleanroom fabrication process, electrical, material, and biochemical characterization techniques, with significant research experience in immunoassay development, clinical studies, and statistical data analysis.

CURRICULUM VITAE

Ambalika Sanjeev Tanak

PhD Biomedical Engineering, University of Texas at Dallas Nov 2021

MS Biomedical Engineering, University of Texas at Dallas July 2016

BE Biomedical Engineering, Mumbai University May 2013

HONORS and AWARDS

- **Jess Hay Endowment Research Fellowships,** UT system 2021
- **Baxter Young Investigator Award,** Baxter 2020
- **Tony B. Travel Award,** Society of Laboratory Automation 2019
- **Louis Beecherl, Jr. Graduate Fellowship,** UT Dallas 2018
- **IAB Graduate Fellowship,** The University of Texas at Dallas 2018
- **Distinguished Abstract Award,** American Association of Clinical Chemists 2018
- **First Place - Poster Competition,** American Association of Clinical Chemists 2018
- **Travel Grant**, American Association of Clinical Chemists 2018
- **NSF Travel Grant,** 28th Anniversary world congress on biosensor 2018
- **Tony B. Travel Award,** Society of Laboratory Automation 2018
- **Jonsson Family Graduate Fellowships,** The University of Texas at Dallas 2017
- **Jonsson School Graduate Scholarship,** The University of Texas at Dallas 2014

Peer-reviewed Journal publications

1.Sardesai, A. U., **Tanak, A. S**., et al. (2021). An approach to rapidly assess sepsis through multi-biomarker host response using machine learning algorithm. Scientific Reports, 11(1), 1-10.

2.**Tanak, A.S**., Muthukumar, S., Hashim, I. A., & Prasad, S. (2020). Establish pre-clinical diagnostic efficacy for parathyroid hormone as a point-of-surgery-testing-device (POST). Scientific Reports, 10(1), 19.

3.**Tanak, A. S**., Muthukumar, S., Krishnan, S., Schully, K. L., Clark, D. V., & Prasad, S. (2020). Multiplexed cytokine detection using electrochemical POC sensing device towards rapid sepsis endotyping. Biosensors and Bioelectronics, 112726.

4.Bhide, A., Jagannath, B., **Tanak, A.S**., Willis, R., & Prasad, S. (2020). CLIP: carbon Dioxide testing suitable for Low power microelectronics and IOT interfaces using Room temperature Ionic Liquid Platform. Scientific reports, 10(1), 1-12.

5.**Tanak, A. S**., Jagannath, B., Tamrakar, Y., Muthukumar, S., & Prasad, S. (2019). Non-faradaic electrochemical impedimetric profiling of procalcitonin and C-reactive protein as a dual marker biosensor for early sepsis detection. Analytica chimica acta: X, 3, 100029.

6.**Tanak, A. S**., Muthukumar, S., Hashim, I. A., & Prasad, S. (2019). Rapid electrochemical device for single-drop point-of-use screening of parathyroid hormone. Bioelectronics in Medicine, 2(1), 13-27.
7.Upasham, S**., Tanak, A. S**., Jagannath, B., & Prasad, S. (2018). Development of ultra-low volume, multi-bio fluid, cortisol sensing platform. Scientific reports, 8(1), 1-12.
8.Kamakoti, V., Shanmugam, N. R., **Tanak, A. S**., Jagannath, B., & Prasad, S. (2018). Investigation of molybdenum-crosslinker interfaces for affinity based electrochemical biosensing applications. Applied Surface Science, 436, 441-450.
9.Shanmugam, N. R., Muthukumar, S., **Tanak, A. S**., & Prasad, S. (2018). Multiplexed electrochemical detection of three cardiac biomarkers cTnI, cTnT and BNP using nanostructured ZnO-sensing platform. Future cardiology, 14(2), 131-141.
10.Upasham, S**., Tanak, A. S,** & Prasad, S. (2018). Cardiac troponin biosensors: where are we now?. Advanced Health Care Technologies, 4, 1-13.